Acta Pharmaceutica Sinica B 2025;15(12):6274−6306

Chinese Pharmaceutical Association
Institute of Materia Medica, Chinese Academy of Medical Sciences

Acta Pharmaceutica Sinica B

www.elsevier.com/locate/apsb
www.sciencedirect.com



REVIEW

ROS-scavenging nanomaterials as emerging tools for bone tissue regeneration: A comprehensive review of recent progress

Wanzhuo He[a,b,d,†], Tian Xu[d,†], Miao Wang[b,e], Ni Ni[a,b,c,d], Yun Su[a,b,c,d,*], Xianqun Fan[a,b,c,d,*]

[a]*Department of Ophthalmology, Shanghai Ninth People's Hospital, Shanghai Jiao Tong University School of Medicine, Shanghai 200011, China*
[b]*Shanghai Key Laboratory of Diseases and Ocular Oncology, Shanghai, 200011, China*
[c]*State Key Laboratory of Eye Health, Department of Ophthalmology, Shanghai Ninth People's Hospital, Shanghai Jiao Tong University School of Medicine, Shanghai 200011, China*
[d]*Shanghai Jiao Tong University School of Medicine, Shanghai 200025, China*
[e]*School of Clinical Medicine, Bengbu Medical University, Bengbu 233004, China*

Received 15 May 2025; received in revised form 19 August 2025; accepted 8 September 2025

KEY WORDS

ROS-scavenging nanomaterials;
Bone defects;
Bone regeneration;
Bone tissue engineering;
Nanoplatforms;
Antioxidant delivery;
Nanozymes;
Clinical translation

Abstract Bone defects, characterized by a loss of skeletal structure integrity, represent a prevalent clinical challenge affecting millions of patients. While bone autografts and allografts offer potential solutions, limitations, including donor scarcity, immune rejection, anatomical constraints, and complications arising from host comorbidities such as diabetes, often lead to unsatisfactory outcomes. This necessitates the need for alternative treatments. Researchers have identified that reactive oxygen species (ROS) play a crucial role in bone regeneration. Although physiological ROS levels are essential for normal healing, excessive ROS accumulation disrupts the balance between bone formation and resorption, hindering regeneration. Antioxidants can mitigate oxidative stress by scavenging ROS or inhibiting their formation, thereby restoring the equilibrium between bone formation and resorption. Advances in nanotechnology have enabled the development of various ROS-scavenging nanomaterials with enhanced therapeutic efficacy. These nanomaterials either function as delivery platforms for conventional antioxidants or as direct

*Corresponding authors.
E-mail addresses: suyun_sy@shsmu.edu.cn (Yun Su), fanxq@sjtu.edu.cn (Xianqun Fan).
[†]These authors made equal contributions to this work.
Peer review under the responsibility of Chinese Pharmaceutical Association and Institute of Materia Medica, Chinese Academy of Medical Sciences.

https://doi.org/10.1016/j.apsb.2025.09.040
2211-3835 © 2025 The Authors. Published by Elsevier B.V. on behalf of Chinese Pharmaceutical Association and Institute of Materia Medica, Chinese Academy of Medical Sciences. This is an open access article under the CC BY-NC-ND license (http://creativecommons.org/licenses/by-nc-nd/4.0/).

ROS-neutralizing agents through intrinsic redox or enzyme-mimicking properties. This review comprehensively summarizes ROS-scavenging nanomaterials for bone tissue regeneration, focusing on their design strategies, underlying mechanisms, applications, and potential for clinical translation.

© 2025 The Authors. Published by Elsevier B.V. on behalf of Chinese Pharmaceutical Association and Institute of Materia Medica, Chinese Academy of Medical Sciences. This is an open access article under the CC BY-NC-ND license (http://creativecommons.org/licenses/by-nc-nd/4.0/).

1. Introduction

Bone defects, often caused by trauma, tumor resection, infection, or congenital disorders, are characterized by a loss of skeletal structure integrity, affecting millions of patients both physically and psychologically[1]. While small defects may heal naturally, critical-sized bone defects or those complicated by diabetes, osteoporosis, or osteomyelitis often require surgical or alternative treatments[2]. Currently, the "gold standard" for treating critical-sized bone defects remains autologous or allogeneic bone grafts; however, they face limitations, including donor scarcity, immune rejection, anatomical constraints, and infection risks, which can potentially lead to poor healing or nonunion[3,4]. In response, bone tissue engineering (BTE) materials such as titanium alloys, ceramics, and hydrogels have been developed to support regeneration by creating a favorable bone microenvironment. Ideal bone substitutes should combine mechanical strength, biocompatibility, biodegradability, and osteoinductivity[5]. Notably, oxidative stress—marked by elevated levels of reactive oxygen species (ROS)—is increasingly recognized as a key factor hindering repair in large bone defects[6]. Therefore, ROS-regulating strategies are gaining attention in BTE to improve healing outcomes[7].

Reactive oxygen species (ROS) are highly reactive oxidants derived from the partial reduction of oxygen[8]. They include free radicals with unpaired electrons (*e.g.*, superoxide anion $O_2^{\cdot-}$, hydroxyl radical $HO^{\cdot}$, alkoxyl radical $RO^{\cdot}$, and peroxyl radical $ROO^{\cdot}$) and non-radicals (*e.g.*, hydrogen peroxide H_2O_2, singlet oxygen $^1O_2$, and ozone O_3). The major source of ROS under physiological conditions is the mitochondrial electron transport chain (ETC)[9]. During aerobic respiration, 2%−3% of electrons may leak from complexes I and III, reducing oxygen to form $O_2^{\cdot-}$. Normally, ROS are minor byproducts of metabolism, but in pathological states—such as large bone defects—mitochondrial dysfunction, ETC disruption can dramatically increase ROS production[10]. Another significant source of ROS is the NADPH oxidase (NOX) complexes, located on the plasma membrane, which primarily generate signaling ROS that function as second messengers in various cellular pathways[11]. Other contributors include the endoplasmic reticulum enzymes, cytochrome P450, nitric oxide synthase, and various oxidases[12] (Fig. 1A). To maintain redox homeostasis, cells rely on sophisticated antioxidant defense systems consisting of both enzymatic and non-enzymatic components[13]. Key enzymatic parts include superoxide dismutase (SOD), catalase (CAT), glutathione peroxidase (GPx), and peroxiredoxins (Prxs)[14]. The non-enzymatic antioxidant primarily involves thiol-based redox buffering systems like glutathione (GSH) and thioredoxin (Trx)[15]. Additionally, small-molecule antioxidants such as vitamins A, C, and E also contribute to ROS scavenging[16–18] (Fig. 1B).

At physiological levels, ROS support normal cellular homeostasis and function[19]. However, excessive ROS fluctuations disrupt cellular functions—low ROS may arrest the cell cycle, while high levels can induce stress responses or cell death[20,21]. In pathological bone microenvironments—such as large defects, infections, or those complicated by diabetes and osteoporosis—ROS production becomes excessive and persistent. This overproduction, coupled with inflammation and hypoxia, gradually weakens antioxidant defenses. For example, hypoxia and pro-inflammatory signals upregulate nitric oxide synthase (NOS), leading to the formation of peroxynitrite ($ONOO^-$) from NO and $O_2^{\cdot-}$[22,23]. $ONOO^-$ can oxidize or nitrate the catalytic centers of Cu/Zn-SOD and GPX, impairing their enzymatic activity[24]. Meanwhile, non-enzymatic antioxidants are depleted by continuous oxidative attacks, leaving insufficient reserves to combat ongoing stress[25,26]. In summary, the interplay between hypoxia, oxidative stress, and inflammation ultimately overwhelms ROS defense mechanisms. Accumulated ROS damages osteogenic proteins and DNA, inhibiting osteoblast differentiation and function, and activating pro-inflammatory pathways that lead to osteoclast overactivation. This pathological shift promotes excessive bone resorption and ultimately leads to bone loss[27]. Therefore, strategies aimed at ROS clearance, particularly ROS-scavenging nanotechnology, emerged as a particularly promising approach.

Nanomaterials, defined as materials with at least one dimension between 1 and 100 nm, include nanoparticles, nanofibers, and nanosheets[28]. The transition from macro-to nanoscale leads to unique physicochemical properties such as size effects, electronic effects, crystal effects, and interface effects[29]. These distinctive properties enhance their interactions with biological systems at cellular and molecular levels, conferring excellent ROS-regulating capabilities.

Recently, several high-impact reviews have explored ROS-scavenging nanomaterials, particularly nanozymes, and their applications in various pathological conditions such as cancer, cardiovascular, and neurodegenerative diseases[30–32]. These reviews have provided solid frameworks, outlining the classification, mechanisms, and biomedical applications of ROS-scavenging materials. However, few have delved into bone repair, and those that do often lack clear categorization, overlook key design considerations, or fail to capture the unique advantages of nanoscale design. In this review, we focus specifically on the interplay between ROS and bone healing, and address key questions: how ROS levels fluctuate during bone healing, how excessive ROS disrupts cellular components involved in bone regeneration, and how ROS-scavenging nanomaterials can improve healing outcomes. We provide a comprehensive and structured classification of ROS-scavenging nanomaterials, integrating underlying mechanisms with representative examples, and highlighting how nanoscale properties improve material performance. Furthermore, by discussing current challenges and future directions, we aim to provide a forward-looking perspective to inspire further development in this field. Thus, this review extends existing literature and offers guidance for the rational design of ROS-scavenging nanomaterials to improve bone defect repair.

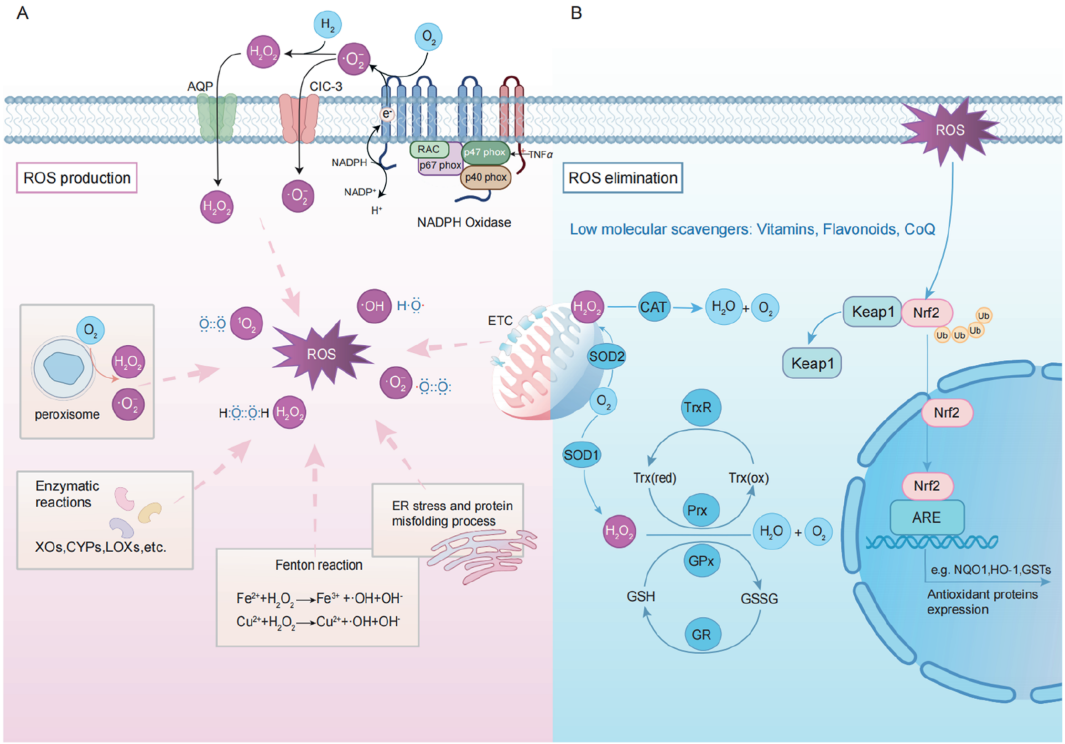


Figure 1 Production and elimination of ROS. (A) ROS are produced through several cellular processes, including mitochondrial electron transport chains (ETC), NADPH oxidases (NOX), endoplasmic reticulum (ER) stress, Fenton reactions, and enzymatic reactions in peroxisomes. The generated ROS mainly include superoxide anions (O_2^-), hydrogen peroxide (H_2O_2), and hydroxyl radicals (OH·). (B) ROS are eliminated *via* endogenous antioxidant systems, including enzymatic antioxidants such as catalase (CAT), superoxide dismutases (SOD1 and SOD2), thioredoxin reductase (TrxR), and glutathione peroxidase (GPx), as well as low-molecular-weight scavengers like vitamins, flavonoids, and coenzyme Q (CoQ). The Nrf2/Keap1 pathway is activated in response to oxidative stress, resulting in the expression of antioxidant proteins that contribute to cellular defense against ROS-induced damage. These systems work in concert to maintain cellular homeostasis and prevent oxidative damage. AQP, aquaporin; CIC-3, cytochrome *c* oxidase subunit III; RAC, ras-related C3 botulinum toxin substrate; Phox, phagocytic oxidase; TNFα, tumor necrosis factor α; ETC, electron transport chain; XOs, xanthine oxidases; CYPs, cytochrome P450s; LOXs, lipoxygenases; Prx, peroxiredoxin; GSH, glutathione; GSSG, oxidized glutathione; GR, glutathione reductase; NF-κB, nuclear factor κB; Nrf2, nuclear factor erythroid 2-related factor 2; ARE, antioxidant response element; Keap1, Kelch-Like ECH-Associated Protein 1; Ub, ubiquitin; NQO1, NAD(P)H quinone oxidoreductase 1; HO-1, heme oxygenase-1; GSTs, glutathione *S*-transferases.

2. The role of ROS in fracture healing

2.1. Time course of fracture healing events

Fracture healing is characterized by three overlapping phases: inflammation, repair, and remodeling.

The inflammatory cascade is initiated immediately after fracture when local blood vessels in the bone tissue, bone marrow, and surrounding soft tissues are disrupted. This vascular damage leads to hematoma formation, creating a microenvironment characterized by hypoxia, low pH, and high inflammatory activity[33]. Within this hematoma, fibrin networks form a temporary matrix that facilitates immune cell infiltration. Neutrophils are the first to arrive within 24 h, drawn by platelet-derived factors, complement fragments, and damage-associated molecular patterns (DAMPs) released from necrotic cells[34]. They are followed by macrophages and lymphocytes, which secrete various cytokines, chemokines, and growth factors[35,36]. This acute inflammatory response typically lasts 4−7 days and is essential for debris clearance and the recruitment of progenitor cells to initiate repair[37] (Fig. 2A).

The repair phase involves two ways of bone formation: direct (primary) and indirect (secondary) healing—largely determined by mechanical stability at the fracture site[38,39]. Direct healing occurs in fractures with minimal interfragmentary motion, where extreme mechanical stability favors the direct differentiation of osteoprogenitor cells into osteoblasts, resembling intramembranous ossification. In this process, osteoclasts first create cutting cones across the fracture line, which are then filled by osteoblasts with new bone, restoring continuity between fragments[40,41]. In contrast, indirect healing, which is more common, involves both intramembranous and endochondral ossification[42,43]. Intramembranous ossification occurs in the periosteum, where conditions are stable and well-vascularized. Meanwhile, in the central fracture zone with greater mechanical strain and limited vascularity, endochondral ossification prevails. There, mesenchymal stem cells (MSCs) differentiate into chondrocytes that form a cartilaginous callus bridging the fracture[39]. As healing progresses, chondrocytes become hypertrophic, the cartilage matrix calcifies, and blood vessels invade, bringing osteoprogenitor cells that replace the cartilage with woven bone[44]. This results in the formation of a hard callus that stabilizes the fracture over weeks to months (Fig. 2B).

The final remodeling phase involves the gradual replacement of woven bone with lamellar bone through coordinated actions of

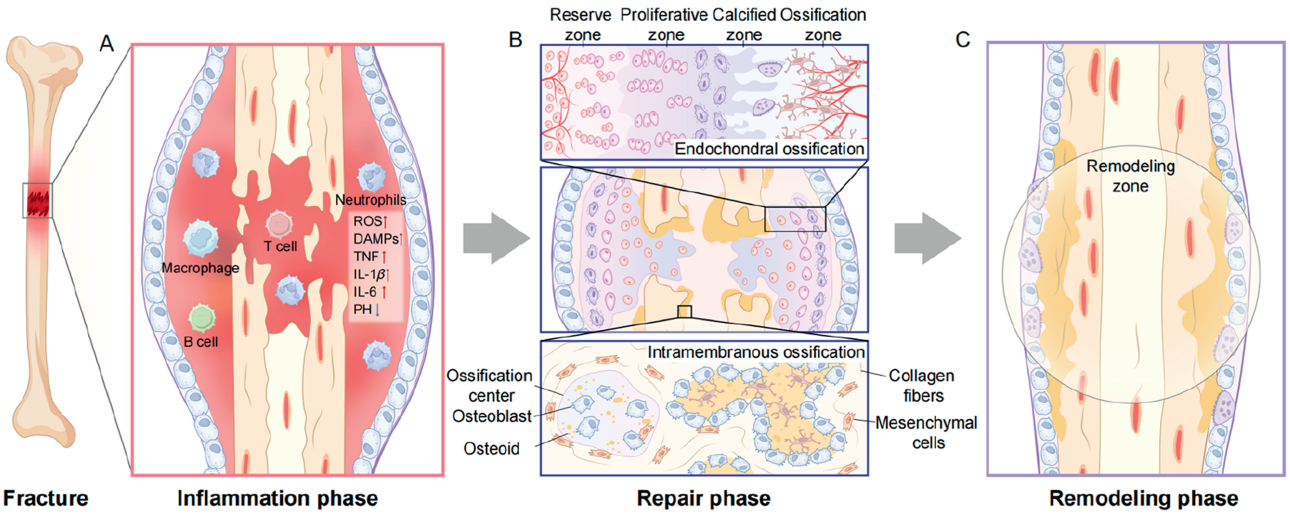


Figure 2 Bone fracture healing process. (A) Inflammation phase: The healing process is initiated by an acute inflammatory response, during which immune cells such as macrophages, T cells, B cells, and neutrophils are recruited to the fracture site. These cells release inflammatory cytokines and reactive oxygen species (ROS) to mediate immune activation and tissue clearance. (B) Bone formation *via* endochondral and intramembranous ossification: Intramembranous ossification occurs at the periosteal region, typically distant from the fracture gap, where mechanical stability and vascularization are sufficient. Mesenchymal stem cells (MSCs) condense beneath the periosteum and differentiate into osteoblasts, forming ossification centers that produce trabecular bone, which later remodels into mature cortical bone. In contrast, endochondral ossification occurs within the fracture gap and involves MSC proliferation and differentiation into chondrocytes that form a cartilage template. These chondrocytes hypertrophy, the matrix calcifies, and the cells undergo apoptosis. Subsequent vascular invasion delivers osteoprogenitor cells, which replace the calcified cartilage with woven bone. (C) Remodeling phase: The final stage involves the coordinated action of osteoclasts and osteoblasts to restore the original bone structure and function. This dynamic process is essential for maintaining bone health and adapting to mechanical stresses. DAMPs, damage-associated molecular patterns; TNF, tumor necrosis factor; IL-1β, interleukin-1β; IL-6, interleukin-6.

osteoclasts and osteoblasts. This process restores the bone's original architecture and mechanical strength, ultimately returning it to its pre-injury state[45] (Fig. 2C). Remodeling may continue for months to years, depending on factors such as fracture severity, patient age, and overall health status.

In the overall process of bone regeneration, the transition from inflammation to repair represents a critical turning point that determines repair outcomes[46]. This transition is marked by shifts in immune cell populations and cytokine expression profiles[47,48]. Pro-inflammatory cytokines (*e.g.*, IL-1β, IL-6, TNF-α) gradually decline, while anti-inflammatory mediators (*e.g.*, IL-10, TGF-β) increase[49]. Central to this process is the phenotypic switch of macrophages from the pro-inflammatory M1 subtype to the pro-reparative M2 subtype[50,51]. This transition is regulated by a coordinated interplay of microenvironmental cues, including cytokine dynamics, metabolic reprogramming, and redox homeostasis[50]. Together, these changes create a microenvironment conducive to the recruitment and osteogenic differentiation of MSCs, thereby initiating the repair phase[52].

From this overview, it is clear that bone healing is a dynamic process coordinated by inflammation, angiogenesis, as well as stem cell recruitment and differentiation. Within this process, spatiotemporal changes in ROS levels critically influence the repair outcome[53]. The following sections will discuss in detail how ROS functions at each critical stage—inflammatory phase, transition period, and repair phase—as well as how pathologically elevated ROS impairs these processes, highlighting the complex interplay between redox signaling and bone regeneration. A better understanding of these mechanisms will guide the design of ROS-modulating nanomaterials to enhance bone repair.

2.2. *Physiological roles of ROS during bone healing*

Inflammation is the initiating phase of bone repair, during which a marked increase in ROS levels is observed in the bone microenvironment[54]. This increase mainly results from the respiratory burst of infiltrating immune cells (*e.g.*, neutrophils and macrophages) *via* NOX, as well as mitochondrial leakage from necrotic debris and damaged tissues[55]. Temporarily elevated ROS helps clear pathogens and debris, creating an aseptic environment[56,57]. Moreover, they amplify NF-κB and MAPK pathways in immune cells, possibly through (1) oxidative modification of key signaling nodes (*e.g.*, TRAF6, IKK complex) to enhance their activity, and (2) inhibition of negative regulators such as MAPK phosphatases (MKPs), which normally restrain MAPK activation[58–61]. This triggers a broad immune response, including increased secretion of pro-inflammatory cytokines and enhanced activation of inflammatory cells[62–64]. ROS also helps maintain the M1 pro-inflammatory phenotype by stabilizing HIF-1α and favoring a glycolytic metabolic shift[65]. These early ROS-driven events are crucial for initiating immune clearance and subsequent tissue repair[66]. In addition to immune modulation, ROS also acts as a secondary messenger to amplify RANKL/RANK signaling in osteoclast precursors by activating NF-κB/MAPK pathways, common downstream effectors of ROS signaling[67–69]. This may lead to the nuclear translocation of NFATc1 and upregulation of osteolytic enzymes such as cathepsin K and TRAP, thus promoting osteoclast differentiation and maturation[70–72]. Furthermore, ROS synergizes with endoplasmic reticulum stress and TGF-β signaling to activate osteoclast autophagy, which provides energy and proteases (*e.g.*, MMP-9) for cellular migration and bone

resorption[73]. Meanwhile, ROS cooperate with hypoxia to stabilize HIF-1α and transiently enhance VEGF and FGF2 expression, thereby promoting endothelial progenitor cell recruitment and early angiogenesis to support subsequent tissue regeneration[74−76]. Collectively, these mechanisms accelerate pathological bone degradation, creating space for subsequent regeneration.

As inflammation progresses, endogenous antioxidant systems such as the nuclear factor erythroid 2-related factor 2 (Nrf2)/antioxidant response element (ARE) pathway are activated to neutralize ROS and restore redox balance[77,78]. The resulting decline in ROS levels not only alleviates oxidative stress but also promotes M1-to-M2 transition by disrupting pro-inflammatory metabolic and signaling programs, restoring mitochondrial oxidative phosphorylation (OXPHOS), reactivating STAT6 signaling, and inducing downstream M2-associated transcription factors such as PPARγ[79]. This phenotypic switch marks the beginning of the repair phase. Subsequently, M2 also helps maintain a low-ROS state by secreting antioxidant enzymes (*e.g.*, extracellular SOD), releasing immunosuppressive cytokines that disrupt the positive feedback loop between inflammation and oxidative stress, and shifting their metabolism toward fatty acid oxidation (FAO)-dependent OXPHOS[80−82]. Unlike the glycolytic metabolism of M1, which disrupts the TCA cycle and promotes mitochondrial ROS production *via* reverse electron transport, the FAO-supported OXPHOS in M2 enables efficient electron flow and minimizes ROS leakage[83]. In addition, reduced ROS levels also enhance the recruitment and osteogenic differentiation of MSCs by relieving FOXO-mediated suppression of Wnt/β-catenin signaling[84,85]. The upregulation of ROS-sensitive pathways, such as PI3K/Akt and BMP, further promotes osteoblast function[86]. Meanwhile, moderate ROS levels alleviate oxidative damage in endothelial cells and support vascular network formation through VEGF and FGF-2 signaling[87]. ROS-dependent activation of Notch signaling, particularly *via* Jagged1, further drives endothelial sprouting and tube formation, contributing to angiogenesis[88,89].

As bone healing progresses into the reparative and remodeling phases, the excessive ROS generated during inflammation is largely eliminated, leaving behind tightly regulated, physiological ROS levels[86,90]. These ROS are produced on demand—primarily *via* NOX4 and ETCs—and act as second messengers within osteogenic cells[91,92]. They activate PI3K/Akt, Wnt/β-catenin, and BMP2 pathways, thereby promoting bone marrow stromal cells (BMSCs) osteogenic differentiation and osteoblast function to support bone formation and maturation[93,94]. Simultaneously, ROS modulates the RANKL/OPG ratio to coordinate osteoblast−osteoclast coupling, which is essential for bone remodeling[67,86,95]. ROS also stabilizes HIF-1α in osteoblasts by inhibiting prolyl hydroxylase (PHD). In contrast to its pro-inflammatory role under oxidative stress, moderately stabilized HIF-1α maintains the expression of angiogenic factors such as VEGF and FGF-2[96,97]. These factors promote vascular maturation through the PI3K−Akt−eNOS pathway, supporting the vascular network necessary for bone development[98,99].

2.3. *Pathological effects of excessive ROS*

Although ROS plays a regulatory role in bone healing, persistently elevated levels can lead to pathological consequences (Fig. 3A and B). Firstly, excessive ROS levels impair the M1-to-M2 transition through multiple mechanisms. They activate NF-κB and STAT1 pathways, stabilize HIF-1α, which sustains the M1 phenotype by preserving its pro-inflammatory gene expression and glycolytic metabolism[100,101]. Meanwhile, ROS impairs IL-4/STAT6 signaling, which is critical for M2 polarization, and suppresses the expression of M2-promoting transcription factors such as PPARγ and KLF4[102−104]. In addition, ROS-induced mitochondrial dysfunction disrupts OXPHOS—a metabolic feature essential for M2 polarization[105]. Collectively, sustained oxidative stress locks macrophages in a pro-inflammatory M1 state, impeding their phenotypic switch and thereby delaying inflammation resolution and bone repair.

Secondly, osteoblasts are also affected by excessive ROS levels. Extracellular ROS can damage cell membranes, leading to necrosis or apoptosis, while intracellular ROS overload may induce apoptosis through the mitochondrial-dependent caspase-3/9 pathway[106]. Simultaneously, excessive ROS strongly activates FoxO transcription factors (*e.g.*, FoxO1/3a) in multiple ways, such as inhibiting the PI3K/Akt pathway and blocking FoxO phosphorylation[107−109]. Unphosphorylated FoxO translocates to the nucleus, competing with TCF/LEF factors, and 'hijacking' β-catenin to the promoter regions of antioxidant genes (such as SOD and peroxidase)[110]. These actions prioritize antioxidant programs to clear excess ROS, which may suppress Wnt-related osteogenic differentiation[111]. Consequently, expression of key osteogenic genes, such as Runx2 and Osterix, is downregulated, resulting in decreased alkaline phosphatase (ALP) activity and osteocalcin secretion, significantly inhibiting osteoblast function[112,113]. Additionally, ROS influences the bone metabolic microenvironment through paracrine signaling. For example, excessive ROS directly upregulates RANKL expression and inhibits osteoprotegerin (OPG) secretion in osteoblasts *via* MAPK (*e.g.*, ERK and JNK) or NF-κB activation, causing an imbalance in the RANKL/OPG ratio[114,115]. This imbalance strongly activates RANK receptor signaling in neighboring osteoclast precursors, driving osteoclast differentiation and bone resorption[116].

Thirdly, ROS disrupts MSC function. High ROS levels suppress osteogenic differentiation by inhibiting Wnt/Notch signaling, while simultaneously promoting adipogenesis *via* upregulation of PPARγ and C/EBP[117]. This shift directly reduces bone formation and causes abnormal marrow adiposity, further deteriorating the bone microenvironment[118]. Additionally, high levels of ROS can induce apoptosis or senescence in MSCs. Senescent MSCs develop a senescence-associated secretory phenotype (SASP), releasing pro-inflammatory cytokines that synergize with ROS[119,120] to promote RANKL expression and amplify RANKL−RANK signaling[121]. If inflammation and oxidative stress persist, the above events will form a vicious cycle of "inflammation−ROS−osteoclast activation−osteogenesis inhibition".

Moreover, ROS impacts the vascular niche. While early high levels of ROS promote angiogenesis, their sustained elevation can disrupt endothelial tight junctions by activating the RhoA/ROCK pathway, leading to abnormal vascular permeability and compromising vascular integrity[122,123].

In summary, while high ROS levels during the acute inflammatory phase are essential for immune activation and debris clearance, their sustained elevation inhibits osteogenic signaling and disrupts inflammatory balance, resulting in tissue destruction, MSC apoptosis, osteoclast overactivation, and suppressed osteoblast function, ultimately impairing bone healing. Therefore, the timely resolution of oxidative stress is crucial for initiating effective repair.

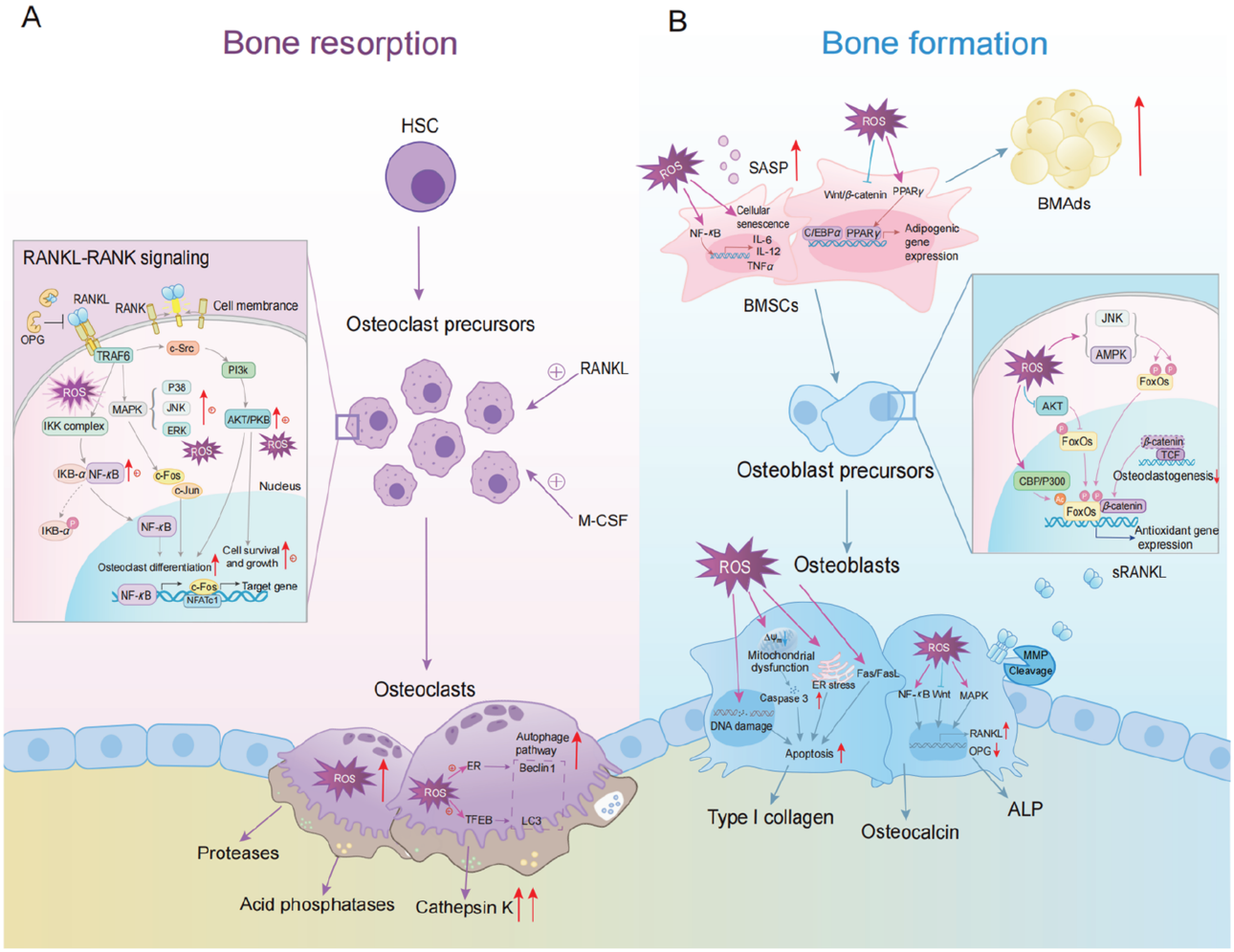


Figure 3 The role of ROS in bone resorption and formation. Excessive ROS promotes bone resorption (A) and impairs bone formation (B) by modulating multiple osteogenic signaling pathways. In osteoclasts, ROS activate the RANKL—RANK signaling cascade, promoting differentiation and resorptive function, and induce autophagy to further enhance bone degradation. In osteoblasts, ROS causes mitochondrial dysfunction and apoptosis, sequesters β-catenin to suppress osteogenic differentiation, and upregulates RANKL while downregulating osteoprotegerin (OPG), indirectly augmenting osteoclastogenesis. In bone marrow stromal cells (BMSCs), ROS drive adipogenic commitment and trigger a senescence-associated secretory phenotype (SASP), thereby disrupting normal lineage differentiation and regenerative capacity. Collectively, ROS-induced dysregulation of the coupling between bone formation and resorption compromises the bone healing process. HSC, hematopoietic stem cell; RANKL, receptor activator of nuclear factor κB ligand; TRAF6, TNF receptor-associated factor 6; PI3K, phosphoinositol-3 kinase; MAPK, mitogen-activated protein kinase; IKK complex, IκB kinase complex; NF-κB, nuclear factor κB; IKK-β, IκB kinase β; c-Fos, cellular FBJ murine osteosarcoma viral oncogene homolog; c-Jun, cellular avian sarcoma virus 17 oncogene homolog; AKT, protein kinase B; ER, endoplasmic reticulum; LC3, microtubule-associated protein 1A/1B-light chain 3; TFEB, transcription factor EB; Beclin1, BCL2-interacting protein 1; M-CSF, macrophage colony-stimulating factor; BMAds, bone marrow adipocytes; IL-12, interleukin-12; TNFα, tumor necrosis factor α; PPARγ, peroxisome proliferator-activated receptor γ; CEBPs, CCAAT/enhancer-binding proteins; AMPK, AMP-activated protein kinase; CBP/p300, CREB-binding protein/p300; FoxOs, forkhead box Os; TCF, T-cell factor; sRANKL, soluble RANKL; ALP, alkaline phosphatase.

3. ROS-scavenging nanomaterials in bone repair

Generally, living organisms maintain a delicate balance between the generation and elimination of ROS through their intracellular antioxidant defense systems. However, under pathological conditions—such as large-scale bone defects, bone damage resulting from suppurative inflammation, osteoarthritis, periodontitis, or bone defects complicated by systemic diseases like diabetes or osteoporosis—ROS can be overproduced and accumulate. The elevated ROS levels lead to severe inflammation, and these two factors exacerbate each other, creating a vicious cycle that hinders bone regeneration[124–128]. Furthermore, although implanted biomaterials for bone repair are typically considered biocompatible, they can still induce local inflammatory responses and ROS production to varying degrees[129,130]. Accumulating evidence suggests that reducing ROS may help alleviate oxidative stress-induced damage and establish a more favorable microenvironment for osteogenesis[36,131]. Therefore, incorporating ROS-reducing strategies into the design of bone repair scaffolds is crucial.

3.1. Overview of current ROS-scavenging strategies

The design principles for ROS-reducing materials primarily follow two simple mechanisms: inhibiting ROS production or enhancing ROS scavenging. The former targets key ROS-generating enzymes, such as NADPH oxidase (NOX), xanthine oxidase (XO), and lipoxygenase (LOX). For example, apocynin, a natural compound, inhibits NOX activity and shows protective effects in inflammatory disease models[132]. However, ROS after bone injury originates from multiple sources, and targeting a single enzymatic pathway is often insufficient[36]. In addition, moderate ROS levels—especially those generated by NOX—are essential for cellular signaling; excessive inhibition may disrupt regeneration[133]. Thus, this strategy is less favored in scaffold design. In contrast, enhancing ROS scavenging is more widely adopted and includes two main strategies: one is boosting endogenous antioxidant systems using enzyme-regulating substances (*e.g.*, Nrf2 activators or natural enzyme modulators), and the other is introducing exogenous antioxidants, which may directly neutralize ROS or mimic antioxidant enzyme activities. In practice, many antioxidant materials exhibit synergistic effects. For example, cerium oxide nanoparticles (nanoceria) can not only mimic SOD/CAT activity but also inhibit excessive ROS production[134,135]. Similarly, *N*-Acetyl-L-cysteine (NAC) can directly scavenge ROS *via* thiol groups and provide cysteine to promote GSH synthesis, facilitating GSH-mediated ROS clearance[136]. As such, current material design trends favor multifunctional agents or combinations to achieve enhanced effects.

Among available antioxidant materials, reductive small organic compounds—such as polyphenols and terpenoids—were among the earliest studied. Beyond direct ROS elimination, they also exhibit anti-inflammatory and osteoinductive properties, making them attractive candidates for BTE applications. These compounds can be incorporated into scaffolds *via* physical interactions (*e.g.*, adsorption, surface coating, pore embedding), chemical bonding, ionic bonding, or copolymerization[137,138]. However, their application is limited by several factors, including poor stability, low drug loading capacity, and lack of spatiotemporal release control, which may result in reduced efficacy, cytotoxicity, or off-target effects[139,140]. Some compounds also exhibit low bioavailability due to poor solubility (*e.g.*, quercetin) or limited membrane permeability (*e.g.*, hydrophilic molecules), further compromising their therapeutic[141,142]. Recently, with the development of nanoscience and nanotechnology, multifunctional nanomaterials have been increasingly employed to design ROS-scavenging agents. Their unique biophysical (*e.g.*, thermodynamics, 2D surface topography, and 3D architecture) and biochemical features (*e.g.*, surface chemical reactivity and enzymatic interaction) contribute to various advantages, including enhanced reaction efficiency, improved stability, and more precise delivery and therapeutic targeting, thereby enabling more effective antioxidant therapies[143]. Accordingly, recent efforts focus on developing nanomaterials with intrinsic ROS-scavenging capabilities, or nanoengineering traditional antioxidants—either by chemical modification into nanostructures or encapsulation within nanoplatforms.

Taken together, ROS-scavenging nanomaterials (NMs) can be broadly divided into two well-established categories according to their specific roles in bone repair scaffolds: I) nanomaterials serving as delivery platforms for traditional ROS scavengers (*e.g.*, polyphenols), which enhance pharmacokinetic properties and achieve targeted, controlled drug delivery[144,145]. II) Nanomaterials themselves function as ROS-quenching sources, directly functioning as antioxidants. Their ROS-quenching ability mainly originates from their unique nanostructures. These materials can be further classified into: enzyme-like NPs (nanozymes), free-radical trapping NPs, and redox-active ROS-scavenging NPs[146–148]. In addition, a growing class of ROS-responsive nanomaterials has emerged. These materials are typically functionalized with ROS-reactive moieties (*e.g.*, thioketal, boronic esters). While primarily designed as targeted carriers, these systems can also scavenge ROS during the response process. This dual function—ROS activation and concurrent redox modulation—distinguishes them mechanistically and warrants separate discussion in this review. In the following sections, we will summarize recent advancements in the application of these ROS-scavenging nanomaterials for bone repair according to this classification.

3.2. Nanoplatforms for antioxidant delivery in bone repair

Nanocarrier-based delivery platforms are widely used to address the limitations of directly incorporating traditional antioxidants into scaffolds (as discussed earlier)[149]. Both small-molecule antioxidants (*e.g.*, vitamins, polyphenols, melanin, NAC) and endogenous antioxidant enzymes or modulators can be encapsulated within these platforms, offering several distinct advantages.

First, nanocarriers can encapsulate antioxidants within their core or on their surface, forming protective barriers that shield against degradation and preserve bioactivity[150–152]. For antioxidants with poor solubility or tendencies to aggregate, such as polyphenols, nanocarriers prevent aggregation or precipitation, thereby enhancing their stability and bioavailability[153–156]. Second, the high surface area-to-volume ratio of nanomaterials and the presence of numerous reactive surface atoms allow for flexible surface modification, enabling responsive release and targeted delivery[157–159]. An example is membrane-decorated nanovehicles, which have gained significant attention recently. A study[160] developed nanocomplexes containing CAT, short stromal-derived factor-1α (sSDF-1α) peptide, and Ckip-1 siRNA, which were then coated with macrophage membranes. The modified nanocomplexes were able to target inflammatory sites, efficiently accumulate at the fractured femur, and release their contents to exert their effects. Third, nanoplatforms facilitate precise controlled, sustained release through tunable degradation profiles and customizable chemical/ionic bonds[161,162]. This release profile aligns with the dynamic process of bone healing, helping reduce systemic toxicity by lowering required doses[163]. Fourth, by encapsulating various functional agents within different nanocarriers, these platforms enable simultaneous, non-interfering incorporation into scaffolds. This also allows the controlled and sequential delivery of multiple factors, providing spatio-temporal control over their release and bioactivity[164–166]. For example, Xue et al.[167] developed a dual-drug delivery nanoplatform with rapamycin encapsulated in mesoporous polydopamine and bilirubin loaded onto an MOF shell. The system enabled sequential release—bilirubin scavenged ROS and inhibited apoptosis, while rapamycin enhanced autophagy—collectively delaying cartilage degeneration in an osteoarthritis model. Fifth, by modifying nanoparticle characteristics such as hydrophilicity, charge, shape, and size, the cellular uptake and internalization of nanoparticles and their carried antioxidants can be altered[168,169]. In addition, these nanoplatforms exhibit good biocompatibility and biodegradability, low immunogenicity and toxicity, further supporting

their application in bone regeneration[170,171]. Next, we will focus on commonly used nanocarriers, discussing their advantages and limitations, along with representative applications in bone repair (as shown in Table 1[172−179]).

3.2.1. *Liposomes*

Liposomes are spherical vesicles composed of phospholipids and cholesterol, structurally resembling natural biological membranes[180]. These nanocarriers feature one or more concentric lipid bilayers enclosing an internal aqueous core, allowing for the simultaneous encapsulation of hydrophilic molecules (*e.g.*, polyphenols, peptides, and proteins) in the aqueous interior and hydrophobic compounds in the lipid bilayers[181]. Moreover, the lipid-based structure closely mimics cell membranes, creating an internal environment similar to that of living cells, which helps to stabilize and protect sensitive biomolecules, while also ensuring excellent biocompatibility, biodegradability, and low immunogenicity[182]. The polar lipid surface can also be functionalized with hydrophilic polymers such as polyethylene glycol (PEGylation) to prolong systemic circulation, or conjugated with targeting ligands, including antibodies or peptides, to enhance tissue-specific delivery[183]. Collectively, these advantages have made liposomes the most common class of US Food and Drug Administration (FDA)-approved nanomedicines[184]. However, they also have some limitations, including poor stability of surface modifications, limited loading capacity, susceptibility to drug leakage, and recognition by the immune system, which shortens their circulation time[185,186].

In BTE, liposomes have been widely used. For example, Sun et al.[187] developed a novel composite hydrogel with liposomes that co-delivered CAT and ROS-responsive oxygen-loaded nanoparticles, effectively protecting them and maintaining their activity. This system enabled long-term ROS scavenging and oxygen supplementation, which helped restore redox balance, thus promoting bone regeneration in a mouse calvarial defect model. Similarly, Yang et al.[172] designed a 3D-printed hydrogel scaffold integrating liposomes to co-deliver hydrophilic glycyrrhizic acid (GA) and hydrophobic epigallocatechin gallate (EGCG), both of which possess anti-inflammatory and antioxidant properties. This system demonstrated effective ROS scavenging and promoted bone regeneration. Another study[188] used melatonin (MT)-loaded liposomes in a hydrogel, enabling stable and prolonged MT release. MT upregulated intracellular antioxidant genes, restored cell function by activating endogenous antioxidant systems, thus improving peri-implant bone formation in an ovariectomized rat model.

3.2.2. *Polymeric nanoparticles*

Polymeric nanoparticles (PNPs) are a collection of structures synthesized from natural (*e.g.*, chitosan) or synthetic (*e.g.*, polylactic acid, polycaprolactone) materials using techniques like emulsification, nanoprecipitation, ionic gelation, and microfluidics[189]. These structures commonly include nanocapsules, nanospheres, polymersomes, and micelles[171]. Among them, poly (lactic-*co*-glycolic acid) (PLGA) and poly(butyl cyanoacrylate) (PBCA) nanoparticles are the most commonly employed[190]. Drugs can be either dispersed within the polymer matrix or adsorbed onto the nanoparticle surface, making PNPs suitable for delivering hydrophobic small molecules and large molecules like siRNA or plasmid DNA[191]. A major advantage of PNPs lies in their strong stability, precise control over drug loading, and tunable release profiles achieved by adjusting polymer composition, molecular weight, and fabrication method. Moreover, their abundant surface functional groups allow facile modifications, including PEGylation, conjugation of targeting ligands, and incorporation of stimuli-responsive linkages (*e.g.*, pH or ROS-responsive bonds), thereby enhancing targeting specificity and therapeutic efficiency[192]. However, issues such as aggregation, potential toxicity, and immunogenicity have constrained their clinical translation, with only a few formulations currently FDA-approved[184].

Several studies have demonstrated the potential of PLGA nanoparticles for antioxidant delivery in bone regeneration. For example, Park et al.[193] developed a polyethylenimine (PEI)-coated PLGA nanoparticle (mPDN) carrying both Nrf2 mRNA and dexamethasone (Dex) to MSCs (Fig. 4A and B). Specifically, Dex was encapsulated in the PLGA core, while mRNA was electrostatically adsorbed onto the PEI shell. Nrf2 protein was produced, upregulating antioxidants and exhibiting dynamic control of mitochondrial fission and fusion, which was important in the proliferation and differentiation of MSCs (Fig. 4C−F). Histological analysis implied Dex encapsulated in PDN played a significant role in bone regeneration, and its side effect was resolved in the early stage by *Nrf2* mRNA (Fig. 4G and H). Another study[194] encapsulated melatonin (MT) into PLGA nanoparticles and incorporated them into a 3D-printed polycaprolactone/β-tricalcium phosphate (PCL/β-TCP) scaffold. This design leverages the sustained-release properties of PLGA to achieve long-term localized MT delivery. In a diabetic bone defect model, the scaffold effectively restored redox balance, improved bone regeneration, and reestablished angiogenesis−osteogenesis coupling.

Micelles are another commonly used subclass of PNPs with unique structures[195]. They spontaneously form through the self-assembly of amphiphilic block copolymers in aqueous environments[196]. Their characteristic core−shell structure, composed of a hydrophobic core and a hydrophilic shell, enables efficient encapsulation of poorly water-soluble drugs and improves the dispersion of these drugs under physiological conditions[197,198]. In addition, their small size, good colloidal stability, and improved tissue penetration further enhance drug delivery capabilities[199,200]. For example, He et al.[201] developed a ROS-scavenging system by loading the hydrophobic drug rapamycin into diselenide-containing nanomicelles, which were then incorporated into an injectable hydrogel. In this design, the micelles easily enter the cells and respond to elevated intracellular ROS levels in senescent BMSCs, enabling ROS reduction and rapamycin release. Meanwhile, the hydrogel matrix helps regulate extracellular ROS through iron ion complexation. This dual-level ROS modulation combined with rapamycin effectively rejuvenated senescent BMSCs and enhanced bone regeneration in aged mice with femoral defects.

3.2.3. *Silica nanoparticles*

Inorganic nanomaterials such as gold, iron oxide, and silica have also attracted wide interest in biomedical applications due to their unique optical, magnetic, and structural properties[171]. Among these, silica nanoparticles (SiNPs) are one of the most commonly used platforms[202]. SiNPs are amorphous, spherical structures with adjustable sizes and silanol-rich (−SiOH) modifiable surfaces. They exhibit excellent biocompatibility and high chemical stability, remaining resistant to heat, organic solvents, and biological fluids[203]. Moreover, their degradation product, soluble silicic acid (H_4SiO_4), is non-toxic, making SiNPs suitable for long-term biomedical applications. Studies suggest this degradation product may further support osteogenic activity *via* Wnt/β-catenin signaling[204]. However, concerns including accumulation in reticuloendothelial organs, slow degradation rates, and long-term

Table 1 Nanocarriers for antioxidant delivery in bone regeneration.

Nanocarrier	Advantage and limitation	Representative example	Therapeutic effect	Ref.
Liposomes	Biomimetic structure, good biocompatibility and biodegradability, suitable for hydrophilic and hydrophobic drugs; but poor stability and limited encapsulation efficiency.	3D-printed hydrogel scaffold incorporating liposomes co-loaded with GA and EGCG	(1) Scavenged ROS; (2) Promoted macrophage M2 polarization and osteogenic gene expression; (3) Accelerated bone regeneration in the rat cranial defect model.	172
Polymeric NPs	Controlled release, payload flexibility, easy surface modification; but potential for aggregation, cytotoxicity, and immunogenicity.	Polydopamine-modified titanium implants coated with electrospun nanofibers containing melatonin-loaded PLGA NPs	(1) Suppressed diabetes-induced ROS overproduction; (2) Promoted osteogenic differentiation *via* BMP-4/WNT pathway; (3) Enhanced bone formation and osteointegration in the T1DM mouse tibial defect model.	173
Micelles	Well-suited for hydrophobic antioxidants, small-sized; but limited loading capacity and poor stability.	Injectable PEGS/γ-PGA hydrogel incorporating rapamycin-loaded poly (diselenide-carbonate) nanomicelles (PSeR)	(1) Eliminated extracellular and intracellular ROS in senescent BMSCs; (2) Rejuvenated stem cell function and promoted BMP/Smad-mediated osteogenesis; (3) Enhanced bone regeneration in aged mouse femoral defect model.	174
Mesoporous silica NPs	High drug load due to mesoporous structure, controlled release *via* pore size tuning, chemically stable; but poorly biodegradable.	Injectable chitosan-based hydrogel incorporating puerarin-loaded mesoporous silica NPs (CH@PUE&MSN)	(1) Eliminated local ROS and inhibited M1 polarization; (2) Promoted M2 polarization and suppressed osteoclast formation; (3) Accelerated bone regeneration and matrix remodeling in rat femoral defect model.	175
Hydroxyapatite (HA) NPs	Bone-mimetic, osteoconductive, and highly biocompatible; but limited mechanical strength and difficult-to-control degradation rate.	Biomimetic Se-nHA/PC composite microspheres	(1) Effectively scavenged ROS and induced M2 polarization; (2) Promoted osteogenic differentiation of human periodontal ligament stem cells (hPDLSCs); (3) Reduced alveolar bone loss and accelerated bone regeneration in the rat periodontitis model.	176
Bioactive glass NPs	High bioactivity, osteoconductive, tunable ion release, good drug loading (MBG); but rapid degradation rate and limited mechanical strength.	3D-printed scaffold incorporating selenium-doped mesoporous bioactive glass (Se-MBG)	(1) Scavenged intracellular ROS and enhanced glutathione peroxidase expression; (2) Promoted M2 polarization and mitochondrial metabolism; (3) Enhanced bone regeneration in the rat critical-sized calvarial defect model.	177

Table 1 (*continued*)

Nanocarrier	Advantage and limitation	Representative example	Therapeutic effect	Ref.
Carbon dots	Excellent biocompatibility, optical properties, diverse surface functional groups, and multifunctionality; but low quantum yield and complex synthesis.	Red fluorescent carbonized polymer dots derived from *N*-acetyl-L-cysteine (NAC-CPDs)	(1) Scavenged ROS *via* Keap1−Nrf2 pathway and inhibited NF-κB-mediated inflammation; (2) Promoted osteogenic differentiation in hPDLCs under oxidative stress; (3) Reduced alveolar bone loss in ligature-induced periodontitis mouse model.	178
High-dimensional nanostructures	Enhanced structural support and multifunctionality; enables surface immobilization of antioxidants; but complex synthesis, potential loss of antioxidant activity, and limited cellular uptake or targeting efficiency.	EGCG-coated extracellular matrix-mimicking nanofibers incorporated into stem cell spheroids	(1) Scavenged intracellular ROS and upregulated antioxidant genes; (2) Promoted osteogenic differentiation and cell viability under oxidative stress; (3) Enhanced calvarial bone regeneration in the mouse defect model.	179

ROS, reactive oxygen species; NPs, nanoparticles; EGCG, (−)-epigallocatechin-3-*O*-gallate; GA, glycolic acid; PLGA, poly (lactic-*co*-glycolic acid); PEGS, poly(ethylene glycol) succinate; γ-PGA, poly(γ-glutamic acid); BMSC(s), bone marrow mesenchymal stem cell(s); M1, classically activated macrophage (pro-inflammatory); M2, alternatively activated macrophage (pro-repair); T1DM, type 1 diabetes mellitus.

biosafety remain barriers to clinical translation[205,206]. Li et al.[207] developed a porous selenium (Se)-doped silica nanocomposite ($Se@SiO_2$), where the porous SiO_2 structure not only provided a biocompatible framework but also enabled controlled, sustained selenium release, effectively avoiding the toxicity associated with high local Se concentrations while preserving therapeutic benefits. In a rat femoral fracture model, $Se@SiO_2$ significantly accelerated bone healing.

Mesoporous silica nanoparticles (MSNs) are a structurally advanced subclass of SiNPs that have found broader applications compared to their conventional counterparts[208]. Their uniqueness lies in the highly ordered and tunable pore structure (typically 2−10 nm) and exceptionally high surface area (up to 500−1000 m^2/g), which provides abundant adsorption sites for drugs[209,210]. These features result in significantly higher loading capacities compared to liposomes or PNPs. In addition, the MSN surface possesses more reactive silanol (−SiOH) groups, facilitating surface functionalization[211]. However, MSN synthesis is more complex—requiring templating agents and tight reaction control—and their porous structure compromises mechanical strength compared to dense SiNPs[212]. Thus, conventional SiNPs remain advantageous for simpler delivery tasks, while MSNs offer a superior platform for bone regeneration applications that require higher drug loading and better protection of drug bioactivity.

For example, He et al.[175] developed an injectable hydrogel by integrating MSNs, puerarin (PUE), and chitosan (CH) through *in situ* self-assembly. MSNs served as nanocarriers to enhance the drug loading, solubility, stability, and sustained release of PUE—a polyphenolic compound with intrinsic antioxidant and anti-inflammatory properties. In a rat femoral defect model, this system reduced local oxidative stress and significantly promoted new bone formation. Similarly, Wang et al.[213] developed a core−shell codelivery system. In this design, the antioxidant and anti-inflammatory compound emodin was first encapsulated into MSNs, enabling stable drug loading and protection. The MSNs were then thiolated and conjugated with growth differentiation factor (GDF). Under oxidative stress, emodin was released to neutralize ROS and suppress inflammation, followed by controlled GDF release to stimulate fibrocartilage regeneration. This system effectively supported cell survival and scaffold integration *in vitro* and *in vivo*.

3.2.4. *Nanoscale hydroxyapatite particles*

Hydroxyapatite (HA), with the formula $Ca_{10}(PO_4)_6(OH)_2$, is the main inorganic component of human bone and teeth. Among its various forms, nanoscale hydroxyapatite particles (nHA, 1−100 nm) closely mimicking the composition and crystalline structure of native bone mineral[214]. This biomimicry provides exceptional osteocompatibility, minimizing immune responses upon implantation. Moreover, nHA is biodegradable *in vivo*, gradually dissolving or being resorbed by osteoclasts into calcium and phosphate ions that can be reutilized during bone remodeling. It also promotes osteoblast adhesion, proliferation, and differentiation, serving as a bioactive scaffold that supports new bone formation and guides cellular orientation[215]. nHA can also load drugs *via* surface adsorption, or in some cases, small molecules may be doped into its crystal lattice or confined within porous structures. These properties allow nHA to function as both a carrier and a structural matrix in bone regeneration strategies. However, some limitations remain. nHA typically degrades slowly, may not match desired release kinetics. To address this, doping with other elements is often employed to modulate degradation and release behavior[216]. Furthermore, its drug-loading capacity, especially for hydrophobic agents, is limited. And

surface functionalization can be technically challenging, potentially compromising crystallinity. Despite these challenges, the biomimetic composition and multifunctionality of nHA make it a promising platform for simple, basic drug delivery in bone repair.

For example, a study[176] developed a composite microsphere system by embedding Se-doped nHA and proanthocyanidins (PC) into a biopolymer matrix. Both Se and PC contributed to effective ROS scavenging, alleviating oxidative stress and inflammation. In synergy with nHA's excellent osteocompatibility and osteoinductivity, the microspheres enhanced the osteogenic differentiation of periodontal ligament stem cells *in vitro* and significantly reduced alveolar bone resorption in a rat periodontitis model. Porous carbonated hydroxyapatite (CHAp), a modified form of nHA with incorporated carbonate ions and a porous architecture, offers enhanced biomimicry, surface area, and drug-loading capacity compared to conventional nHA[217]. Li et al.[218] utilized CHAp microspheres to co-load resveratrol and dexamethasone and embedded them into a hydrogel matrix. The CHAp microspheres were capable of penetrating the microvoids and irregular regions of osteoporotic bone, enabling the sustained release of hydrophobic drugs. *In vitro* and *in vivo* studies demonstrated its effectiveness in ROS clearance, immune modulation, and osteoinduction.

3.2.5. *Bioactive glass nanoparticles*

Another type of inorganic material is bioactive glass (BAG), typically composed of silica (SiO_2), calcium oxide (CaO), sodium oxide (Na_2O), and phosphorus pentoxide (P_2O_5)[219]. Upon degradation, BAG releases Ca^{2+}, PO_4^{3-}, and H_4SiO_4, promoting osteogenesis and modulating immune responses[220]. When fabricated into nanoscale particles (20−200 nm), nano bioactive glass (NBG) combines the bioactivity of BAG with the delivery advantages of nanocarriers. However, as a drug carrier, NBG only adsorbs antioxidants onto its surface, which limits the overall drug-loading capacity, release control, and surface modifiability. An improved variant, mesoporous bioactive glass (MBG), features well-defined pores and a large surface area (200−500 m^2/g), significantly improving drug adsorption and delivery efficiency[221]. For example, Chen et al.[177] developed a Se-doped MBG scaffold that leveraged MBG's high surface area and pore volume for efficient Se loading and sustained release. The released Se scavenged ROS in macrophages, promoting M2 polarization and enhancing osteogenesis. Meanwhile, MBG itself also provided osteoconductive cues to further support osteogenesis. In a rat calvarial defect model, Se-MBG significantly enhanced bone regeneration. Similarly, Yao et al.[222] developed an L-arginine−modified MBG (MBG@L-Arg), which utilized MBG's porous structure for efficient loading. The grafted L-Arg neutralized excess ROS and released NO in the inflammatory microenvironment. Both *in vitro* and *in vivo*, MBG@L-Arg effectively reduced inflammation-induced damage and promoted periodontal bone regeneration.

3.2.6. *Carbon dots*

Carbon dots (CDs) are a class of fluorescent, carbon-based nanomaterials typically smaller than 10 nm, consisting of a sp^2/sp^3 carbon core and various surface functional groups (*e.g.*, −COOH, $-NH_2$)[223]. While sharing this basic structure, CDs can be synthesized from different carbon-rich precursors, such as citric acid, glucose, or biomass, resulting in diverse surface functional groups and biological properties (*e.g.*, osteoinductive activity)[224]. CDs may possess antioxidant properties, which could stem from their surface reductive groups, or external antioxidants loaded onto CDs *via* surface adsorption or covalent bonding[225]. Owing to their ultrasmall size, CDs are efficiently cleared by the kidneys, reducing long-term organ accumulation. They also exhibit excellent water solubility, low toxicity, and good biocompatibility[226]. Additionally, their stable fluorescence allows for real-time drug delivery tracking and bioimaging[227,228]. However, due to their small size and limited surface area, CDs generally exhibit low antioxidant-loading capacity[229].

Currently, CDs have been extensively studied for bioimaging, diagnostics, monitoring, and sensing[230]. However, their use in bone regeneration, particularly in scaffold-integrated CD systems, remains limited, likely due to poor drug delivery performance and challenges in scaffold integration. Most bone-related studies rely on local injection or simple hydrogel encapsulation for treating small bone defects that do not require mechanical strength[231]. For example, Liu et al.[178] developed *N*-acetylcysteine-derived carbonized polymer dots (NAC-CPDs), which combine strong ROS-scavenging capacity with intrinsic red fluorescence for bioimaging. In a periodontitis mouse model, NAC-CPDs preferentially accumulated in alveolar bone, regulated redox homeostasis and inflammation, supported bone regeneration, and enabled fluorescence tracking, demonstrating their dual function in therapy and imaging. Similarly, Xin et al.[232] synthesized MT-derived carbon dots (MT-CDs). Compared to free MT, MT-CDs exhibited improved water solubility and bioavailability, enabling more effective antioxidant and anti-inflammatory properties. In a periodontitis mouse model, MT-CDs reduced alveolar bone loss and inflammation.

3.2.7. *High-dimensional nanostructures*

In addition to nanoparticles, one-dimensional (*e.g.*, nanorods, nanotubes, nanofibers) and two-dimensional (*e.g.*, nanosheets) nanostructures composed of the aforementioned materials can also serve as effective platforms for integrating antioxidants. Rather than being encapsulated in the core, antioxidants are often immobilized on the surface or chemically coordinated within the nanostructure network. While this may provide less protective shielding, it still enables controlled release, sustained bioactivity, and functional synergy. Incorporating such nanostructures can enhance the mechanical strength, stiffness, and multifunctionality of scaffolds[233]. In addition, three-dimensional nanostructures, including metal−organic frameworks (MOFs) and covalent organic frameworks (COFs), offer more complex structures and properties (as will be discussed later), and also show promise as antioxidant nanocarriers. Notably, incorporating specific metal ions, such as zinc ions in ZIF-8, has been found to regulate osteogenesis[234,235].

Several studies have validated the potential of these nanostructures in antioxidant bone scaffolds. Byun et al.[179] developed mineral nanofibers coated with EGCG, mimicking the extracellular matrix. These nanofibers were then combined with human adipose-derived stem cells (hADSCs) to form stem cell spheroids. In this design, the EGCG-coated nanofibers enhanced both the antioxidant capacity and osteogenic differentiation of the hADSCs, significantly promoting calvarial bone regeneration. Additionally, Wang et al.[173] designed MT-loaded PLGA nanofibers, which were coated onto polydopamine-modified titanium surfaces, forming a durable nanofiber layer. This layer provided sustained MT release, a structural matrix for osteointegration, and supported cell adhesion and proliferation. In a diabetic mouse tibial defect model, this system inhibited excessive ROS production and significantly enhanced bone regeneration and osteointegration. Another study[236] employed electrospinning technology to fabricate a NAC-loaded biomimetic mineralized hydroxyapatite/

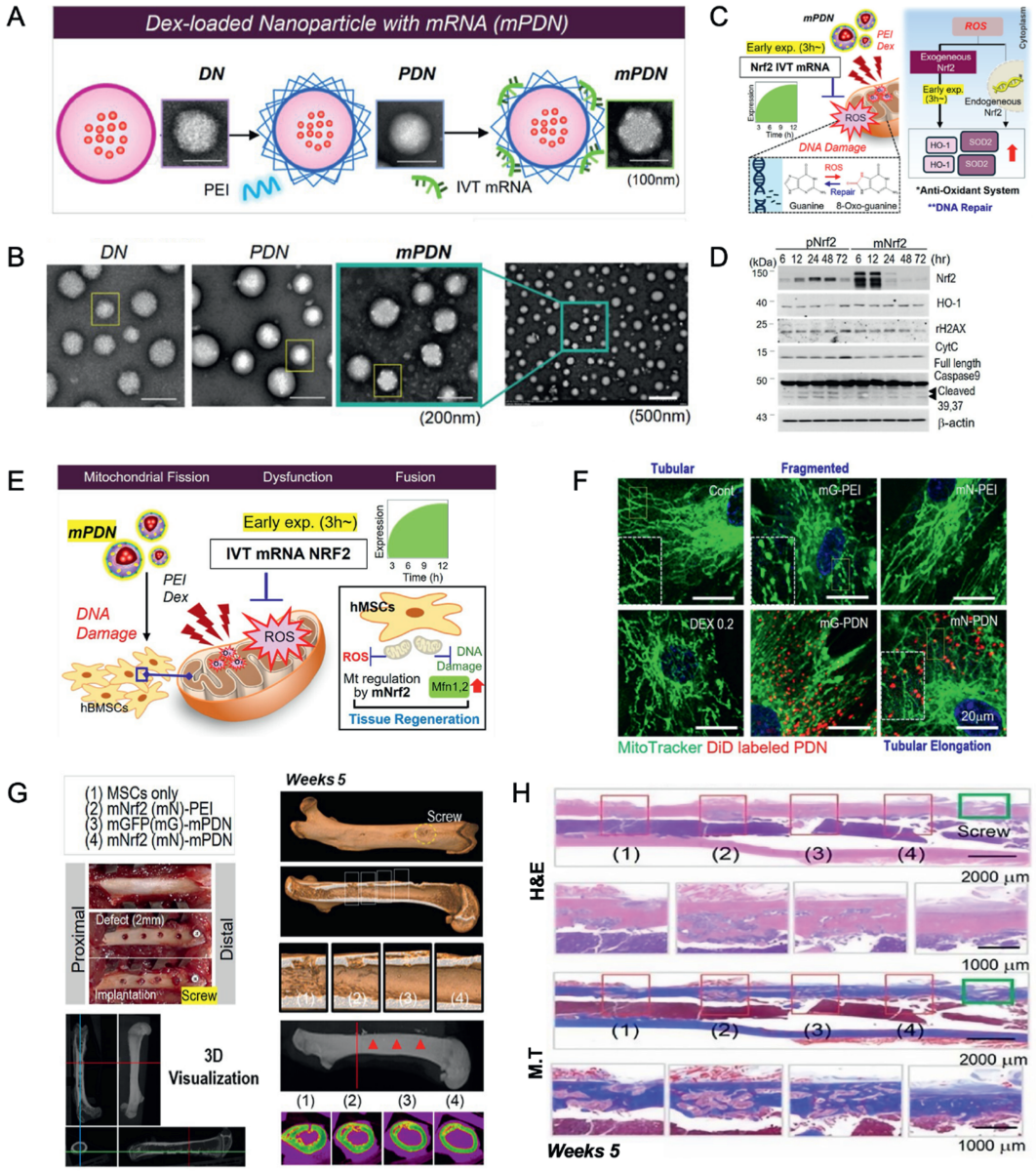


Figure 4 Nanoparticles (NPs)-based codelivery of nuclear factor erythroid 2-related factor 2 (*Nrf2*)-mRNA and dexamethasone (Dex) for bone regeneration. (A) Schematic preparation of polyethylenimine (PEI)-coated poly(lactic-*co*-glycolic acid) (PLGA) NPs loading Dex and mRNA. (B) Scanning electron microscopy images of the NPs. (C) pDNA(pG, pN)-PDN *via* the nucleus to express the target protein in the cytoplasm after 12 h, and mRNA (mG, mN)-PDN does not have to localize to the nucleus and expresses the target protein 3 h after cytoplasmic absorption. (D) Comparative protein expression analysis of antioxidant in human mesenchymal stem cells (hMSCs) treated with pNrf2 and mNrf2-PDNs. (E) Schematic diagram of mitochondrial dysfunction induced by PEI and Dex and increased mitochondrial fusion *via* early Nrf2 expression. (F) Confocal microscopy confirmation of mitochondrial morphological changes following treatment with DiD-labeled PDNs. (G) Evaluation of changes in 3D micro-CT images in a rat femur defect model after treatment with (1) control hMSCs, (2) mN-PEI-engineered hMSCs, (3) mG-PDN-treated hMSCs, and (4) mN-PDN-treated hMSCs. (H) Histological assessment *via* H&E and Masson's trichrome staining showing collagen deposition and new bone formation at 5 weeks post-treatment. Reprinted with permission from Ref. 194. Copyright © 2024, American Chemical Society.

silk fibroin nanofibrous scaffold that could sustainably release high concentrations of NAC, thereby significantly scavenging ROS, promoting the osteogenic differentiation of iPSC-derived MSCs, and bone regeneration.

In conclusion, we have discussed several commonly used nanocarriers for delivering antioxidants in bone regeneration, outlining their advantages, limitations, and representative applications. Selecting suitable antioxidant-nanocarrier combinations requires a comprehensive consideration of their physicochemical properties, antioxidant mechanisms, and target application, while balancing factors such as loading efficiency, release kinetics, biocompatibility, and the preservation of antioxidant activity. Future research should focus on developing novel combinations, exploring synergistic effects with other bioactive

molecules, and, most importantly, evaluating their long-term safety and efficacy in preclinical and clinical settings.

In the following section, we turn to a distinct class of nanomaterials that scavenge ROS through their intrinsic activity, functioning without the need for externally loaded antioxidant agents. This transition reflects a conceptual shift from nanocarriers as passive delivery vehicles to therapeutic nanomaterials that actively neutralize oxidative stress.

3.3. Nanomaterials as direct ROS scavengers

Intrinsic ROS-scavenging nanomaterials can be classified into nanozymes, free radical trappers, and redox-active scavengers (as shown in Table 2[54,237−244]). Nanozymes mimic the catalytic mechanisms of natural enzymes, eliminating ROS through repetitive catalytic cycles. Free radical trappers, on the other hand, bind to and stabilize ROS, rendering them inactive. Redox-active scavengers, in contrast, convert ROS into stable substances through redox reactions. While this classification is based on the predominant ROS-scavenging mechanism, it is worth noting that each type of nanomaterial may utilize multiple antioxidant pathways.

3.3.1. Nanozymes

SOD, CAT, and GPx are key antioxidant enzymes that work together to effectively maintain cellular redox balance. SOD consists of dimers or tetramers of β-barrel subunits, each containing one or two metal ions in the active center. Based on the metal cofactor, SOD is classified into Cu/Zn-SOD, Mn-SOD, and Fe-SOD. The metal ions help maintain the catalytic conformation through coordination with surrounding amino acid residues and drive the cyclic dismutation of O_2^- to O_2 and H_2O_2 *via* valence changes (*e.g.*, Cu^{2+}/Cu^{+}, Mn^{3+}/Mn^{2+})[245]. CAT is a tetrameric heme enzyme, with each subunit containing a high-spin Fe^{3+}-heme. In the active center, Fe^{3+} reacts with H_2O_2, oxidizing to Fe^{4+} and forming a peroxide intermediate. Subsequently, Fe^{4+} decomposes H_2O_2 into water and oxygen, while being reduced back to Fe^{3+}, thus completing the catalytic cycle[246]. GPx is a selenium-containing tetramer with a selenocysteine (Sec) residue in the active site. It reduces H_2O_2 and other peroxides to corresponding alcohols or water using glutathione (GSH) as an electron donor[247]. From these, it can be seen that metals (such as Mn, Cu, Fe) or the metalloid selenium help facilitate the most efficient electron transfer pathways, playing a crucial role in enzyme-catalyzed ROS removal reactions.

However, the direct clinical use of these enzymes faces challenges like high preparation costs, poor stability, and easy inactivation. Recently, metal ions, metal oxides, and some carbon-based materials have been found to mimic enzymatic redox activity[248]. Furthermore, when prepared at the nanoscale, these materials—termed nanozymes—exhibit enhanced catalytic efficiency due to their high surface area, active sites, and quantum effects[249]. Compared to natural enzymes, nanozymes also offer better stability, tunable activity, and easier large-scale production[250]. In bone repair, redox-active nanozymes are promising. They can be integrated into scaffolds through physical adsorption, covalent coupling, or carrier loading. Certain metal-based nanozymes, especially those forming metal-organic frameworks (MOFs), can further enhance catalytic performance and reaction selectivity[240,251−253]. Beyond antioxidation, metal nanoparticles also improve scaffold mechanics, promote mineralization, and exhibit intrinsic osteoinductive activity[237]. In summary, scaffolds with redox nanozymes offer a promising new approach for treating bone defects.

3.3.1.1. CeO_2 nanoparticles. Among various nanozymes, cerium oxide nanoparticles (CeO_2 NPs) are extensively used in bone repair due to their unique crystal structure and reversible redox behavior[254−256]. CeO_2 has a fluorite-type face-centered cubic structure, with each cerium ion surrounded by 8 oxygen ions[257]. Under certain external conditions (*e.g.*, high temperature, reducing atmosphere, etc.), oxygen ions on the lattice surface may escape, forming oxygen vacancies and reducing Ce^{4+} to Ce^{3+} to maintain electroneutrality, resulting in a non-stoichiometric material (CeO_2-δ, where δ represents the number of oxygen vacancies)[258−260]. This coexistence of Ce^{3+} and Ce^{4+} endows CeO_2 to mimic the catalytic activities of both SOD and CAT[261]. Specifically, Ce^{3+} possesses an unpaired 4f1 electron, exhibiting strong reducibility and readily losing electrons to be oxidized; while Ce^{4+} (with no electrons in the 4f orbital) is relatively stable but can act as an oxidant, accepting electrons under reducing conditions to convert to Ce^{3+}. The Ce^{3+} on the surface of CeO_2 NPs can reduce superoxide anion radicals to O_2 and H_2O_2, mimicking SOD activity; the generated or pre-existing Ce^{4+} can further react with H_2O_2, reducing to Ce^{3+} and producing O_2 and H_2O, similar to the catalytic process of CAT[262,263]. However, the CAT-like activity of CeO_2 NPs is relatively lower than their SOD-like activity due to the slower reduction of Ce^{4+} and limited catalytic sites[264,265]. Furthermore, the electron transfer between Ce ions and oxygen vacancies, coupled with the dynamic creation and annihilation of these vacancies, greatly promotes Ce valence shifts[266,267]. In other words, oxygen vacancies increase the reactivity of CeO_2. The higher the oxygen vacancy density, the faster Ce^{3+}/Ce^{4+} cycling and the greater catalytic efficiency. More oxygen vacancies can be introduced through surface modification or by reducing particle size[268,269]. Nanostructured CeO_2 exhibits higher vacancy densities due to its large surface area, high surface energy, and unsaturated surface coordination, all of which promote oxygen loss and vacancy formation[270,271]. Additionally, due to the size effect, the Ce^{3+} content on the surface of nanoparticles is significantly higher than that of the bulk, indicating more active sites involved in the catalytic process[272−274]. In summary, the reversible redox cycling between Ce^{3+}/Ce^{4+} in CeO_2 NPs, facilitated by oxygen vacancies and nanostructure, is the key to their excellent enzyme-mimetic activity and ROS scavenging performance. Besides their antioxidant activity, CeO_2 NPs can directly upregulate osteogenic gene expression, enhance ALP activity and mineral deposition, and modulate immunity, improve mechanical properties, all of which enhance their potential in bone repair applications[255].

Several studies have demonstrated the applications of CeO_2 NPs in BTE. Zhang et al.[237] integrated cerium oxide nanoparticles (CeO2 NPs) into bioactive glass (BG) to fabricate three-dimensional(3D)-printed scaffolds (Fig. 5A and B). In the early stage, the incorporated CeO2 NPs exhibited SOD and CAT-mimicking activities, alleviating oxidative stress at bone defect sites. Later, they further enhanced osteoblast differentiation, promoting mineral deposition and ALP activity. They also improved the mechanical properties of the scaffolds. In a rat tibial defect model, CeO_2−BG scaffolds demonstrated superior osteogenic performance (Fig. 5C−G). Similarly, Ren et al.[275] developed PCL/gelatin fibrous membranes loaded with CeO_2 NPs. These membranes exhibited enhanced mechanical properties and provided sustained release of CeO_2 NPs. The released CeO_2 NPs demonstrated antioxidant activity, restored redox balance, and promoted

Table 2 Summary of intrinsically ROS-scavenging nanomaterials for bone regeneration.

Nanomaterial		ROS-scavenging mechanism	Representative example	Therapeutic effect	Ref.
Nanozyme	CeO_2 NPs	(1) Dual enzyme-mimetic activity (SOD and CAT-like) due to reversible Ce^{3+}/Ce^{4+} redox transitions; (2) High density of oxygen vacancies enhances catalytic efficiency and ROS scavenging capacity; (3) Nanostructure and surface defects increase active sites, improving ROS clearance.	CeO_2 NPs incorporated into 3D-printed bioactive glass scaffolds (CeO_2-BG scaffolds)	(1) Alleviated oxidative stress around bone defects *in vitro* and *in vivo*; (2) Promoted proliferation and osteogenic differentiation; (3) Enhanced mechanical strength and bone regeneration in the rat tibial defect model.	237
	MnO_2 NPs	(1) Inherent SOD and CAT-like activities; (2) Releases oxygen in the bone injury microenvironment; (3) Biodegradable and releases Mn^{2+} ions that stimulate osteoblast function and inhibit osteoclast activity.	Hollow MnO_2 NPs (hMNPs) in GelMA composite hydrogels	(1) Eliminated intracellular ROS and promoted cell growth by releasing oxygen; (2) Enhanced osteogenic differentiation of BMSCs; (3) Facilitated bone regeneration in the rat calvarial defect model.	54
	Multi-metal nanozymes	(1) Exhibits multiple enzyme-like activities (SOD, CAT, GPx); (2) Synergistic effect between metal components increases electron density, facilitating redox reactions.	Ru−Cu/EDHJ (electron-donable heterojunction with synergetic Ru−Cu pair sites)	(1) Cleared ROS in stem cells, protecting against oxidative damage; (2) Promoted osteogenic differentiation of hMSCs; (3) Enhanced mandible defect repair in mice with excellent biocompatibility and anti-inflammatory properties. (4) Exhibited pH-responsive catalytic behavior (ROS scavenging in neutral media, ROS generation in acidic media to enable antibacterial effects).	238
	SeNPs	(1) Convert to selenocysteine (Sec_2) *in vivo*, which activates Keap1−Nrf2 pathways and stabilizes GPx active sites; (2) Intrinsic POD-like activity through redox cycling between Se(0) and Se(+4).	Ultrasound-controlled SeNPs-loaded hydrogel (O_2-PSSG)	(1) Reduced ROS and maintained homeostasis in BMSCs; (2) Promoted osteogenic differentiation through Wnt/β-catenin activation;	239

(*continued on next page*)

Table 2 (*continued*)

Nanomaterial		ROS-scavenging mechanism	Representative example	Therapeutic effect	Ref.
		(3) Enhance osteogenic differentiation, angiogenesis, and bone matrix mineralization.		(3) Enhanced bone regeneration and cranial bone repair in rat models.	
	MOFs	(1) Catalytic active sites within the framework mimic SOD and CAT activities, scavenging ROS; (2) Tunable pore size and surface chemistry enhance selective catalytic processes; (3) Synergistic effects from metal ions (*e.g.*, Zn, Co) for enhanced ROS scavenging and biological function.	Zn/Co-MOF functionalized β-TCP scaffolds (MOF-TCP)	(1) Enhanced ROS scavenging in osteochondral defects; (2) Improved osteogenic and chondrogenic differentiation of rBMSCs and chondrocytes; (3) Inhibited inflammatory responses and promoted osteochondral regeneration in rabbit models.	240
Free radical trappers	C_{60} and its derivatives	(1) Strong $\pi-\pi$ interactions and electron affinity enable capture and stabilization of ROS; (2) Conjugated π−electron system facilitates electron transfer, neutralizing captured ROS; (3) Fullerenol derivatives enhance water solubility and biocompatibility, expanding biological applications.	Fullerol-hydrogel microfluidic spheres (FMSs)	(1) Efficiently quenched both intracellular and extracellular ROS, protecting stem cells from oxidative stress; (2) Promoted osteogenic differentiation of BMSCs *via* FoxO1 signaling activation; (3) Enhanced bone healing in rat calvarial defects by improving stem cell survival and osteogenesis.	241
Redox-active NPs	PDA NPs	(1) Catechol groups can reactions with ROS, and forming stable quinone structures to neutralize additional radicals; (2) $\pi-\pi$ stacking and cation$-\pi$ interactions facilitate ultrafast electron transfer and redox cycling; (3) Chelates free metal ions (Fe^{2+}, Cu^{2+}) to inhibit Fenton reactions; (4) Improves mitochondrial function and reduces mitochondrial ROS production	PDA@Au-HA nanocomposite	(1) Eliminated ROS and promoted osteoblast function; (2) Promoted M2 macrophage polarization and osteogenesis-related cytokines secretion; (3) Enhanced bone regeneration and vascularization in bone defect models.	242
	MPNs	(1) Synergistic antioxidant activity from polyphenols and metal ions;	PMPNs-modified extracellular matrix (ECM) and hydroxyapatite nanowires (nHAW) scaffold	(1) Scavenged ROS and enhanced angiogenesis and osteogenesis;	243

	(2) Metal ions (*e.g.*, Sr) act as nanozymes and functional ions, enhancing ROS scavenging and osteogenic effects; (3) MPNs form stable, flexible coatings on scaffolds, improving their functionalities.	(PMPNs@ECM/nHAW)	(2) Promoted stem cell osteogenic differentiation *via* ROS-dependent signaling; (3) Improved bone healing and vascularization in rat calvarial defects.	
H_2	(1) Donates electrons to directly scavenge ROS, especially ·OH and ONOO−; (2) Enhances endogenous antioxidant defense systems; (3) Acts as a mild antioxidant without interfering with essential ROS.	H_2-releasing RA-MC/nSi scaffold	(1) Regulated redox homeostasis and reduced inflammation in bone defect models; (2) Enhanced bone regeneration in mouse calvarial defect model with H_2 gas release.	244

NPs, nanoparticles; ROS, reactive oxygen species; BMSC(s), bone marrow mesenchymal stem cell(s); M1, classically activated macrophage (pro-inflammatory); M2, alternatively activated macrophage (pro-repair); MOFs, metal-organic frameworks; PDA, polydopamine; MPNs, metal-phenolic networks; SOD, superoxide dismutase; CAT, catalase; GPx, glutathione peroxidase; POD, peroxidase; hMSCs, human mesenchymal stem cells; RA-MC, radially aligned mineralized collagen fibers.

the osteogenic differentiation of human periodontal ligament stem cells (hPDLSCs). When implanted into rat cranial defect models, these membranes significantly accelerated new bone formation. However, one of the challenges faced by CeO_2 NPs in practical applications is the poor stability of Ce^{3+} in biological fluids, particularly in phosphate-containing environments[276]. Phosphate ions easily coordinate with Ce^{3+} to form Ce-phosphate complexes, which reduces the free Ce^{3+} concentration and blocks its active sites[277]. To overcome this challenge, Shao et al.[265] utilized titanium oxide nanotube arrays (TiNTA) as a support material to composite with CeO_2 NPs. The CeO_2 NPs are stabilized through electronic interactions with the TiNTA surface, forming a Ce-Ti mixed oxide interface that prevents phosphate ions from directly binding to Ce^{3+}. Additionally, TiNTA can also adsorb phosphate ions. These factors enable CeO_2 to maintain enzyme-mimetic activity in PBS for an extended period, effectively protecting pre-osteoblasts from ROS inhibition and improving osteoporosis in rats.

3.3.1.2. Nanozymes derived from transition metals and their oxides. Transition metals and their oxides are also widely employed as nanozymes. While exhibiting diverse catalytic mechanisms, they share common characteristics: their catalytic processes involve direct adsorption-activation and redox reactions, generally following Michaelis-Menten kinetics[278,279]. Furthermore, their ROS scavenging mechanisms mainly involve valence state shifts, unsaturated coordination sites, and surface charges[280]. Given the diversity of metal nanozymes, detailed catalytic processes and mechanisms will not be elaborated here.

3.3.1.2.1. Single-metal nanozymes. Among single-metal nanozymes, MnO_2 NPs stand out due to their low cost, abundant availability, strong acid tolerance, and dual antioxidant-osteogenic properties. With intrinsic SOD- and CAT-like activities, they scavenge ROS and release oxygen at injury sites, reducing oxidative damage[281]. MnO_2 is also biocompatible and biodegradable, gradually degrading *in vivo* and releasing Mn^{2+} ions. These released Mn^{2+} ions exert immunostimulatory effects, enhance osteoblast adhesion, viability, and function, while also inhibiting osteoclast activity[282−284]. In a study, Li et al.[54] developed a hydrogel that incorporated hollow MnO_2 NPs loaded with bone morphogenetic protein-2 (BMP-2). This composite material enabled H_2O_2 scavenging, oxygen release, and sustained BMP-2 delivery, which collectively enhanced bone regeneration in a rat critical-sized calvarial defect model. Similarly, Yang et al.[285] designed a 3D-printed scaffold made of poly-L-lactide (PLLA) and MnO_2 NPs. This scaffold effectively scavenged ROS, promoted M2 polarization, and upregulated the TGF-β/Smad signaling pathway in human BMSCs, leading to enhanced bone regeneration in refractory bone defects.

In addition to MnO_2 NPs, iron-derived nanozymes, such as Prussian blue NPs (PBNPs), also show promise in bone defect repair due to their POD- and CAT-mimetic properties[286]. Chen et al.[287] demonstrated this potential by guiding various types of cells to self-organize into multicellular spheroids (MCSs), which were then hybridized with PBNPs to form Prussian blue nanohybridized multicellular spheroids (PBNPs@MCSs). The resulting material exhibited potent antioxidant properties, effectively reducing cell apoptosis under oxidative stress and promoting bone repair both *in vitro* and *in vivo*. Additionally, their photoacoustic properties enabled real-time monitoring of the healing process after transplantation.

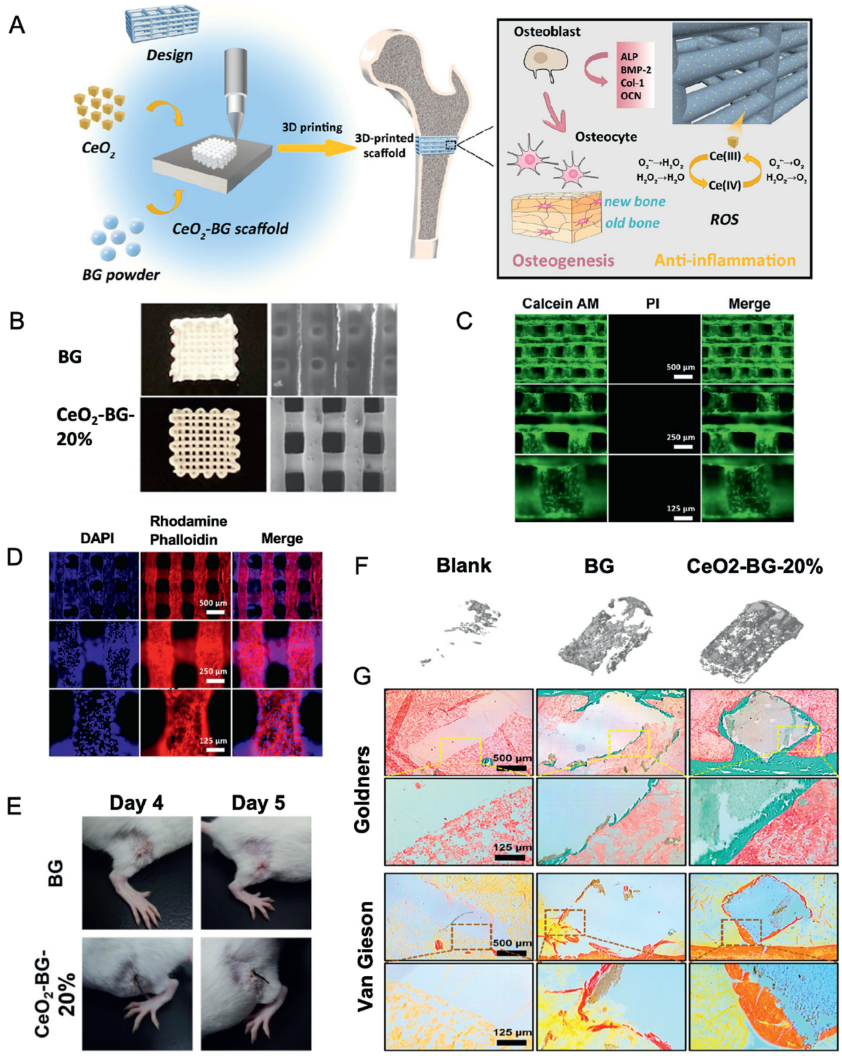


Figure 5 Cerium oxide-reinforced 3D-printed bioactive glass scaffolds (CeO_2−BG scaffold) for Bone Regeneration. (A) Schematic illustration of the preparation of 3D-printed CeO_2−BG scaffold. (B) Digital photographs of CeO_2−BG 3D-printed scaffolds with different concentrations of incorporated CeO_2 NPs. (C) Live/dead staining images and (D) Cytoskeleton staining images of the adhered osteoblasts cultured on CeO_2−BG-20% scaffolds for 3 days. (E) Photographs of the inflammatory condition of the wounds after implantation in rat tibial defects with different scaffolds. (F) Micro-CT images of rat tibial bone defects implanted with different scaffolds after 12 weeks of implantation. (G) Goldner's staining and van Gieson staining of hard tissue sections of tibial bone defects. Reprinted with permission from Ref. 238. Copyright © 2023, American Chemical Society.

Ruthenium (Ru), a member of the platinum group elements, has low electronegativity and a unique metallic electronic structure. Compared to Fe, it possesses more d-electrons, unoccupied orbitals, and superior redox stability, which enhance its catalytic activities[288]. Leveraging these advantages, Lin et al.[289] developed a multienzymatic hydrogel scaffold (MEBTHS) incorporating Ru nanozymes in both Ru^0 and Ru^{4+} oxidation states. The Ru^0 component effectively eliminates NO, while the Ru^{4+} moiety scavenges ROS. When applied to a diabetic mandibular defect model, MEBTHS promoted macrophage repolarization, stimulated osteogenesis and angiogenesis, and ultimately restored the physiological bone remodeling process. Similarly, Wang et al.[290] designed a Ru-doped layered double hydroxide (Ru-hydroxide) artificial antioxidase, which effectively regulates redox homeostasis and promotes maxillofacial bone regeneration.

Molybdenum (Mo) ions can also exhibit enzyme-mimicking activity by converting between Mo^{5+} and Mo^{6+} oxidation states. Leveraging this property, Liao et al.[291] developed an injectable nanohydrogel containing molybdenum-based polyoxometalate (POM) nanoclusters. These nanoclusters scavenged ROS and activated the PI3K/Akt signaling pathway, leading to the upregulation of BMP2 and RUNX2. This, in turn, promoted osteoblast differentiation, enhancing osteogenesis in a diabetic femoral defect model.

Beyond nanoparticles, nanostructure design also influences catalytic performance. For example, Wang et al.[292] developed ultrathin tungsten oxide (WOx) nanoribbons with a 2D sheet-like morphology, which enhances electron conductivity and accelerates electron transfer. Moreover, their one-dimensional extensibility and specific crystal orientation promote the formation of high-density oxygen vacancies on the surfaces and edges, boosting ROS scavenging activity. This ROS scavenging reshaped metabolic activity and promoted M2 polarization in hyperglycemic conditions. Combined with photothermal antibacterial effects,

these nanoribbons effectively reduced inflammation and repaired infected bone defects in diabetic mice.

3.3.1.2.2. Multi-metal nanozymes. Recently, multi-metal nanozymes have attracted attention in BTE due to their superior catalytic performance compared to single-metal counterparts. The introduction of metal dopants can create structural defects, such as oxygen vacancies and substitutional sites, which provide additional catalytic sites and promote electron transfer[293]. A prime example of this is the Fe-doped vanadium oxide (Fe-VOx) nanozymes developed by Cheng et al.[294] The incorporation of Fe induces structural reconstruction, resulting in abundant defects, including Fe substitution and oxygen vacancies, which markedly enhance their multi-enzyme mimicking activities. These nanozymes effectively scavenged reactive oxygen and nitrogen species (RONS), restored mitochondrial function, and promoted bone regeneration in osteoradionecrosis models.

Furthermore, the synergistic effect between different metal components also enhances catalytic efficiency. This synergy arises from electronic interactions and charge transfer between the metal elements, which may increase the electron density of the primary catalytic metal, thereby accelerating redox reactions[295,296]. Alternatively, the metals may work in concert to catalyze different steps of the reaction, with one metal ion responsible for redox reactions and another for coordination activation or electron shuttling, thereby expediting the overall process[297]. For example, Bai et al.[238] utilized the high catalytic efficiency of Ru and the electron-donating capability of copper (Cu) to develop a Ru-Cu electron-donating heterojunction (Ru-Cu/EDHJ) system, driven by strong electronic metal-support interactions (Fig. 6A and B). This unique design optimizes the electronic configuration of catalytic centers, increasing the electron density of Ru atoms and enhancing the binding affinity for ROS at the active sites, resulting in superior enzyme-mimicking catalytic performance. This system exhibited ROS-scavenging under neutral conditions and ROS-generation under acidic conditions, showing excellent bone repair and antibacterial efficacy in mandibular defect models (Fig. 6C−H).

Lastly, multi-metal nanozymes enable the integration of multiple enzyme-mimicking functions. For example, Hui et al.[298] designed Au@Pt bimetallic nanozymes, where the Au core mimicked glucose oxidase-like activity, enabling glucose consumption, and the Pt shell possesses CAT-like activity, facilitating ROS scavenging. Incorporated into GelMA microspheres, this system regulated hyperglycemia and oxidative stress in diabetic environments, protected BMSCs, enhanced osteogenesis and angiogenesis, and promoted bone regeneration.

3.3.1.3. Metal-organic frameworks. Metal-organic frameworks (MOFs) are crystalline porous materials formed by the coordination of metal ions or clusters with organic ligands[299]. Compared to other porous materials, MOFs' key advantage lies in their highly tunable composition and structure. By selecting different metal ions and organic ligands, researchers can precisely control the pore size, surface area, and chemical properties to suit specific biological applications[300]. In BTE, MOFs are primarily used as nanocarriers for bioactive molecules delivery, leveraging their high loading capacity, stability, and excellent surface modifiability[301−303]. Notably, MOFs offer functional integration—serving not only as carriers but also as active components. The incorporation of specific metal ions (*e.g.*, Zn, Mg, Sr) adds extra biological functions, including osteogenic, angiogenic, antibacterial, and immunomodulatory effects, thus extending MOFs' capabilities beyond simple drug delivery[304−306]. For example, ZIF-8 has been preliminarily applied in BTE research, showing promising osteogenic induction activity[307].

MOFs can also function as redox-nanozymes when incorporating metals with inherent enzyme-like activity[253,308]. Their unique structure further enhances catalytic performance[309]. Firstly, the regular framework facilitates the introduction of other synergistic catalysts, which may activate reactants, stabilize intermediates, and guide reactions along more efficient pathways[310,311]. For example, Shu et al.[240] designed a zinc-cobalt bimetallic MOF (Zn/Co-MOF)-functionalized bioceramic scaffold. This scaffold exhibited stronger POD-like activity, effectively scavenging ROS and accelerating the integrated regeneration of cartilage and subchondral bone in severe osteochondral defects[297]. Secondly, by adjusting the size and shape of MOF nanopores, the selectivity and efficiency of catalytic reactions can be improved[312]. Functional group modifications within the pores further refine interactions between substrates and active sites, thus optimizing reaction kinetics[313]. Furthermore, the well-defined pore channels of MOFs provide a stable microenvironment that confines reaction intermediates, preventing their diffusion or aggregation, thus reducing side reactions and enhancing catalytic selectivity and efficiency[314,315]. For example, a recent study[316] introduced a Zr-based MOF (HMUiO-66-NH_2) with large pores and amino modification. Within its nanostructure, the large-pore framework facilitates the adsorption and diffusion of H_2O_2 molecules. The unsaturated Zr−OH sites subsequently activate H_2O_2 for catalytic decomposition. Meanwhile, the amino groups donate electrons and hydrogen atoms to stabilize H_2O_2, and also enhance the reducibility and catalytic activity of Zr centers. In addition, the Zr−OH sites capture and stabilize the decomposition products, collectively improving the overall ROS-scavenging efficiency. In a periodontitis-induced bone resorption model, this nanozyme exhibited excellent ROS scavenging and bone formation capability, effectively reducing alveolar bone loss *in vivo*.

3.3.1.4. Se nanoparticles. Exogenous selenium supplementation can enhance cellular antioxidant defenses. *In vivo*, selenium compounds are first metabolized into active forms such as selenocysteine ($SeCys_2$), which are then incorporated into selenoproteins such as GPx, to support their activity. These selenoproteins contribute to redox homeostasis by catalyzing ROS detoxification or modulating antioxidant pathways such as Keap1−Nrf2 [317−319]. However, traditional selenium agents suffer from a narrow therapeutic window, highlighting the need for controlled-release systems[320]. Selenium nanoparticles (SeNPs) offer a promising alternative due to their lower toxicity. They can both release bioactive selenocysteine and exhibit intrinsic POD-like activity—likely through a redox cycle between Se^0 and Se^{4+} valence states[321,322]. Beyond their antioxidant properties, SeNPs also promote osteogenesis, angiogenesis, anti-inflammation, and matrix mineralization, making them an ideal candidate for BTE applications[207,323]. For example, Xu et al.[239] developed an ultrasound-responsive hydrogel embedded with selenium-doped hollow silica nanoparticles (O_2-PSSG). Upon ultrasound stimulation, the system rapidly released selenocystine and oxygen, promoting intracellular selenoprotein synthesis and enhancing antioxidant enzyme activity in BMSCs. This helped scavenge ROS, alleviate hypoxia, and activate the Wnt/β-catenin pathway, thereby accelerating bone regeneration in a rat cranial

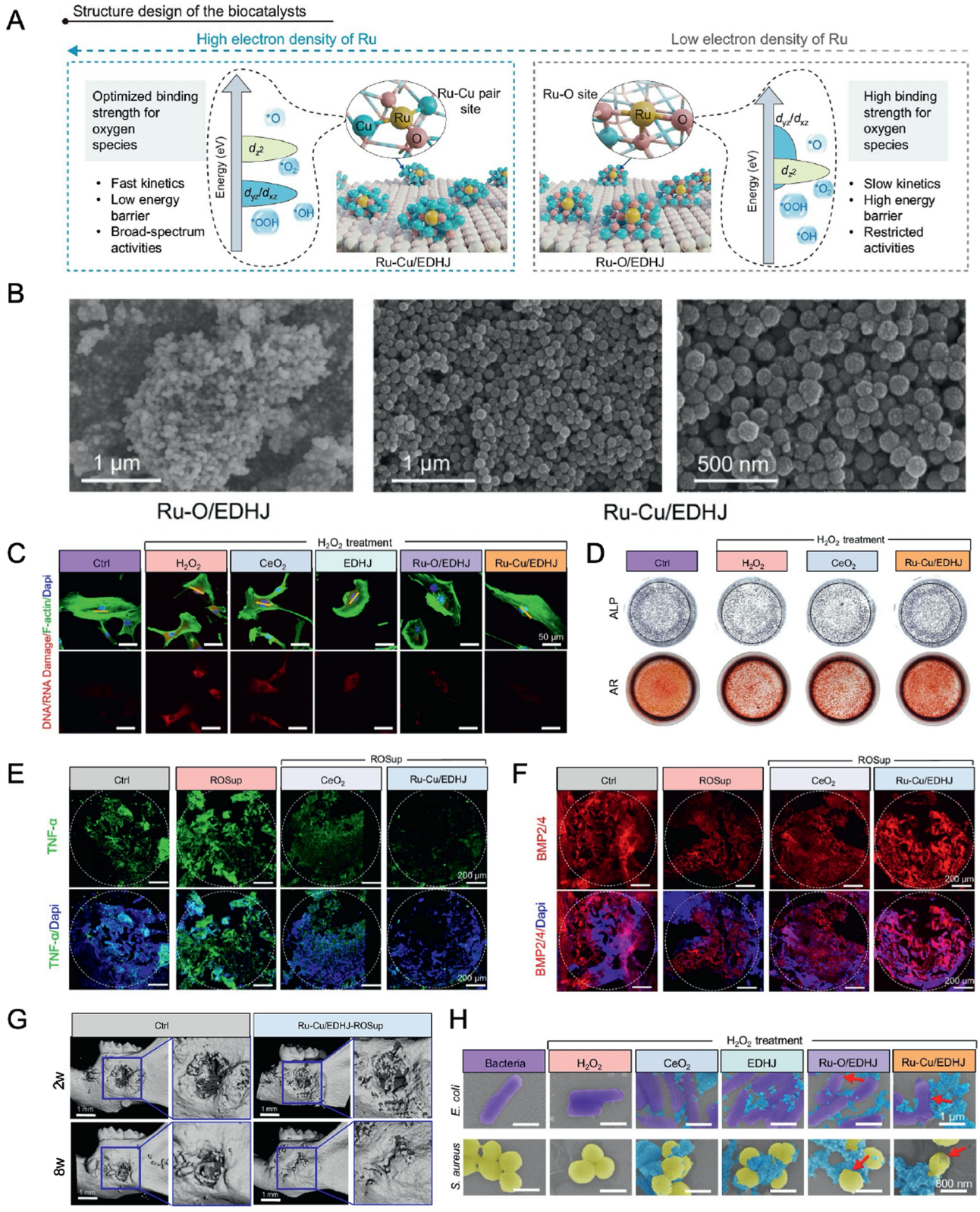


Figure 6 Electron-donable heterojunction with synergetic Ru−Cu pair sites (Ru-Cu/EDHJ) for biocatalytic regeneration. (A) Structural and biocatalytic advantages of Ru-Cu/EDHJ when compared with Ru-O/EDHJ. (B) Scanning electron microscope (SEM) images of Ru-O/EDHJ and Ru-Cu/EDHJ. (C) Fluorescence images of the signals of DNA/RNA damage marker in nuclei in the mesenchymal stem cells (MSCs). (D) Alkaline Phosphatase (ALP) staining after 3-day *in vitro* osteo-induction and AR staining after 21-day *in vitro* osteo-induction using the MSCs. (E) Fluorescence staining images of TNF-α and (F) BMP2/4 after mandible defect surgery for 1 week. (G) 3D reconstruction of micro-CT images at different times post-surgery. (H) SEM images of *E. coli* and *S. aureus* after treatments. Blue: materials, purple: *E. coli*, yellow: *S. aureus*. Reprinted with permission from Ref. 239. Copyright © 2024, Springer Nature.

defect model. Another study[324] developed lentinan-coated selenium nanoparticles (LNT-Se) as a therapeutic agent for oxidative stress−related bone loss. LNT-Se showed enhanced cellular uptake and was rapidly converted to $SeCys_2$ *in vivo*. This upregulated GPx1, suppressed inflammation and osteoclastogenesis, and ultimately alleviated bone loss in arthritis and osteoporosis models.

In summary, nanozymes hold great promise in BTE due to their unique antioxidant advantages. However, several challenges remain. Their catalytic mechanisms are insufficiently studied, limiting insights into structure−activity relationships and hindering theoretical guidance for performance optimization. Additionally, their activity and specificity are highly sensitive to environmental conditions[325,326]. For example, Prussian blue nanozymes display pH-dependent catalytic behaviors: in acidic microenvironments (*e.g.*, pH 4−6), their iron-active sites decompose H_2O_2 into $HO^{\cdot}$, while under neutral conditions (*e.g.*, pH 7−7.4), these same sites switch to CAT-like activity, converting H_2O_2 into harmless H_2O and O_2[327]. This variability stems from the redox-based catalytic nature of nanozymes, in which the oxidation states of metal centers and their standard redox potentials (E°) shift dynamically with changes in pH. These pH-induced variations in E° values directly determine the catalytic direction (promoting H_2O_2 dismutation or generating harmful free radicals like $HO^{\cdot}$). While this pH-responsiveness enables adaptive therapies, it also complicates the control and stability needed for clinical use[328]. Moreover, as inorganic agents, concerns about their metabolism, long-term toxicity, and immunogenicity persist. To advance clinical translation, future research should focus on elucidating structure−activity correlations, optimizing nanozyme design, and systematically evaluating biosafety and pharmacokinetics[329].

3.3.2. *Free radical trappers*

Fullerenes (C_{60}) are spheroidal carbon molecules with conjugated double bonds, known for their strong electron affinity. They have shown therapeutic potential in fields such as chemotherapy protection, neurodegeneration, and, more recently, bone tissue engineering[330−332]. Although their antioxidant mechanism is not fully understood, the widely accepted "cage capture" theory suggests that the π-conjugated surface of fullerenes interacts with ROS *via* van der Waals forces, electrostatic attraction, and, most importantly, $\pi-\pi$ interactions, enabling them to trap and stabilize ROS by accepting unpaired electrons[333]. Studies have confirmed the immobilization of both superoxide and hydroxyl radicals on the fullerene surface, rendering them inactive and limiting their diffusion[334]. The conjugated π−electron system then may facilitate electron transfer, neutralizing the captured ROS into low-activity or inactive products[335]. This antioxidant function helps reduce cellular toxicity, mitochondrial dysfunction, and lipid peroxidation, thereby supporting bone regeneration[334,336]. Furthermore, fullerene nanoparticles have shown potential as surface coatings to enhance osteoblast adhesion and migration while possibly suppressing osteoclast activity[337,338]. However, pristine fullerenes are hydrophobic and tend to self-aggregate, which reduces their accessible surface area and weakens biological performance. To address this, derivatives such as fullerol—polyhydroxylated fullerenes—have been developed. Fullerol retains antioxidant activity while offering better solubility and biocompatibility, thus broadening the biomedical applications, especially in bone repair[339]. In one study[241], researchers incorporated highly dispersed fullerol nanocrystals into the hydrogel matrix to develop fullerol-hydrogel microspheres (FMSs) and used them as a BMSCs delivery platform. The FMSs effectively scavenged both intracellular ROS in BMSCs and extracellular ROS in the bone defect microenvironment. When transplanted into rat calvarial defects, BMSC-loaded FMSs significantly promoted bone regeneration. In another study, Yang et al.[340] developed a 3D-printed porous scaffold (FPBS) by integrating fullerol nanoparticles into a PDA-coated bredigite scaffold. Under oxidative stress, the PDA coating degraded, releasing fullerol NPs that eliminated intracellular ROS and upregulated osteogenic marker expression. In a rat calvarial defect model, FPBS significantly improved bone regeneration.

TEMPO (2,2,6,6-tetramethylpiperidine-1-oxyl) nanoparticles and their derivatives are also effective ROS-trappers due to their stable nitroxide radical structure[341]. The unpaired electron on the nitroxide group enables radical-radical recombination to neutralize ROS. Additionally, TEMPO undergoes reversible redox cycling among its nitroxide, oxoammonium cation, and hydroxylamine states, which further enhances its antioxidant capacity. Its membrane permeability also allows efficient targeting of intracellular ROS[342]. In BTE, research on TEMPO-based nanomaterials is still in the early stages, with limited studies mainly focusing on cellular-level effects. For example, TEMPO-conjugated gold nanoparticles have been shown to reduce ROS in hMSCs under oxidative stress, promote osteogenesis, and inhibit adipogenesis[343]. This is possibly due to concerns about low stability, poor compatibility with biomaterials, and potential cytotoxicity[344]. Further research is needed to optimize their design for bone regeneration.

3.3.3. *Redox-active scavengers*

3.3.3.1. Antioxidant-derived nanoparticles. In the previous section, we summarized the application of traditional antioxidant-loaded nanocarriers in BTE. As discussed, while the use of nanocarriers offers several advantages, it also raises concerns about long-term degradation, systemic elimination, and potential toxicity[145,345]. Interestingly, certain natural antioxidants—particularly polyphenols—can self-assemble into nanoparticles through hydrogen bonding, $\pi-\pi$ stacking, electrostatic interactions, or hydrophobic effects under specific conditions, eliminating the need for exogenous carriers[346]. These self-assembled antioxidant nanoparticles retain their inherent bioactivity, including antioxidant, immunomodulatory, and osteoinductive properties, while also achieving nanoscale benefits. Moreover, they avoid the biocompatibility and degradation concerns associated with carriers. As a result, they represent a carrier-free delivery system that combines therapeutic efficacy with fabrication flexibility and are increasingly applied in bone repair.

Polydopamine nanoparticles (nPDA) are a prime example. They are formed by dopamine self-polymerization under alkaline conditions. nPDA possesses redox-active catechol and amine groups, which efficiently scavenge ROS *via* oxidizing to quinone structures[347,348]. The resulting quinones can neutralize additional free radicals, further enhancing ROS scavenging efficiency[349]. Additionally, nPDA's molecular architecture includes $\pi-\pi$ stacking and cation$-\pi$ interactions, facilitating ultrafast electron transfer and accelerating redox cycling[350]. Beyond direct ROS scavenging, nPDA also chelates metal ions (particularly Fe^{2+}, Cu^{2+}) to inhibit Fenton reactions, and enhances mitochondrial ETC efficiency to reduce ROS production. Moreover, nPDA exhibits anti-inflammatory and immunomodulatory effects, collectively fostering a regenerative microenvironment. In addition to its biochemical properties, nPDA exhibits excellent adhesive

capabilities due to the presence of lysine and 3,4-dihydroxyphenylalanine (DOPA). This enables them to form a stable coating on a wide range of surfaces, improving scaffold hydrophilicity, biocompatibility, and bioactivity[351−353]. Many studies have validated the application of nPDA in bone regeneration. For example, Qin et al.[242] developed a PDA@Au-HA nanoplatform that combines the osteoinductive effects of Au-HA with the antioxidant and immunomodulatory properties of nPDA, resulting in enhanced vascularized bone regeneration in a rat cranial defect model. In another study, Yu et al.[354] formed an HA/nPDA composite through the metal chelation of nPDA's catechol groups with calcium ions in HA, along with additional ionic interactions. This composite was then co-deposited onto titanium alloy surfaces. The resulting scaffold effectively scavenged ROS and promoted osteogenesis under oxidative conditions. Furthermore, the surface chemistry of nPDA improved the cell affinity of the implant, enhancing its osseointegration. Similarly, Li et al.[355] incorporated nPDA-modified graphene oxide and nHA into alginate-based scaffolds, successfully supporting bone regeneration in diabetic periodontal defects.

Gallic acid (GA) and tannic acid (TA), due to their unique polyphenolic structures and biological activities, have also emerged as promising building blocks for self-assembling antioxidant nanoparticles in bone regeneration applications. For example, Yu et al.[356] utilized EGCG and cysteine to self-assemble into mitochondria-targeting nanoparticles (EC NPs), which could achieve intracellular ROS scavenging, especially for mtROS and recover the mitochondrial membrane potential (Fig. 7A and B). Under ROS-induced oxidative stress, EC NPs were able to recover the aggregate/monomer ratio of mitochondria and decrease mtROS production (Fig. 7C). Both *in vitro* and *in vivo* experiments indicated that EC NPs could protect BMSCs from ROS impairment and demonstrate the inherent promotion of osteogenesis even in a high ROS environment (Fig. 7D−F). Likewise, mineral-tannic acid nanoparticles (mTNs) were prepared by self-assembling tannic acid in simulated body fluid containing calcium and phosphate ions. The catechol groups in tannic acid chelated with mineral ions and formed hydrogen bonds, resulting in nanoparticles with a diameter of approximately 250−350 nm. *In vitro*, mTNs effectively scavenged ROS, promoted osteogenic differentiation and function[357]. Similarly, Byun et al.[358] developed gelatin-based cryogels embedded with tannic acid-mineral nanoparticles (TMP/Gel). These composites exhibited excellent osteoinductive properties and biocompatibility, suppressed inflammation and osteoclastogenesis, significantly enhanced bone formation and quality in a murine calvarial defect model.

3.3.3.2. Metal-phenolic networks. Metal−phenolic networks (MPNs) are amorphous nanomaterials formed *via* coordination between metal ions and polyphenol ligands[359−361]. Their amorphous and flexible nature allows them to easily form uniform coatings on complex scaffold surface[362,363]. By combining the antioxidant capacity of polyphenols with the immunoregulatory or osteoinductive functions of metal ions, MPNs provide stable, multifunctional coatings well-suited for bone tissue engineering[364]. For example, a study[365] developed a multifunctional composite material by embedding TA-magnesium nanoparticles (TMgP) into gelatin cryogels. TA reduced oxidative stress and inflammation, while Mg^{2+} promoted M2 polarization, facilitating tissue repair. These nanoparticles also enhanced osteogenic differentiation and supported angiogenesis, synergistically enhancing bone formation and mineralization in a murine calvarial defect model. In another study, Liu et al.[243] constructed a biomimetic scaffold reinforced with PDA-coated strontium-EGCG MPNs. In this design, EGCG scavenged ROS and reduced inflammation, Sr^{2+} enhanced osteogenesis and angiogenesis, and the PDA coating improved the scaffold's photothermal and antioxidant properties. *In vivo*, the scaffold significantly promoted cranial bone defect repair by regulating the microenvironment and enhancing bone tissue regeneration.

3.3.3.3. H_2-based nanomaterials. Hydrogen gas (H_2) is also a promising antioxidant commonly used to combat cellular aging. It scavenges ROS both by directly donating electrons and by indirectly enhancing endogenous antioxidant defense systems[366]. Compared to other antioxidants, H_2 offers several advantages. First, its small molecular size allows for rapid diffusion and penetration into the cytosol, mitochondria, and nucleus, thus enabling effective protection. Second, as an endogenous inert gas, H_2 is highly safe and biocompatible. Most importantly, H_2 exhibits moderate reducing activity, reacting primarily with highly toxic oxidants like $HO^{\cdot}$ and $ONOO^{-}$, while preserving physiological ROS involved in normal cell signaling, thereby minimizing potential side effects[367]. In addition to its antioxidative properties, H_2 exerts immunomodulatory, anti-inflammatory, and anti-apoptotic effects[366]. These multifaceted benefits make H_2 a promising therapeutic agent for various oxidative stress-related diseases[368].

However, the low solubility and high diffusivity of H_2 in body fluids present challenges in maintaining high local concentrations at disease sites. To overcome this limitation, recent advancements have focused on developing *in situ* H_2-releasing systems. For example, Zhou et al.[369] engineered an injectable Mg@PEG-PLGA hydrogel that releases H_2 upon reacting with water, thus enabling ROS scavenging and *in situ* scaffold formation. This hydrogel enhanced osteogenesis, promoted M2 polarization, and suppressed osteoclastogenesis, significantly improving bone repair in an osteoporotic rat model. Similarly, Chen et al.[370] constructed an in-situ H_2-releasing scaffold by electrospraying PHA-encapsulated $CaSi_2$ nanoparticles onto mesoporous bioactive glass. Upon water exposure, the scaffold released high-dose H_2 (911 mL/g over one week), which reduced ROS levels, alleviated cellular senescence, and preserved stem cell function. *In vivo* studies, this scaffold transformed the pathological niche—characterized by the superposition of aging, inflammation, and oxidative stress—into a pro-regenerative one, ultimately repairing critical-size femoral defects in aged mice. Moreover, Chan et al.[244] developed a biomimetic scaffold made of mineralized collagen fibers with nanosilicon (RA-MC/nSi), which released H_2 upon contact with body fluids. The released H_2 maintained redox homeostasis, suppressed inflammation, and promoted osteogenic differentiation. In a mouse calvarial defect model, the scaffold doubled the bone volume fraction compared to controls, significantly enhancing regeneration. These examples highlight the potential of H_2-releasing nanomaterials in promoting bone regeneration.

3.4. ROS-activated ROS-scavenging nanomaterials

In recent years, smart ROS-responsive systems—typically hydrogels and nanocarriers functionalized with ROS-sensitive moieties—have garnered increasing attention in BTE. These systems selectively respond to elevated ROS levels within inflammatory or injury-related microenvironments, enabling targeted therapeutic release. In addition to their targeting capability,

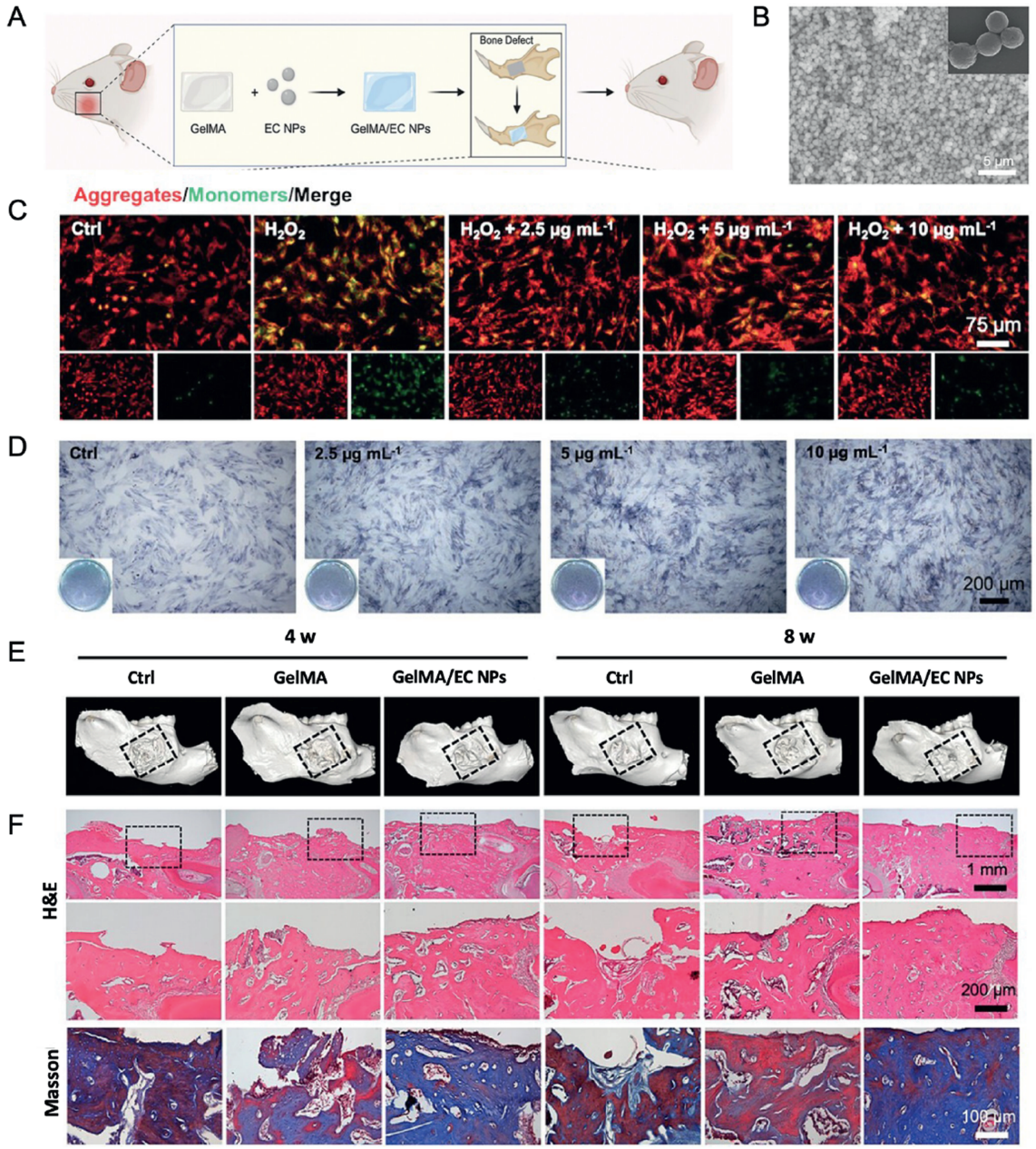


Figure 7 Epigallocatechin-3-gallate (EGCG)—cysteine (Cys) assembled nanoparticles (NPs) for enhanced bone regeneration. (A) Schematic illustration of EGCG-Cys (EC) assembled NPs. (B) Scanning electron microscopy (SEM) images of EC NPs at 30 min of synthesis. (C) Fluorescence images of MMP using JC-1 after different treatments. (D) Alkaline phosphatase (ALP) staining after incubation with EC NPs for 7 days. (E) 3D-reconstructed micro-CT scanning images of rat mandibular bone defects at 4- and 8-weeks post-operation. (F) H&E staining and Masson trichrome staining of the mandibular bone defect at 4- and 8-week post-operation. Reprinted with permission from Ref. 357. Copyright © 2024, John Wiley and Sons.

this review also highlights the concurrent antioxidant function of ROS-responsive systems—namely, the ability to scavenge excess ROS while responding to oxidative stress. When loaded with antioxidant agents, such systems can further amplify their ROS-scavenging efficacy. For clarity and emphasis, we refer to them as ROS-activated antioxidant nanomaterials throughout this section. Their activation typically involves either ROS-activated alterations in physical properties—particularly solubility—or ROS-mediated cleavage of specific chemical bonds[371,372]. In the former, polymers containing hydrophobic groups (*e.g.*, thioethers, tellurethers, selenoethers), which form the core of the nanoparticles, undergo oxidation reactions with ROS, producing more hydrophilic species such as sulfoxides (−SO−), sulfones ($-SO_2-$), tellurium oxides (−TeO−), and selenium oxides (−SeO−). This conversion destabilizes the hydrophobic core, increases solubility, and leads to particle disassembly, thereby facilitating drug release[373]. In the latter mechanism, chemical bonds such as disulfide, thioketal, poly(proline), phenylboronic acid, and esters are

cleaved through direct reaction with ROS[374−376]. Since these linkages often serve as crosslinking points or structural components, their cleavage compromises the physical integrity of the carrier, ultimately resulting in therapeutic release.

The application of ROS-activated ROS-scavenging strategies in bone repair is illustrated by the following examples. Zhang et al.[377] developed a ROS-responsive, factor-free hydrogel based on thioketal (TK) (+) crosslinks. Under elevated ROS levels, the TK (+) bonds undergo degradation while concurrently consuming excessive ROS. This redox-regulating process restored cell viability, enhanced BMSC migration, and reversed adipogenic differentiation, thereby promoting osteogenesis. In diabetic calvarial defect models, the system significantly improved bone regeneration without the need for exogenous growth factors. Another example is provided by Fang et al.[378], who constructed resveratrol-loaded cyclodextrin nanomicelles (RSV-NMs) functionalized with phenylboronic esters. In ROS-rich inflammatory environments, the boronic ester bonds cleave, causing the nanomicelles to rapidly disassemble and release resveratrol. This process was accompanied by a significant reduction in intracellular ROS levels, as demonstrated by fluorescence imaging. The controlled release of resveratrol effectively inhibited osteoclastogenesis and protected bone from LPS-induced destruction.

4. Summaries and perspectives

This review comprehensively summarizes three major categories of ROS-scavenging nanomaterials—nanocarriers that deliver traditional antioxidants, nanomaterials with intrinsic ROS-scavenging activity, and ROS-activated ROS-scavenging systems—highlighting their distinct advantages in bone regeneration. These emerging strategies represent a shift from traditional passive bone scaffolds toward active, microenvironment-responsive regenerative therapies. Looking ahead, advances in smart biomaterials, such as self-healing coatings and nanoscopic sensors, will enable materials to precisely sense and respond to redox fluctuations in real-time, triggering antioxidant release at optimal timing and dosage. Moreover, the integration of these materials with multifunctional platforms (*e.g.*, osteoinductive, immunomodulatory, and antibacterial components), coupled with AI-assisted 3D bioprinting techniques, will significantly enhance therapeutic precision and allow tailored solutions for specific clinical scenarios. Collectively, these innovations have the potential to establish ROS-scavenging nanoscaffolds as next-generation standards for bone defect repair, especially for challenging conditions such as diabetic osteonecrosis and osteoporosis-related bone defects.

However, despite the rapid progress and promising prospects in this field, no ROS-scavenging scaffolds have yet entered clinical evaluation specifically for bone defect repair. Multiple factors continue to hinder their clinical translation. Among these, biosafety concerns remain paramount. Uncertainties surrounding immune rejection, tissue integration, metabolic profiles, and long-term toxicity—especially for inorganic or metal-based materials that may accumulate *in vivo*—raise substantial safety issues. Although short-term biocompatibility and systemic toxicity are routinely assessed, long-term evaluations are limited by experimental duration and model constraints. Moreover, toxicity reports on antioxidant scaffolds remain scarce, potentially due to publication bias. In addition, optimization procedures for improving scaffold biocompatibility are often underreported, limiting reproducibility and hindering future material refinement.

The complexity of synthesis and large-scale production presents another challenge. Most ROS-scavenging platforms involve multi-component architectures designed for high therapeutic efficacy, which inevitably results in low yields, time-consuming purification, and difficulties in maintaining batch-to-batch consistency. The lack of standardized quality control and performance metrics further complicates industrial scalability and clinical-grade material preparation.

Transitioning from preclinical models to clinical evaluation also presents substantial challenges. Unlike standardized animal models, patient conditions vary widely in fracture type, defect size, comorbidities, and healing response, making it difficult to establish universal treatment guidelines or evaluate therapeutic outcomes consistently. Moreover, the lack of standardized efficacy endpoints and follow-up protocols hampers material benchmarking and cross-study comparisons.

From a mechanistic perspective, current research predominantly centers on osteoblasts, osteoclasts, macrophages, and stem cells, while other relevant cell types—such as neural and immune cells—receive limited attention. ROS-scavenging nanomaterials may modulate broader cellular networks involved in bone repair, yet this potential remains underexplored. In addition, most studies adopt a practical approach based on the observed benefits of ROS elimination, yet often lack clear theoretical guidance. As discussed earlier, the physiological role of ROS varies across different stages of bone healing; thus, whether ROS should be continuously removed, transiently controlled, or allowed to fluctuate remains an open question.

To overcome these barriers, future research should focus on the following areas.

(1) Prioritize long-term biocompatibility and safety evaluations. Metabolic tracking, biodistribution profiling, and chronic toxicity assessment in large animal models are essential. Negative findings and long-term follow-up data should be encouraged to avoid publication bias and promote transparency. Moreover, leveraging FDA-approved materials—such as titanium-based scaffolds—as foundational platforms may enhance safety and streamline clinical acceptance.
(2) Applying artificial intelligence (AI) for high-throughput screening and material optimization. Machine learning algorithms can extract patterns from large physicochemical and biological datasets to predict ROS clearance efficiency, osteogenic potential, and toxicity risks. AI-guided inverse design can accelerate the development of next-generation biomaterials tailored for specific oxidative environments.
(3) Deepen the mechanistic understanding of bone repair. Despite growing interest, the precise molecular pathways through which elevated ROS levels influence bone repair remain unclear, including their interactions with osteogenic, immune, and neural cells, as well as the optimal ROS levels required at different stages of healing. Without answers to these questions, it remains difficult to determine when and how much ROS should be regulated, making material design uncertain and imprecise. Therefore, future studies should focus on uncovering the specific mechanisms by which ROS participate in bone repair and how they influence communication between different cell types. These insights will provide a stronger foundation for designing more precise and controllable antioxidant materials, moving from empirical benefit to mechanism-driven precision.

(4) Establish standardized evaluation systems. A robust framework for assessing efficacy, toxicology, and long-term performance is critical. Furthermore, standardized protocols for patient inclusion, clinical endpoints, and multicenter trials will facilitate consistent evaluation and cross-study comparison of different materials, laying the foundation for future industrial translation and broader clinical application.

In conclusion, ROS-scavenging nanomaterials hold tremendous potential for enhancing bone repair. By addressing current limitations in biosafety, manufacturing, and clinical evaluation, and by embracing emerging tools such as AI-driven optimization and integrative mechanistic research, this field is poised for transformative progress. We hope this review provides a useful reference for researchers and clinicians working to accelerate the development and translation of effective bone-regenerative therapies. Ultimately, antioxidant nanoscaffolds may become vital components in future bone repair strategies, offering new hope for patients suffering from bone defects and related conditions.

Acknowledgments

This study was supported by the National Natural Science Foundation of China (No. 82371102, China), and the Key program of Shanghai Science and Technology Commission (No. 23JC1402400, China). The author would like to thank Dr. Chen Guo (Department of Spine Surgery, Peking University People's Hospital, Beijing, China) for his insightful guidance on manuscript writing. The graphic abstract was created with BioRender.com.

Author contributions

Wanzhuo He, Yun Su, and Xianqun Fan jointly conceptualized the topic and designed the overall structure of the review. Wanzhuo He, Miao Wang, and Ni Ni contributed to literature investigation and data curation. Wanzhuo He and Tian Xu wrote the original draft and prepared the figures and tables. Yun Su and Xianqun Fan revised the manuscript. All of the authors have read and approved the final manuscript.

Conflicts of interest

The authors have no conflicts of interest to declare.

References

1. Xue NN, Ding XF, Huang RZ, Jiang RH, Huang HY, Pan X, et al. Bone tissue engineering in the treatment of bone defects. *Pharmaceuticals (Basel)* 2022;**15**:879.
2. Łuczak JW, Palusińska M, Matak D, Pietrzak D, Nakielski P, Lewicki S, et al. The future of bone repair: emerging technologies and biomaterials in bone regeneration. *Int J Mol Sci* 2024;**25**:12766.
3. Smith BD, Grande DA. The current state of scaffolds for musculoskeletal regenerative applications. *Nat Rev Rheumatol* 2015;**11**: 213−22.
4. Roberts SJ, Howard D, Buttery LD, Shakesheff KM. Clinical applications of musculoskeletal tissue engineering. *Br Med Bull* 2008; **86**:7−22.
5. Bauso LV, La Fauci V, Longo C, Calabrese G. Bone tissue engineering and nanotechnology: a promising combination for bone regeneration. *Biology (Basel)* 2024;**13**:207−37.
6. Wang J, Zhang Y, Tang Q, Zhang Y, Yin Y, Chen L. Application of antioxidant compounds in bone defect repair. *Antioxidants* 2024;**13**: 789.
7. Xu YY, Luo YF, Weng ZZ, Xu HC, Zhang W, Li Q, et al. Microenvironment-responsive metal-phenolic nanozyme release platform with antibacterial, ROS scavenging, and osteogenesis for periodontitis. *ACS Nano* 2023;**17**:18732−46.
8. Sies H, Jones DP. Reactive oxygen species (ROS) as pleiotropic physiological signalling agents. *Nat Rev Mol Cell Biol* 2020;**21**: 363−83.
9. de Almeida A, de Oliveira J, da Silva Pontes LV, de Souza Júnior JF, Gonçalves TAF, Dantas SH, et al. ROS: basic concepts, sources, cellular signaling, and its implications in aging pathways. *Oxid Med Cell Longev* 2022;**2022**:1225578.
10. Marques-Carvalho A, Kim HN, Almeida M. The role of reactive oxygen species in bone cell physiology and pathop hysiology. *Bone Rep* 2023;**19**:101664.
11. Taylor JP, Tse HM. The role of NADPH oxidases in infectious and inflammatory diseases. *Redox Biol* 2021;**48**:102159.
12. Förstermann U, Xia N, Li H. Roles of vascular oxidative stress and nitric oxide in the pathogenesis of atherosclerosis. *Circ Res* 2017; **120**:713−35.
13. Halliwell B. Understanding mechanisms of antioxidant action in health and disease. *Nat Rev Mol Cell Biol* 2024;**25**:13−33.
14. Fridovich I. Superoxide radical and superoxide dismutases. *Annu Rev Biochem* 1995;**64**:97−112.
15. Das KC, Kundumani-Sridharan V, Subramani J. Role of thioredoxin in age-related hypertension. *Curr Hypertens Rep* 2018;**20**:6.
16. Shastak Y, Alvaro G, Pelletier W. The relationship between vitamin a status and oxidative stress in animal production. *J Appl Anim Res* 2023;**51**:546−53.
17. Zheng H, Xu Y, Liehn EA, Rusu M. Vitamin C as scavenger of reactive oxygen species during healing after myocardial infarction. *Int J Mol Sci* 2024;**25**:3114.
18. Lee GY, Han SN. The role of vitamin E in immunity. *Nutrients* 2018; **10**:1614.
19. Sies H, Mailloux RJ, Jakob U. Fundamentals of redox regulation in biology. *Nat Rev Mol Cell Biol* 2024;**25**:758.
20. Xu T, Ding W, Ji X, Ao X, Liu Y, Yu WP, et al. Oxidative stress in cell death and cardiovascular diseases. *Oxid Med Cell Longev* 2019; **2019**:9030563.
21. Checa J, Aran JM. Reactive oxygen species: drivers of physiological and pathological processes. *J Inflamm Res* 2020;**13**:1057−73.
22. Chenevier-Gobeaux C, Simonneau C, Lemaréchal H, Bonnefont-Rousselot D, Poiraudeau S, Rannou F, et al. Effect of hypoxia/reoxygenation on the cytokine-induced production of nitric oxide and superoxide anion in cultured osteoarthritic synoviocytes. *Osteoarthr Cartil* 2013;**21**:874−81.
23. Pacher P, Beckman JS, Liaudet L. Nitric oxide and peroxynitrite in health and disease. *Physiol Rev* 2007;**87**:315−424.
24. Beckman JS, Carson M, Smith CD, Koppenol WH. ALS, SOD and peroxynitrite. *Nature* 1993;**364**:584.
25. Nwanjo H, Oze G, Okafor M, Nwosu D, Nwankpa P. Oxidative stress and non-enzymic antioxidant status in hypertensive patients in Nigeria. *Afr J Biotechnol* 2007;**6**:1681−4.
26. Bonnefont Rousselot D, Mc J, Issad B, Cacoub P, Congy F, Jardel C, et al. Antioxidant status of elderly chronic renal patients treated by continuous ambulatory peritoneal dialysis. *Nephrol Dial Transplant* 1997;**12**:1399−405.
27. Cerqueni G, Scalzone A, Licini C, Gentile P, Mattioli-Belmonte M. Insights into oxidative stress in bone tissue and novel challenges for biomaterials. *Mater Sci Eng C Mater Biol Appl* 2021;**130**:112433.
28. Mekuye B, Abera B. Nanomaterials: an overview of synthesis, classification, characterization, and applications. *Nano Select* 2023;**4**: 486−501.

29. Roduner E. Size matters: why nanomaterials are different. *Chem Soc Rev* 2006;**35**:583−92.
30. Wang LY, Zhu BH, Deng YT, Li TT, Tian QY, Yuan ZG, et al. Biocatalytic and antioxidant nanostructures for ROS scavenging and biotherapeutics. *Adv Funct Mater* 2021;**31**:2101804.
31. Wang L, Chen FX, Zhang CL, Cheng YY, Bu WB, Liu YY. Reactive oxygen species and neurodegenerative diseases: insights into nanozyme therapeutics. *Med Mat* 2024;**1**:55−73.
32. Li H, Zhang ZH, Liu J, Wang HW. Antioxidant scaffolds for enhanced bone regeneration: recent advances and challenges. *Biomed Eng Online* 2025;**24**:41.
33. ElHawary H, Baradaran A, Abi-Rafeh J, Vorstenbosch J, Xu L, Efanov JI. Bone healing and inflammation: principles of fracture and repair. *Semin Plast Surg* 2021;**35**:198−203.
34. Chung R, Cool JC, Scherer MA, Foster BK, Xian CJ. Roles of neutrophil-mediated inflammatory response in the bony repair of injured growth plate cartilage in young rats. *J Leukoc Biol* 2006;**80**: 1272−80.
35. Xing ZQ, Lu CY, Hu D, Yu YY, Wang XD, Colnot C, et al. Multiple roles for CCR2 during fracture healing. *Dis Model Mech* 2010;**3**: 451−8.
36. Sheppard AJ, Barfield AM, Barton S, Dong Y. Understanding reactive oxygen species in bone regeneration: a glance at potential therapeutics and bioengineering applications. *Front Bioeng Biotechnol* 2022;**10**:836764.
37. Bahney CS, Zondervan RL, Allison P, Theologis A, Ashley JW, Ahn J, et al. Cellular biology of fracture healing. *J Orthop Res* 2019; **37**:35−50.
38. Loi F, Córdova LA, Pajarinen J, Lin TH, Yao Z, Goodman SB. Inflammation, fracture and bone repair. *Bone* 2016;**86**:119−30.
39. Li X, Li Be, Shi Y, Wang Cl, Ye L. Targeting reactive oxygen species in stem cells for bone therapy. *Drug Discov Today* 2021;**26**:1226−44.
40. Saul D, Khosla S. Fracture healing in the setting of endocrine diseases, aging, and cell ular senescence. *Endocr Rev* 2022;**43**:984−1002.
41. Einhorn TA. The science of fracture healing. *J Orthop Trauma* 2005; **19**:S4−6.
42. Claes L, Recknagel S, Ignatius A. Fracture healing under healthy and inflammatory conditions. *Nat Rev Rheumatol* 2012;**8**:133−43.
43. Marsell R, Einhorn TA. The biology of fracture healing. *Injury* 2011; **42**:551−5.
44. Einhorn TA. The cell and molecular biology of fracture healing. *Clin Orthop Relat Res* 1998;**355**:S7−21.
45. Baker CE, Moore-Lotridge SN, Hysong AA, Posey SL, Robinette JP, Blum DM, et al. Bone fracture acute phase response—a unifying theory of fracture repair: clinical and scientific implications. *Clin Rev Bone Miner Metab* 2018;**16**:142−58.
46. Newman H, Shih YV, Varghese S. Resolution of inflammation in bone regeneration: from understandings to therapeutic applications. *Biomaterials* 2021;**277**:121114.
47. Caballero-Sánchez N, Alonso-Alonso S, Nagy L. Regenerative inflammation: when immune cells help to re-build tissues. *FEBS J* 2024;**291**:1597−614.
48. Schlundt C, Saß RA, Bucher CH, Bartosch S, Hauser AE, Volk HD, et al. Complex spatio−temporal interplay of distinct immune and bone cell subsets during bone fracture healing. *Cells* 2023;**13**:40.
49. Gibon E, Lu L, Goodman SB. Aging, inflammation, stem cells, and bone healing. *Stem Cell Res Ther* 2016;**7**:44.
50. Schlundt C, Fischer H, Bucher CH, Rendenbach C, Duda GN, Schmidt-Bleek K. The multifaceted roles of macrophages in bone regeneration: a story of polarization, activation and time. *Acta Biomater* 2021;**133**:46−57.
51. Xue JD, Gao J, Tang AF, Feng C. Shaping the immune landscape: multidimensional environmental stimuli refine macrophage polarization and foster revolutionary approaches in tissue regeneration. *Heliyon* 2024;**10**:e37192.
52. Pajarinen J, Lin T, Gibon E, Kohno Y, Maruyama M, Nathan K, et al. Mesenchymal stem cell-macrophage crosstalk and bone healing. *Biomaterials* 2019;**196**:80−9.
53. Denu RA, Hematti P. Effects of oxidative stress on mesenchymal stem cell biology. *Oxid Med Cell Longev* 2016;**2016**:2989076.
54. Li JY, Han FX, Ma JJ, Wang H, Pan J, Yang GB, et al. Targeting endogenous hydrogen peroxide at bone defects promotes bone repair. *Adv Funct Mater* 2022;**32**:2111208.
55. Symons MC. Radicals generated by bone cutting and fracture. *Free Radic Biol Med* 1996;**20**:831−5.
56. Li H, Zhou XD, Huang YY, Liao BY, Cheng L, Ren B. Reactive oxygen species in pathogen clearance: the killing mechanisms, the adaption response, and the side effects. *Front Microbiol* 2020;**11**: 622534.
57. Nauseef WM. The phagocyte NOX2 NADPH oxidase in microbial killing and cell signaling. *Curr Opin Immunol* 2019;**60**:130−40.
58. Zhang JX, Wang XL, Vikash V, Ye Q, Wu DD, Liu YL, et al. ROS and ROS-mediated cellular signaling. *Oxid Med Cell Longev* 2016; **2016**:4350965.
59. Kaul N, Forman HJ. Activation of NF-κB by the respiratory burst of macrophages. *Free Radic Biol Med* 1996;**21**:401−5.
60. Morgan MJ, Liu ZG. Crosstalk of reactive oxygen species and NF-κB signaling. *Cell Res* 2011;**21**:103−15.
61. Toledano MB, Leonard WJ. Modulation of transcription factor NF-κB binding activity by oxidation-reduction *in vitro*. *Proc Natl Acad Sci U S A* 1991;**88**:4328−32.
62. Yang YH, Bazhin AV, Werner J, Karakhanova S. Reactive oxygen species in the immune system. *Int Rev Immunol* 2013;**32**:249−70.
63. Blaser H, Dostert C, Mak TW, Brenner D. TNF and ROS crosstalk in inflammation. *Trends Cell Biol* 2016;**26**:249−61.
64. Xiong H, Zhao YZ, Xu QY, Xie X, Wu JR, Hu B, et al. Biodegradable hollow-structured nanozymes modulate phenotypic polarization of macrophages and relieve hypoxia for treatment of osteoarthritis. *Small* 2022;**18**:2203240.
65. Liang S, Dong SH, Liu WW, Wang M, Tian SS, Ai Y, et al. Accumulated ROS activates HIF-1α-induced glycolysis and exerts a protective effect on sensory hair cells against noise-induced damage. *Front Mol Biosci* 2021;**8**:806650.
66. Nathan C. Neutrophils and immunity: challenges and opportunities. *Nat Rev Immunol* 2006;**6**:173−82.
67. Lee NK, Choi YG, Baik JY, Han SY, Jeong DW, Bae YS, et al. A crucial role for reactive oxygen species in RANKL-induced osteoclast differentiation. *Blood* 2005;**106**:852−9.
68. Kim HJ, Chang EJ, Kim HM, Lee SB, Kim HD, Su Kim G, et al. Antioxidant α-lipoic acid inhibits osteoclast differentiation by reducing nuclear factor-κB DNA binding and prevents *in vivo* bone resorption induced by receptor activator of nuclear factor-κB ligand and tumor necrosis factor-α. *Free Radic Biol Med* 2006;**40**:1483−93.
69. Ha H, Kwak HB, Lee SW, Jin HM, Kim HM, Kim HH, et al. Reactive oxygen species mediate RANK signaling in osteoclasts. *Exp Cell Res* 2004;**301**:119−27.
70. Lorenzo J. The many ways of osteoclast activation. *J Clin Investig* 2017;**127**:2530−2.
71. Takayanagi H, Kim S, Koga T, Nishina H, Isshiki M, Yoshida H, et al. Induction and activation of the transcription factor NFATc1 (NFAT2) integrate RANKL signaling in terminal differentiation of osteoclasts. *Dev Cell* 2002;**3**:889−901.
72. Takayanagi H. Mechanistic insight into osteoclast differentiation in osteoimmunology. *J Mol Med (Berl)* 2005;**83**:170−9.
73. Wang K, Niu J, Kim H, Kolattukudy PE. Osteoclast precursor differentiation by MCPIP *via* oxidative stress, endoplasmic reticulum stress, and autophagy. *J Mol Cell Biol* 2011;**3**:360−8.
74. Nguyen VT, Canciani B, Cirillo F, Anastasia L, Peretti GM, Mangiavini L. Effect of chemically induced hypoxia on osteogenic and angiogenic differentiation of bone marrow mesenchymal stem cells and human umbilical vein endothelial cells in direct coculture. *Cells* 2020;**9**:757.
75. Schröder K. Redox control of angiogenesis. *Antioxid Redox Signal* 2019;**30**:960−71.
76. Black SM, DeVol JM, Wedgwood S. Regulation of fibroblast growth factor-2 expression in pulmonary arterial smooth muscle cells

involves increased reactive oxygen species generation. *Am J Physiol Cell Physiol* 2008;**294**:C345−54.
77. Ozgocmen S, Kaya H, Fadillioglu E, Aydogan R, Yilmaz Z. Role of antioxidant systems, lipid peroxidation, and nitric oxide in postmenopausal osteoporosis. *Mol Cell Biochem* 2007;**295**:45−52.
78. Domazetovic V, Marcucci G, Iantomasi T, Brandi ML, Vincenzini MT. Oxidative stress in bone remodeling: role of antioxidants. *Clin Cases Miner Bone Metab* 2017;**14**:209−16.
79. Su JC, Zhang Y, Cheng C, Zhu YN, Ye YM, Sun YK, et al. Hydrogen regulates the M1/M2 polarization of alveolar macrophages in a rat model of chronic obstructive pulmonary disease. *Exp Lung Res* 2021; **47**:301−10.
80. Sica A, Mantovani A. Macrophage plasticity and polarization: *In vivo* veritas. *J Clin Investig* 2012;**122**:787−95.
81. Mosser DM, Edwards JP. Exploring the full spectrum of macrophage activation. *Nat Rev Immunol* 2008;**8**:958−69.
82. Lv L, Xie Y, Li K, Hu T, Lu X, Cao Y, et al. Unveiling the mechanism of surface hydrophilicity-modulated macrophage polarization. *Adv Healthc Mater* 2018;**7**:1800675.
83. Chambers M, Rees A, Cronin JG, Nair M, Jones N, Thornton CA. Macrophage plasticity in reproduction and environmental influences on their function. *Front Immunol* 2020;**11**:607328.
84. Rached MT, Kode A, Silva BC, Jung DY, Gray S, Ong H, et al. FoxO1 expression in osteoblasts regulates glucose homeostasis through regulation of osteocalcin in mice. *J Clin Investig* 2010;**120**: 357−68.
85. Iyer S, Ambrogini E, Bartell SM, Han L, Roberson PK, de Cabo R, et al. FoxOs attenuate bone formation by suppressing Wnt signaling. *J Clin Investig* 2013;**123**:3409−19.
86. Wauquier F, Leotoing L, Coxam V, Guicheux J, Wittrant Y. Oxidative stress in bone remodelling and disease. *Trends Mol Med* 2009;**15**: 468−77.
87. Fay J, Varoga D, Wruck CJ, Kurz B, Goldring MB, Pufe T. Reactive oxygen species induce expression of vascular endothelial growth factor in chondrocytes and human articular cartilage explants. *Arthritis Res Ther* 2006;**8**:1−8.
88. Wang YX, Zang QS, Liu ZJ, Wu Q, Maass D, Dulan G, et al. Regulation of VEGF-induced endothelial cell migration by mitochondrial reactive oxygen species. *Am J Physiol Cell Physiol* 2011; **301**:C695−704.
89. Benedito R, Roca C, Sörensen I, Adams S, Gossler A, Fruttiger M, et al. The notch ligands Dll4 and Jagged1 have opposing effects on angiogenesis. *Cell* 2009;**137**:1124−35.
90. Schröder K. NADPH oxidases in bone homeostasis and osteoporosis. *Free Radic Biol Med* 2019;**132**:67−72.
91. Zhu XW, Ding K, Dai XY, Ling WQ. β-aminoisobutyric acid accelerates the proliferation and differentiation of MC3T3-E1 cells *via* moderate activation of ROS signaling. *J Chin Med Assoc* 2018;**81**: 611−8.
92. Tao HQ, Ge GR, Liang XL, Zhang WC, Sun HY, Li M, et al. ROS signaling cascades: dual regulations for osteoclast and osteoblast. *Acta Biochim Biophys Sin (Shanghai)* 2020;**52**:1055−62.
93. Mandal Chandi C, Ganapathy S, Gorin Y, Mahadev K, Block K, Abboud Hanna E, et al. Reactive oxygen species derived from NOX4 mediate *BMP2* gene transcription and osteoblast differentiation. *Biochem J* 2010;**433**:393−402.
94. Lennicke C, Cochemé HM. Redox metabolism: ROS as specific molecular regulators of cell signaling and function. *Mol Cell* 2021; **81**:3691−707.
95. Agidigbi TS, Kim C. Reactive oxygen species in osteoclast differentiation and possible pharmaceutical targets of ROS-mediated osteoclast diseases. *Int J Mol Sci* 2019;**20**:3576.
96. Qutub AA, Popel AS. Reactive oxygen species regulate hypoxia-inducible factor 1α differentially in cancer and ischemia. *Mol Cell Biol* 2008;**28**:5106−19.
97. Lee G, Won HS, Lee YM, Choi JW, Oh TI, Jang JH, et al. Oxidative dimerization of PHD2 is responsible for its inactivation and contributes to metabolic reprogramming *via* HIF-1α activation. *Sci Rep* 2016;**6**:18928.
98. Cross MJ, Claesson-Welsh L. FGF and VEGF function in angiogenesis: signalling pathways, biological responses and therapeutic inhibition. *Trends Pharmacol Sci* 2001;**22**:201−7.
99. Dimmeler S, Fleming I, Fisslthaler B, Hermann C, Busse R, Zeiher AM. Activation of nitric oxide synthase in endothelial cells by AKT-dependent phosphorylation. *Nature* 1999;**399**:601−5.
100. Rendra E, Riabov V, Mossel DM, Sevastyanova T, Harmsen MC, Kzhyshkowska J. Reactive oxygen species (ROS) in macrophage activation and function in diabetes. *Immunobiology* 2019;**224**: 242−53.
101. Guo Q, Jin YZ, Chen XY, Ye XM, Shen X, Lin MX, et al. NF-κB in biology and targeted therapy: new insights and translational implications. *Signal Transduct Target Ther* 2024;**9**:53.
102. Dwivedi G, Gran MA, Bagchi P, Kemp ML. Dynamic redox regulation of IL-4 signaling. *PLoS Comput Biol* 2015;**11**:e1004582.
103. Scott TE, Lewis CV, Zhu M, Wang C, Samuel CS, Drummond GR, et al. IL-4 and IL-13 induce equivalent expression of traditional M2 markers and modulation of reactive oxygen species in human macrophages. *Sci Rep* 2023;**13**:19589.
104. Kapoor N, Niu J, Saad Y, Kumar S, Sirakova T, Becerra E, et al. Transcription factors STAT6 and KLF4 implement macrophage polarization *via* the dual catalytic powers of MCPIP. *J Immunol* 2015; **194**:6011−23.
105. Zhou NJ, Bao WQ, Zhang CF, Jiang ML, Liang TL, Ma GY, et al. Immunometabolism and oxidative stress: roles and therapeutic strategies in cancer and aging. *NPJ Aging* 2025;**11**:59.
106. Wu CL, Huang AC, Yang JS, Liao CL, Lu HF, Chou ST, et al. Benzyl isothiocyanate (BITC) and phenethyl isothiocyanate (PEITC)-mediated generation of reactive oxygen species causes cell cycle arrest and induces apoptosis *via* activation of caspase-3, mitochondria dysfunction and nitric oxide (NO) in human osteogenic sarcoma U-2 OS cells. *J Orthop Res* 2011;**29**:1199−209.
107. Hoogeboom D, Burgering BM. Should I stay or should I go: β-catenin decides under stress. *Biochim Biophys Acta* 2009;**1796**:63−74.
108. Almeida M. Unraveling the role of FoxOs in bone-insights from mouse models. *Bone* 2011;**49**:319−27.
109. Van der Horst A, de Vries-Smits AM, Brenkman AB, van Triest MH, van den Broek N, Colland F, et al. FOXO4 transcriptional activity is regulated by monoubiquitination and USP7/HAUSP. *Nat Cell Biol* 2006;**8**:1064−73.
110. Essers MA, de Vries-Smits LM, Barker N, Polderman PE, Burgering BM, Korswagen HC. Functional interaction between β-catenin and FOXO in oxidative stress signaling. *Science* 2005;**308**:1181−4.
111. Almeida M, Han L, Martin-Millan M, O'Brien CA, Manolagas SC. Oxidative stress antagonizes Wnt signaling in osteoblast precursors by diverting β-catenin from T cell factor-to forkhead box O-mediated transcription. *J Biol Chem* 2007;**282**:27298−305.
112. Manolagas SC, Almeida M. Gone with the Wnts: β-catenin, T-cell factor, forkhead box O, and oxidative stress in age-dependent diseases of bone, lipid, and glucose metabolism. *Mol Endocrinol* 2007; **21**:2605−14.
113. Kousteni S. FoxOs: unifying links between oxidative stress and skeletal homeostasis. *Curr Osteoporos Rep* 2011;**9**:60−6.
114. Fontani F, Marcucci G, Iantomasi T, Brandi ML, Vincenzini MT. Glutathione, *N*-acetylcysteine and lipoic acid down-regulate starvation-induced apoptosis, RANKL/OPG ratio and sclerostin in osteocytes: involvement of JNK and ERK1/2 signalling. *Calcif Tissue Int* 2015;**96**:335−46.
115. He XF, Zhang L, Zhang CH, Zhao CR, Li H, Zhang LF, et al. Berberine alleviates oxidative stress in rats with osteoporosis through receptor activator of NF-κB/receptor activator of NF-κB ligand/osteoprotegerin (RANK/RANKL/OPG) pathway. *Bosn J Basic Med Sci* 2017;**17**:295−301.
116. Theoleyre S, Wittrant Y, Tat SK, Fortun Y, Redini F, Heymann D. The molecular triad OPG/RANK/RANKL: involvement in the

orchestration of pathophysiological bone remodeling. *Cytokine Growth Factor Rev* 2004;**15**:457−75.
117. Atashi F, Modarressi A, Pepper MS. The role of reactive oxygen species in mesenchymal stem cell adipogenic and osteogenic differentiation: a review. *Stem Cells Dev* 2015;**24**:1150−63.
118. Moerman EJ, Teng K, Lipschitz DA, Lecka-Czernik B. Aging activates adipogenic and suppresses osteogenic programs in mesenchymal marrow stroma/stem cells: the role of PPAR-γ2 transcription factor and TGF-β/BMP signaling pathways. *Aging Cell* 2004;**3**: 379−89.
119. Rodrigues M, Turner O, Stolz D, Griffith LG, Wells A. Production of reactive oxygen species by multipotent stromal cells/mesenchymal stem cells upon exposure to fas ligand. *Cell Transplant* 2012;**21**: 2171−87.
120. Zhang CS, Meng Y, Han JH. Emerging roles of mitochondrial functions and epigenetic changes in the modulation of stem cell fate. *Cell Mol Life Sci* 2024;**81**:26.
121. Theill LE, Boyle WJ, Penninger JM. RANK-L and RANK: T cells, bone loss, and mammalian evolution. *Annu Rev Immunol* 2002;**20**: 795−823.
122. Mangialardi G, Katare R, Oikawa A, Meloni M, Reni C, Emanueli C, et al. Diabetes causes bone marrow endothelial barrier dysfunction by activation of the RhoA−Rho-associated kinase signaling pathway. *Arterioscler Thromb Vasc Biol* 2013;**33**:555−64.
123. Zuo XZ, Tian C, Zhao NN, Ren WY, Meng Y, Jin X, et al. Tea polyphenols alleviate high fat and high glucose-induced endothelial hyperpermeability by attenuating ROS production *via* NADPH oxidase pathway. *BMC Res Notes* 2014;**7**:1−8.
124. Oliveira TC, Gomes MS, Gomes AC. The crossroads between infection and bone loss. *Microorganisms* 2020;**8**:1765.
125. Riegger J, Schoppa A, Ruths L, Haffner-Luntzer M, Ignatius A. Oxidative stress as a key modulator of cell fate decision in osteoarthritis and osteoporosis: a narrative review. *Cell Mol Biol Lett* 2023; **28**:76.
126. Bădilă AE, Rădulescu DM, Ilie A, Niculescu AG, Grumezescu AM, Rădulescu AR. Bone regeneration and oxidative stress: an updated overview. *Antioxidants* 2022;**11**:318.
127. Li J, Han F, Ma J, Wang H, Pan J, Yang G, et al. Targeting endogenous hydrogen peroxide at bone defects promotes bone repair. *Adv Funct Mater* 2021;**32**:2111208.
128. Wang BB, Huang Y, Cai Q, Du ZP, Li XM. Biomaterials for diabetic bone repair: influencing mechanisms, multi-aspect progress and future prospects. *Compos Part B: Eng* 2024;**274**:111282.
129. Sheikh Z, Brooks PJ, Barzilay O, Fine N, Glogauer M. Macrophages, foreign body giant cells and their response to implantable biomaterials. *Materials (Basel)* 2015;**8**:5671−701.
130. Mouthuy PA, Snelling SJB, Dakin SG, Milković L, Gašparović A, Carr AJ, et al. Biocompatibility of implantable materials: an oxidative stress viewpoint. *Biomaterials* 2016;**109**:55−68.
131. Ma L, Cheng Y, Feng XB, Zhang XG, Lei J, Wang HC, et al. A janus-ROS healing system promoting infectious bone regeneration *via* sono-epigenetic modulation. *Adv Mater* 2024;**36**:e2307846.
132. Barbieri SS, Cavalca V, Eligini S, Brambilla M, Caiani A, Tremoli E, et al. Apocynin prevents cyclooxygenase 2 expression in human monocytes through NADPH oxidase and glutathione redox-dependent mechanisms. *Free Radic Biol Med* 2004;**37**:156−65.
133. Schrder K. NADPH oxidases in bone homeostasis and osteoporosis. *Cell Mol Life Sci* 2015;**72**:25−38.
134. Li YR, Zhu H. Nanoceria potently reduce superoxide fluxes from mitochondrial electron transport chain and plasma membrane NADPH oxidase in human macrophages. *Mol Cell Biochem* 2021; **476**:4461−70.
135. Wei F, Neal CJ, Sakthivel TS, Kean T, Seal S, Coathup MJ. Multifunctional cerium oxide nanoparticles regulate inflammation and enhance osteogenesis. *Mater Sci Eng C Mater Biol Appl* 2021;**124**: 112041.
136. Liu X, Hou Y, Yang M, Xin X, Deng Y, Fu R, et al. *N*-Acetyl-L-cysteine-derived carbonized polymer dots with ROS scavenging *via* Keap1−Nrf2 pathway regulate alveolar bone homeostasis in periodontitis. *Adv Healthc Mater* 2023;**12**:e2300890.
137. Wang QT, Mu M, Yu W, Fan RR, Chen HF, Han B, et al. Engineering polyphenol-based osteogenic system for bone and cartilage repair: transplantation, tissue engineering, and organoid. *J Adv Res* 2025. S2090-1232(25)00476-X.
138. Gao ZR, Feng YZ, Zhao YQ, Zhao J, Zhou YH, Ye Q, et al. Traditional Chinese medicine promotes bone regeneration in bone tissue engineering. *Chin Med* 2022;**17**:86.
139. Xia E-Q, Deng G-F, Guo Y-J, Li H-B. Biological activities of polyphenols from grapes. *Int J Mol Sci* 2010;**11**:622−46.
140. Kamran S, Sinniah A, Abdulghani MAM, Alshawsh MA. Therapeutic potential of certain terpenoids as anticancer agents: a scoping review. *Cancers* 2022;**14**:1100.
141. Kandemir K, Tomas M, McClements DJ, Capanoglu E. Recent advances on the improvement of quercetin bioavailability. *Trends Food Sci Technol* 2022;**119**:192−200.
142. Orszulak L, Minecka A, Bernat R, Lamrani T, Jurkiewicz K, Hachuła B, et al. Hydrophilic and amphiphilic macromolecules as modulators of the physical stability and bioavailability of piribedil: a study on binary mixtures and micellar systems. *Mol Pharm* 2025;**22**: 4708−30.
143. Zhang M, Xu F, Cao JC, Dou QQ, Wang J, Wang J, et al. Research advances of nanomaterials for the acceleration of fracture healing. *Bioact Mater* 2024;**31**:368−94.
144. Du L, Li J, Chen C, Liu Y. Nanocarrier: a potential tool for future antioxidant therapy. *Free Radic Res* 2014;**48**:1061−9.
145. Li SL, Li HR, Xu XD, Saw PE, Zhang L. Nanocarrier-mediated antioxidant delivery for liver diseases. *Theranostics* 2020;**10**: 1262−80.
146. Zandieh M, Liu J. Nanozymes: definition, activity, and mechanisms. *Adv Mater* 2024;**36**:e2211041.
147. Huang X, He D, Pan Z, Luo G, Deng J. Reactive-oxygen-species-scavenging nanomaterials for resolving inflammation. *Mater Today Bio* 2021;**11**:100124.
148. Ciccarese F, Raimondi V, Sharova E, Silic-Benussi M, Ciminale V. Nanoparticles as tools to target redox homeostasis in cancer cells. *Antioxidants* 2020;**9**:211.
149. Khalil I, Yehye WA, Etxeberria AE, Alhadi AA, Dezfooli SM, Julkapli NBM, et al. Nanoantioxidants: recent trends in antioxidant delivery applications. *Antioxidants* 2019;**9**:24.
150. Birinci Y, Niazi JH, Aktay-Çetin O, Basaga H. Quercetin in the form of a nano-antioxidant ($QTiO_2$) provides stabilization of quercetin and maximizes its antioxidant capacity in the mouse fibroblast model. *Enzyme Microb Technol* 2020;**138**:109559.
151. Anwer MK, Al-Mansoor MA, Jamil S, Al-Shdefat R, Ansari MN, Shakeel F. Development and evaluation of PLGA polymer based nanoparticles of quercetin. *Int J Biol Macromol* 2016;**92**:213−9.
152. Bazylińska U, Pucek A, Sowa M, Matczak-Jon E, Wilk KA. Engineering of phosphatidylcholine-based solid lipid nanocarriers for flavonoids delivery. *Colloids Surf A Physicochem Eng Asp* 2014;**460**: 483−93.
153. Liu CZ, Ge SJ, Yang J, Xu YY, Zhao M, Xiong L, et al. Adsorption mechanism of polyphenols onto starch nanoparticles and enhanced antioxidant activity under adverse conditions. *J Funct Foods* 2016; **26**:632−44.
154. Xie XX, Tao Q, Zou YN, Zhang FY, Guo M, Wang Y, et al. PLGA nanoparticles improve the oral bioavailability of curcumin in rats: characterizations and mechanisms. *J Agric Food Chem* 2011;**59**: 9280−9.
155. Shaikh J, Ankola DD, Beniwal V, Singh D, Kumar MN. Nanoparticle encapsulation improves oral bioavailability of curcumin by at least 9-fold when compared to curcumin administered with piperine as absorption enhancer. *Eur J Pharm Sci* 2009;**37**:223−30.
156. Onoue S, Terasawa N, Nakamura T, Yuminoki K, Hashimoto N, Yamada S. Biopharmaceutical characterization of nanocrystalline solid dispersion of coenzyme Q10 prepared with cold wet-milling system. *Eur J Pharm Sci* 2014;**53**:118−25.

157. Wang S, Yu GC, Wang ZT, Jacobson O, Lin LS, Yang WJ, et al. Enhanced antitumor efficacy by a cascade of reactive oxygen species generation and drug release. *Angew Chem Int Ed Engl* 2019;**58**: 14758−63.
158. Chen WK, Zhang H, Zhou QR, Zhou FJ, Zhang Q, Su JC. *Smart hydrogels for bone reconstruction via modulating the microenvironment*, vol. 6. Research (Wash D C); 2023. p. 89.
159. Shen C, Gao M, Chen HM, Zhan YT, Lan QM, Li ZM, et al. Reactive oxygen species (ROS)-responsive nanoprobe for bioimaging and targeting therapy of osteoarthritis. *J Nanobiotechnology* 2021;**19**: 395.
160. Wu C, Yan J, Ge CL, Xie LC, He YJ, Zhao ZY, et al. Macrophage membrane-reversibly camouflaged nanotherapeutics accelerate fracture healing by fostering MSCs recruitment and osteogenic differentiation. *J Nanobiotechnology* 2024;**22**:411.
161. Gao J, Jiang XY, Lei SM, Cheng WH, Lai Y, Li M, et al. A region-confined PROTAC nanoplatform for spatiotemporally tunable protein degradation and enhanced cancer therapy. *Nat Commun* 2024;**15**: 6608.
162. Siafaka PI, Okur N, Karantas ID, Okur ME, Gündoğdu EA. Current update on nanoplatforms as therapeutic and diagnostic tools: a review for the materials used as nanotheranostics and imaging modalities. *Asian J Pharm Sci* 2021;**16**:24−46.
163. Zhao F, Su YX, Liu H, Zhao Y, Zhang L, Zhuge NS, et al. Facile nanocomposite hydrogel scaffold with sustained drug release and osteo-immunomodulatory effects to enhance bone regeneration. *ACS Appl Mater Interfaces* 2025;**17**:19286−303.
164. Chen FM, Zhang M, Wu ZF. Toward delivery of multiple growth factors in tissue engineering. *Biomaterials* 2010;**31**:6279−308.
165. Basmanav FB, Kose GT, Hasirci V. Sequential growth factor delivery from complexed microspheres for bone tissue engineering. *Biomaterials* 2008;**29**:4195−204.
166. Richardson TP, Peters MC, Ennett AB, Mooney DJ. Polymeric system for dual growth factor delivery. *Nat Biotechnol* 2001;**19**: 1029−34.
167. Xue S, Zhou XJ, Sang WL, Wang C, Lu HM, Xu YM, et al. Cartilage-targeting peptide-modified dual-drug delivery nanoplatform with NIR laser response for osteoarthritis therapy. *Bioact Mater* 2021;**6**:2372−89.
168. Ho LWC, Liu Y, Han R, Bai Q, Choi CHJ. Nano-cell interactions of non-cationic bionanomaterials. *Acc Chem Res* 2019;**52**:1519−30.
169. Behzadi S, Serpooshan V, Tao W, Hamaly MA, Alkawareek MY, Dreaden EC, et al. Cellular uptake of nanoparticles: journey inside the cell. *Chem Soc Rev* 2017;**46**:4218−44.
170. Antônio E, Antunes ODRJ, de Araújo IS, Khalil NM, Mainardes RM. Poly(lactic acid) nanoparticles loaded with ursolic acid: characterization and *in vitro* evaluation of radical scavenging activity and cytotoxicity. *Mater Sci Eng C Mater Biol Appl* 2017;**71**:156−66.
171. Mitchell MJ, Billingsley MM, Haley RM, Wechsler ME, Peppas NA, Langer R. Engineering precision nanoparticles for drug delivery. *Nat Rev Drug Discov* 2021;**20**:101−24.
172. Yang YL, Xiang Y, Xu P, Zhang WB, Wang YW, Feng LB, et al. Immuno-osteoinductive 3D printed hydrogel scaffolds with triple crosslinking and GA/EGCG release for bone healing. *Colloids Surf B Biointerfaces* 2025;**252**:114651.
173. Wang ZJ, Chen TT, Wu ZM, Jiang XZ, Hou QD, Miao SK, et al. The dual-effects of PLGA@MT electrospun nanofiber coatings on promoting osteogenesis at the titanium-bone interface under diabetic conditions. *J Mater Chem B* 2022;**10**:4020−30.
174. He ZR, Sun CH, Ma YF, Chen X, Wang Y, Chen K, et al. Rejuvenating aged bone repair through multihierarchy reactive oxygen species-regulated hydrogel. *Adv Mater* 2024;**36**:e2306552.
175. He YW, Luo ZW, Nie XS, Du YM, Sun R, Sun JM, et al. An injectable multi-functional composite bioactive hydrogel for bone regeneration *via* immunoregulatory and osteogenesis effects. *Adv Compos Hybrid Mater* 2025;**8**:128.
176. Ming PY, Liu YF, Yu PY, Jiang XY, Yuan LL, Cai SY, et al. A biomimetic Se-nHA/PC composite microsphere with synergistic immunomodulatory and osteogenic ability to activate bone regeneration in periodontitis. *Small* 2024;**20**:e2305490.
177. Chen D, Liang ZT, Su ZK, Huang JY, Pi YX, Ouyang YT, et al. Selenium-doped mesoporous bioactive glass regulates macrophage metabolism and polarization by scavenging ROS and promotes bone regeneration *in vivo*. *ACS Appl Mater Interfaces* 2023;**15**:34378−96.
178. Liu XC, Hou YB, Yang MX, Xin XR, Deng Y, Fu RB, et al. *N*-Acetyl-L-cysteine-derived carbonized polymer dots with ROS scavenging *via* Keap1−Nrf2 pathway regulate alveolar bone homeostasis in periodontitis. *Adv Healthc Mater* 2023;**12**:e2300890.
179. Byun H, Jang GN, Lee J, Hong MH, Shin H, Shin H. Stem cell spheroid engineering with osteoinductive and ROS scavenging nanofibers for bone regeneration. *Biofabrication* 2021;**13**:034101.
180. Nsairat H, Khater D, Sayed U, Odeh F, Al Bawab A, Alshaer W. Liposomes: structure, composition, types, and clinical applications. *Heliyon* 2022;**8**:e09394.
181. Torchilin VP. Recent advances with liposomes as pharmaceutical carriers. *Nat Rev Drug Discov* 2005;**4**:145−60.
182. Gonzalez Gomez A, Hosseinidoust Z. Liposomes for antibiotic encapsulation and delivery. *ACS Infect Dis* 2020;**6**:896−908.
183. Di J, Xie F, Xu Y. When liposomes met antibodies: drug delivery and beyond. *Adv Drug Deliv Rev* 2020;**154-155**:151−62.
184. Anselmo AC, Mitragotri S. Nanoparticles in the clinic: an update. *Bioeng Transl Med* 2019;**4**:e10143.
185. Sedighi M, Sieber S, Rahimi F, Shahbazi MA, Rezayan AH, Huwyler J, et al. Rapid optimization of liposome characteristics using a combined microfluidics and design-of-experiment approach. *Drug Deliv Transl Res* 2019;**9**:404−13.
186. Sercombe L, Veerati T, Moheimani F, Wu SY, Sood AK, Hua S. Advances and challenges of liposome assisted drug delivery. *Front Pharmacol* 2015;**6**:286.
187. Sun H, Xu J, WangYANG YF, Shen SY, Xu XQ, Zhang L, et al. Bone microenvironment regulative hydrogels with ROS scavenging and prolonged oxygen-generating for enhancing bone repair. *Bioact Mater* 2023;**24**:477−96.
188. Xiao L, Lin JY, Chen RY, Huang Y, Liu Y, Bai JX, et al. Sustained release of melatonin from GelMA liposomes reduced osteoblast apoptosis and improved implant osseointegration in osteoporosis. *Oxid Med Cell Longev* 2020;**2020**:6797154.
189. Zielińska A, Carreiró F, Oliveira AM, Neves A, Pires B, Venkatesh DN, et al. Polymeric nanoparticles: production, characterization, toxicology and ecotoxicology. *Molecules* 2020;**25**:3731.
190. Sairam AB, Sanmugam A, Pushparaj A, Mahesh Kumar G, Sundarapandian N, Balaji S, et al. Toxicity of polymeric nanodrugs as drug carriers. *ACS Chem Health Saf* 2023;**30**:236−50.
191. Beach MA, Nayanathara U, Gao Y, Zhang C, Xiong Y, Wang Y, et al. Polymeric nanoparticles for drug delivery. *Chem Rev* 2024;**124**: 5505−616.
192. Patra JK, Das G, Fraceto LF, Campos EVR, Rodriguez-Torres MDP, Acosta-Torres LS, et al. Nano based drug delivery systems: recent developments and future prospects. *J Nanobiotechnology* 2018;**16**: 71.
193. Park JS, Jeon HY, Lee Y, Cheon SY, Lee DH, Lim SG, et al. Rapid DNA repair in mesenchymal stem cells and bone regeneration by nanoparticle-based codelivery of *Nrf2*-mRNA and dexamethasone. *ACS Nano* 2024;**18**:31877−90.
194. Chen TT, Wu ZM, Hou QD, Mei YX, Yang KK, Xu J, et al. The dual angiogenesis effects *via* Nrf2/HO-1 signaling pathway of melatonin nanocomposite scaffold on promoting diabetic bone defect repair. *Int J Nanomed* 2024;**19**:2709−32.
195. Ghezzi M, Pescina S, Padula C, Santi P, Del Favero E, Cantù L, et al. Polymeric micelles in drug delivery: an insight of the techniques for their characterization and assessment in biorelevant conditions. *J Control Release* 2021;**332**:312−36.
196. Su H, Wang FH, Ran W, Zhang WJ, Dai WB, Wang H, et al. The role of critical micellization concentration in efficacy and toxicity of supramolecular polymers. *Proc Natl Acad Sci U S A* 2020;**117**: 4518−26.

197. Junnuthula V, Kolimi P, Nyavanandi D, Sampathi S, Vora LK, Dyawanapelly S. Polymeric micelles for breast cancer therapy: recent updates, clinical translation and regulatory considerations. *Pharmaceutics* 2022;**14**:1860.
198. Lu Y, Park K. Polymeric micelles and alternative nanonized delivery vehicles for poorly soluble drugs. *Int J Pharm* 2013;**453**:198−214.
199. Zhang Y, Huang Y, Li S. Polymeric micelles: nanocarriers for cancer-targeted drug delivery. *AAPS PharmSciTech* 2014;**15**:862−71.
200. Wang ZH, Pan JM, Yuan RT, Chen M, Guo X, Zhou SB. Shell-sheddable polymeric micelles alleviate oxidative stress and inflammation for enhanced ischemic stroke therapy. *Nano Lett* 2023;**23**: 6544−52.
201. He ZR, Sun CH, Ma YF, Chen X, Wang Y, Chen K, et al. Rejuvenating aged bone repair through multihierarchy reactive oxygen species-regulated hydrogel. *Adv Mater* 2024;**36**:2306552.
202. Janjua TI, Cao Y, Yu C, Popat A. Clinical translation of silica nanoparticles. *Nat Rev Mater* 2021;**6**:1072−4.
203. McLean B, Yarovsky I. Structure, properties, and applications of silica nanoparticles: recent theoretical modeling advances, challenges, and future directions. *Small* 2024;**20**:e2405299.
204. You YH, Ma WZ, Wang FA, Jiao GJ, Zhang L, Zhou HM, et al. Ortho-silicic acid enhances osteogenesis of osteoblasts through the upregulation of miR-130b which directly targets PTEN. *Life Sci* 2021;**264**:118680.
205. Corma A, Botella P, Rivero-Buceta E. Silica-based stimuli-responsive systems for antitumor drug delivery and controlled release. *Pharmaceutics* 2022;**14**:110.
206. Bruckmann FDS, Nunes FB, Salles TDR, Franco C, Cadoná FC, Bohn Rhoden CR. Biological applications of silica-based nanoparticles. *Magnetochemistry* 2022;**8**:131.
207. Li CL, Wang Q, Gu XH, Kang YJ, Zhang YX, Hu YY, et al. Porous Se@SiO_2 nanocomposite promotes migration and osteogenic differentiation of rat bone marrow mesenchymal stem cell to accelerate bone fracture healing in a rat model. *Int J Nanomed* 2019;**14**: 3845−60.
208. Noureddine A, Maestas-Olguin A, Tang L, Corman-Hijar JI, Olewine M, Krawchuck JA, et al. Future of mesoporous silica nanoparticles in nanomedicine: protocol for reproducible synthesis, characterization, lipid coating, and loading of therapeutics (chemotherapeutic, proteins, siRNA and mRNA). *ACS Nano* 2023;**17**: 16308−25.
209. Xu C, Niu Y, Popat A, Jambhrunkar S, Karmakar S, Yu C. Rod-like mesoporous silica nanoparticles with rough surfaces for enhanced cellular delivery. *J Mater Chem B* 2014;**2**:253−6.
210. Lin YH, Chen YP, Liu TP, Chien FC, Chou CM, Chen CT, et al. Approach to deliver two antioxidant enzymes with mesoporous silica nanoparticles into cells. *ACS Appl Mater Interfaces* 2016;**8**: 17944−54.
211. Zhu JH, Niu YM, Li Y, Gong YX, Shi H, Huo Q, et al. Stimuli-responsive delivery vehicles based on mesoporous silica nanoparticles: recent advances and challenges. *J Mater Chem B* 2017;**5**: 1339−52.
212. Xu BL, Li SS, Shi R, Liu HY. Multifunctional mesoporous silica nanoparticles for biomedical applications. *Signal Transduct Target Ther* 2023;**8**:435.
213. Wang YJ, Tang B, Zhou MH, Li BH, Lu XJ, Geng HM, et al. Core−shell codelivery nanocarrier synergistically regulates cartilaginous immune microenvironment for total meniscus replacement. *ACS Nano* 2025;**19**:15474−90.
214. Zhou H, Lee J. Nanoscale hydroxyapatite particles for bone tissue engineering. *Acta Biomater* 2011;**7**:2769−81.
215. Wang T, Guo S, Zhang Y. Effect of nHA/CS/PLGA delivering adipose stem cell-derived exosomes and bone marrow stem cells on bone healing-*in vitro* and *in vivo* studies. *Sci Rep* 2024;**14**:27502.
216. He YQ, Dong YH, Cui FZ, Chen XJ, Lin RQ. Ectopic osteogenesis and scaffold biodegradation of nano-hydroxyapatite-chitosan in a rat model. *PLoS One* 2015;**10**:e0135366.
217. Mohan N, Palangadan R, Fernandez FB, Varma H. Preparation of hydroxyapatite porous scaffold from a 'coral-like' synthetic inorganic precursor for use as a bone substitute and a drug delivery vehicle. *Mater Sci Eng C Mater Biol Appl* 2018;**92**:329−37.
218. Li JN, Li L, Wu TK, Shi K, Bei ZW, Wang M, et al. An injectable thermosensitive hydrogel containing resveratrol and dexamethasone-loaded carbonated hydroxyapatite microspheres for the regeneration of osteoporotic bone defects. *Small Methods* 2024;**8**:2300843.
219. Skallevold HE, Rokaya D, Khurshid Z, Zafar MS. Bioactive glass applications in dentistry. *Int J Mol Sci* 2019;**20**:5960.
220. Marelli B, Ghezzi CE, Mohn D, Stark WJ, Barralet JE, Boccaccini AR, et al. Accelerated mineralization of dense collagen-nano bioactive glass hybrid gels increases scaffold stiffness and regulates osteoblastic function. *Biomaterials* 2011;**32**:8915−26.
221. Schumacher M, Habibovic P, van Rijt S. Mesoporous bioactive glass composition effects on degradation and bioactivity. *Bioact Mater* 2021;**6**:1921−31.
222. Yao HY, Turali Emre ES, Fan Y, Wang JL, Liu F, Wei JC. L-arginine modified mesoporous bioactive glass with ROS scavenging and NO release for periodontitis treatment. *Bioact Mater* 2025;**48**:200−16.
223. Cui L, Ren X, Sun MT, Liu HY, Xia LX. Carbon dots: synthesis, properties and applications. *Nanomaterials (Basel)* 2021;**11**:3419.
224. Heo SC, Shin HW, Lee DJ, Garcia-Godoy F, Keum BR, Kwon YH, et al. Tartaric acid-branched polyethyleneimine carbon dots promote repair of bone defect *via* osteogenic differentiation. *Regen Biomater* 2025;**12**:rbaf030.
225. Innocenzi P, Stagi L. Carbon dots as oxidant-antioxidant nanomaterials, understanding the structure-properties relationship. A critical review. *Nano Today* 2023;**50**:101837.
226. Liu JJ, Li R, Yang B. Carbon dots: a new type of carbon-based nanomaterial with wide applications. *ACS Cent Sci* 2020;**6**:2179−95.
227. Alafeef M, Srivastava I, Aditya T, Pan D. Carbon dots: from synthesis to unraveling the fluorescence mechanism. *Small* 2024;**20**: e2303937.
228. Gedda G, Sankaranarayanan SA, Putta CL, Gudimella KK, Rengan AK, Girma WM. Green synthesis of multi-functional carbon dots from medicinal plant leaves for antimicrobial, antioxidant, and bioimaging applications. *Sci Rep* 2023;**13**:6371.
229. Kar DK, V P, Si S, Panigrahi H, Mishra S. Carbon dots and their polymeric nanocomposites: insight into their synthesis, photoluminescence mechanisms, and recent trends in sensing applications. *ACS Omega* 2024;**9**:11050−80.
230. Qi J, Zhang PF, Zhang T, Zhang R, Zhang QM, Wang J, et al. Metal-doped carbon dots for biomedical applications: from design to implementation. *Heliyon* 2024;**10**:e32133.
231. Chen QL, Ma JJ, Yu SY, Su Y, Guo HB, Jiang H, et al. "Small dots, multiple functions": unveiling the veil of a bioactive quercetin carbon dot and its multifaceted antibacterial and osteogenesis mechanisms for infectious bone defect repair. *Adv Funct Mater* 2025:2507840.
232. Xin XR, Liu JJ, Liu XC, Xin Y, Hou YB, Xiang XC, et al. Melatonin-derived carbon dots with free radical scavenging property for effective periodontitis treatment *via* the Nrf2/HO-1 pathway. *ACS Nano* 2024;**18**:8307−24.
233. Fu Y, Zhang JB, Lin H, Mo A. 2D titanium carbide (MXene) nanosheets and 1D hydroxyapatite nanowires into free standing nanocomposite membrane: *in vitro* and *in vivo* evaluations for bone regeneration. *Mater Sci Eng C* 2021;**118**:111367.
234. Yang SY, Zhu Y, Ji CX, Zhu HM, Lao A, Zhao R, et al. A five-in-one novel MOF-modified injectable hydrogel with thermo-sensitive and adhesive properties for promoting alveolar bone repair in periodontitis: antibacterial, hemostasis, immune reprogramming, pro-osteo-/angiogenesis and recruitment. *Bioact Mater* 2024;**41**:239−56.
235. Li MM, Yin SH, Lin MZ, Chen XL, Pan Y, Peng YQ, et al. Current status and prospects of metal-organic frameworks for bone therapy and bone repair. *J Mater Chem B* 2022;**10**:5105−28.
236. Li XL, Xiong F, Wang SG, Zhang ZJ, Dai JH, Chen H, et al. *N*-Acetyl-cysteine-loaded biomimetic nanofibrous scaffold for

osteogenesis of induced-pluripotent-stem-cell-derived mesenchymal stem cells and bone regeneration. *Front Bioeng Biotechnol* 2021;**9**:767641.
237. Zhang MZ, Zhai XY, Ma TF, Huang YK, Jin MD, Yang HZ, et al. Sequential therapy for bone regeneration by cerium oxide-reinforced 3D-printed bioactive glass scaffolds. *ACS Nano* 2023;**17**:4433−44.
238. Bai MR, Wang T, Xing ZY, Huang HJ, Wu XZ, Adeli M, et al. Electron-donable heterojunctions with synergetic Ru−Cu pair sites for biocatalytic microenvironment modulations in inflammatory mandible defects. *Nat Commun* 2024;**15**:9592.
239. Xu RH, You YY, Zheng WY, Ma L, Chang YZ, Pan SY, et al. Selenoprotein-regulated hydrogel for ultrasound-controlled microenvironment remodeling to promote bone defect repair. *Adv Funct Mater* 2024;**34**:2313122.
240. Shu CQ, Qin C, Chen L, Wang YF, Shi Z, Yu JM, et al. Metal-organic framework functionalized bioceramic scaffolds with antioxidative activity for enhanced osteochondral regeneration. *Adv Sci* 2023;**10**:e2206875.
241. Yang JL, Liang J, Zhu Y, Hu M, Deng LF, Cui WG, et al. Fullerol-hydrogel microfluidic spheres for *in situ* redox regulation of stem cell fate and refractory bone healing. *Bioact Mater* 2021;**6**:4801−15.
242. Qin DL, Zhao YF, Cheng R, Liu YY, Guo SS, Sun LX, et al. Mussel-inspired immunomodulatory and osteoinductive dual-functional hydroxyapatite nanoplatform for promoting bone regeneration. *J Nanobiotechnol* 2024;**22**:320.
243. Liu ZQ, Wang TL, Zhang L, Luo YP, Zhao JH, Chen YX, et al. Metal-phenolic networks-reinforced extracellular matrix scaffold for bone regeneration *via* combining radical-scavenging and photo-responsive regulation of microenvironment. *Adv Healthc Mater* 2024;**13**:e2304158.
244. Mac CH, Chan HY, Lin YH, Sharma AK, Song HL, Chan YS, et al. Engineering a biomimetic bone scaffold that can regulate redox homeostasis and promote osteogenesis to repair large bone defects. *Biomaterials* 2022;**286**:121574.
245. Sheng Y, Abreu IA, Cabelli DE, Maroney MJ, Miller AF, Teixeira M, et al. Superoxide dismutases and superoxide reductases. *Chem Rev* 2014;**114**:3854−918.
246. Kirkman HN, Gaetani GF. Mammalian catalase: a venerable enzyme with new mysteries. *Trends Biochem Sci* 2007;**32**:44−50.
247. Flohé L, Toppo S, Orian L. The glutathione peroxidase family: discoveries and mechanism. *Free Radic Biol Med* 2022;**187**:113−22.
248. Gao LZ, Zhuang J, Nie L, Zhang JB, Zhang Y, Gu N, et al. Intrinsic peroxidase-like activity of ferromagnetic nanoparticles. *Nat Nanotechnol* 2007;**2**:577−83.
249. Wu JX, Wang XY, Wang Q, Lou ZP, Li SR, Zhu YY, et al. Nanomaterials with enzyme-like characteristics (nanozymes): next-generation artificial enzymes (ii). *Chem Soc Rev* 2019;**48**:1004−76.
250. Yang WP, Yang X, Zhu LJ, Chu HS, Li XY, Xu WT. Nanozymes: activity origin, catalytic mechanism, and biological application. *Coord Chem Rev* 2021;**448**:214170.
251. Yang J, Yang YW. Metal-organic frameworks for biomedical applications. *Small* 2020;**16**:e1906846.
252. Chen MW, Wang D, Li MH, He Y, He TT, Chen MH, et al. Nanocatalytic biofunctional MOF coating on titanium implants promotes osteoporotic bone regeneration through cooperative pro-osteoblastogenesis MSC reprogramming. *ACS Nano* 2022;**16**:15397−412.
253. Lee J, Farha OK, Roberts J, Scheidt KA, Nguyen ST, Hupp JT. Metal-organic framework materials as catalysts. *Chem Soc Rev* 2009;**38**:1450−9.
254. Wu Y, Ta HT. Different approaches to synthesising cerium oxide nanoparticles and their corresponding physical characteristics, and ROS scavenging and anti-inflammatory capabilities. *J Mater Chem B* 2021;**9**:7291−301.
255. Lord MS, Berret JF, Singh S, Vinu A, Karakoti AS. Redox active cerium oxide nanoparticles: current status and burning issues. *Small* 2021;**17**:e2102342.
256. Saifi MA, Seal S, Godugu C. Nanoceria, the versatile nanoparticles: promising biomedical applications. *J Control Release* 2021;**338**:164−89.
257. Zhang Y, Zhao SN, Feng J, Song SY, Shi WD, Wang D, et al. Unraveling the physical chemistry and materials science of CeO_2-based nanostructures. *Chem* 2021;**7**:2022−59.
258. Brandão Da Silva Assis M, Nestal De Moraes G, De Souza KR. Cerium oxide nanoparticles: chemical properties, biological effects and potential therapeutic opportunities. *Biomed Rep* 2024;**20**:48.
259. Skorodumova NV, Simak SI, Lundqvist BI, Abrikosov IA, Johansson B. Quantum origin of the oxygen storage capability of Ceria. *Phys Rev Lett* 2002;**89**:166601.
260. Hojo H, Mizoguchi T, Ohta H, Findlay SD, Shibata N, Yamamoto T, et al. Atomic structure of a CeO_2 grain boundary: the role of oxygen vacancies. *Nano Lett* 2010;**10**:4668−72.
261. Chen SY, Wang YR, Bao SL, Yao L, Fu X, Yu Y, et al. Cerium oxide nanoparticles in wound care: a review of mechanisms and therapeutic applications. *Front Bioeng Biotechnol* 2024;**12**:1404651.
262. Heckert EG, Karakoti AS, Seal S, Self WT. The role of cerium redox state in the SOD mimetic activity of nanoceria. *Biomaterials* 2008;**29**:2705−9.
263. Ma YY, Tian ZM, Zhai WF, Qu YQ. Insights on catalytic mechanism of CeO_2 as multiple nanozymes. *Nano Res* 2022;**15**:10328−42.
264. Wang ZZ, Shen XM, Gao XF, Zhao YL. Simultaneous enzyme mimicking and chemical reduction mechanisms for nanoceria as a bio-antioxidant: a catalytic model bridging computations and experiments for nanozymes. *Nanoscale* 2019;**11**:13289−99.
265. Shao DD, Li K, Hu T, Wang SJ, Xu HW, Zhang SB, et al. Titania nanotube array supported nanoceria with redox cycling stability ameliorates oxidative stress-inhibited osteogenesis. *Chem Eng J* 2021;**415**:128913.
266. Campbell CT, Peden CH. Chemistry. Oxygen vacancies and catalysis on ceria surfaces. *Science* 2005;**309**:713−4.
267. Esch F, Fabris S, Zhou L, Montini T, Africh C, Fornasiero P, et al. Electron localization determines defect formation on ceria substrates. *Science* 2005;**309**:752−5.
268. Zhang JK, Yang Y, Qin FM, Hu TT, Zhao XS, Zhao SC, et al. Catalyzing generation and stabilization of oxygen vacancies on CeO_{2-x} nanorods by Pt nanoclusters as nanozymes for catalytic therapy. *Adv Healthc Mater* 2023;**12**:e2302056.
269. Zhu MY, Wen YF, Song SG, Zheng AQ, Li JC, Sun WW, et al. Synergistic effects between polyvinylpyrrolidone and oxygen vacancies on improving the oxidase-mimetic activity of flower-like CeO_2 nanozymes. *Nanoscale* 2020;**12**:19104−11.
270. Trovarelli A, Llorca J. Ceria catalysts at nanoscale: how do crystal shapes shape catalysis?. *ACS Catal* 2017;**7**:4716−35.
271. Hao X, Yoko A, Chen C, Inoue K, Saito M, Seong G, et al. Atomic-scale valence state distribution inside ultrafine CeO_2 nanocubes and its size dependence. *Small* 2018;**14**:e1802915.
272. Chen BH, Stephen Inbaraj B. Various physicochemical and surface properties controlling the bioactivity of cerium oxide nanoparticles. *Crit Rev Biotechnol* 2018;**38**:1003−24.
273. Deshpande S, Patil S, Kuchibhatla S, Seal S. Size dependency variation in lattice parameter and valency states in nanocrystalline cerium oxide. *Appl Phys Lett* 2005;**87**:133113.
274. Lee SS, Song W, Cho M, Puppala HL, Nguyen P, Zhu H, et al. Antioxidant properties of cerium oxide nanocrystals as a function of nanocrystal diameter and surface coating. *ACS Nano* 2013;**7**:9693−703.
275. Ren SS, Zhou Y, Zheng K, Xu XW, Yang J, Wang XY, et al. Cerium oxide nanoparticles loaded nanofibrous membranes promote bone regeneration for periodontal tissue engineering. *Bioact Mater* 2022;**7**:242−53.
276. Singh R, Singh S. Role of phosphate on stability and catalase mimetic activity of cerium oxide nanoparticles. *Colloids Surf B Biointerfaces* 2015;**132**:78−84.
277. Singh S, Dosani T, Karakoti AS, Kumar A, Seal S, Self WT. A phosphate-dependent shift in redox state of cerium oxide

nanoparticles and its effects on catalytic properties. *Biomaterials* 2011;**32**:6745−53.
278. Panferov VG, Zhang W, D'Abruzzo N, Wang S, Liu J. Kinetic profiling of oxidoreductase-mimicking nanozymes: impact of multiple activities, chemical transformations, and colloidal stability. *ACS Nano* 2024;**18**:34870−83.
279. Shen XM, Liu WQ, Gao XJ, Lu ZH, Wu XC, Gao XF. Mechanisms of oxidase and superoxide dismutation-like activities of gold, silver, platinum, and palladium, and their alloys: a general way to the activation of molecular oxygen. *J Am Chem Soc* 2015;**137**: 15882−91.
280. Gao XC, Zhang JJ, Gong YN, Yan L. The biomedical applications of nanozymes in orthopaedics based on regulating reactive oxygen species. *J Nanobiotechnol* 2024;**22**:569.
281. Liu L, Zhang SF, Chen XZ, Li G, Zhe YD, Li YH, et al. Spin-cooperated catalytic activities in MnN_4-based single-atom nanozyme: mechanisms and a brief charge-spin machine learning model. *Chem Mater* 2024;**36**:2971−84.
282. Wang CG, Guan YK, Lv MZ, Zhang R, Guo ZY, Wei XM, et al. Manganese increases the sensitivity of the cGAS−STING pathway for double-stranded DNA and is required for the host defense against DNA viruses. *Immunity* 2018;**48**:675−87.
283. Li JM, Deng CJ, Liang WY, Kang F, Bai Y, Ma B, et al. Mn-containing bioceramics inhibit osteoclastogenesis and promote osteoporotic bone regeneration *via* scavenging ROS. *Bioact Mater* 2021;**6**: 3839−50.
284. Li Y, Pan Q, Xu JK, He X, Li HA, Oldridge DA, et al. Overview of methods for enhancing bone regeneration in distraction osteogenesis: potential roles of biometals. *J Orthop Translat* 2021;**27**:110−8.
285. Yang YP, Yao ZY, Sun YY, Nie YY, Zhang YC, Li ZY, et al. 3D-printed manganese dioxide incorporated scaffold promotes osteogenic-angiogenic coupling for refractory bone defect by remodeling osteo-regenerative microenvironment. *Bioact Mater* 2025;**44**:354−70.
286. Feng KZ, Wang ZZ, Wang SW, Wang GC, Dong HJ, He HL, et al. Elucidating the catalytic mechanism of prussian blue nanozymes with self-increasing catalytic activity. *Nat Commun* 2024;**15**:5908.
287. Chen L, Tang SJ, Zhang JM, Zhong CY, Xu XQ, Yan J, et al. Prussian blue nanohybridized multicellular spheroids as composite engraftment for antioxidant bone regeneration and photoacoustic tomography. *ACS Nano* 2024;**18**:24770−83.
288. Sun YM, Mu SD, Xing ZY, Guo JS, Wu ZH, Yu FY, et al. Catalase-mimetic artificial biocatalysts with Ru catalytic centers for ROS elimination and stem-cell protection. *Adv Mater* 2022;**34**:e2206208.
289. Lin PH, Qian ZY, Liu SB, Ye X, Xue PP, Shao YJ, et al. A single-cell RNA sequencing guided multienzymatic hydrogel design for self-regenerative repair in diabetic mandibular defects. *Adv Mater* 2024;**36**:e2410962.
290. Wang T, Bai MR, Geng W, Adeli M, Ye L, Cheng C. Bioinspired artificial antioxidases for efficient redox homeostasis and maxillofacial bone regeneration. *Nat Commun* 2025;**16**:856.
291. Liao X, Shen MK, Li TB, Feng L, Lin Z, Shi G, et al. Combined molybdenum gelatine methacrylate injectable nano-hydrogel effective against diabetic bone regeneration. *Int J Nanomed* 2023;**18**: 5925−42.
292. Wang JC, Zhang CG, Zhang WS, Liu WW, Guo YR, Dang PR, et al. Ultrathin WOx nanoribbons with moderate ROS clearance and antibacterial abilities efficiently induce M2 macrophage polarization for diabetic bone defect repair. *Adv Funct Mater* 2024;**34**:2306319.
293. Yuan M, Kermanian M, Agarwal T, Yang Z, Yousefiasl S, Cheng Z, et al. Defect engineering in biomedical sciences. *Adv Mater* 2023;**35**: 2304176.
294. Cheng Z, Wang YC, Lin HB, Chen ZY, Qin R, Wang TX, et al. Engineering dual active sites and defect structure in nanozymes to reprogram jawbone microenvironment for osteoradionecrosis therapy. *Adv Sci* 2025;**12**:2413215.
295. Liu R, Sun MZ, Liu XJ, Lv ZH, Yu XY, Wang JM, et al. Enhanced metal-support interactions boost the electrocatalytic water splitting of supported ruthenium nanoparticles on a Ni_3 N/NiO heterojunction at industrial current density. *Angew Chem Int Ed Engl* 2023;**62**: e202312644.
296. Jiang ZY, Tian MJ, Jing MZ, Chai SN, Jian YF, Chen CW, et al. Modulating the electronic metal-support interactions in single-atom Pt(1)-CuO catalyst for boosting acetone oxidation. *Angew Chem Int Ed Engl* 2022;**61**:e202200763.
297. Bagheri N, Habibi B, Khataee A, Hassanzadeh J. Application of surface molecular imprinted magnetic graphene oxide and high performance mimetic behavior of bi-metal ZnCo MOF for determination of atropine in human serum. *Talanta* 2019;**201**:286−94.
298. Hui YJ, Mao JN, Rui M, Huang YY, Jiang XZ, Xu YC, et al. Hydrogel microsphere-encapsulated bimetallic nanozyme for promoting diabetic bone regeneration *via* glucose consumption and ROS scavenging. *Adv Healthc Mater* 2024;**13**:2402596.
299. Zhou HC, Long JR, Yaghi OM. Introduction to metal-organic frameworks. *Chem Rev* 2012;**112**:673−4.
300. Zhao CQ, Shu CQ, Yu JM, Zhu YF. Metal-organic frameworks functionalized biomaterials for promoting bone repair. *Mater Today Bio* 2023;**21**:100717.
301. Zhang XL, Tu RX, Lu Z, Peng JY, Hou CT, Wang ZH. Hierarchical mesoporous metal−organic frameworks encapsulated enzymes: progress and perspective. *Coord Chem Rev* 2021;**443**:214032.
302. Wang Y, Yan JH, Wen NC, Xiong HJ, Cai SD, He QY, et al. Metal-organic frameworks for stimuli-responsive drug delivery. *Biomaterials* 2020;**230**:119619.
303. Yao XL, Chen XR, Sun Y, Yang PX, Gu XS, Dai X. Application of metal-organic frameworks-based functional composite scaffolds in tissue engineering. *Regen Biomater* 2024;**11**:rbae009.
304. Kang Y, Xu C, Meng LA, Dong XF, Qi M, Jiang DQ. Exosome-functionalized magnesium-organic framework-based scaffolds with osteogenic, angiogenic and anti-inflammatory properties for accelerated bone regeneration. *Bioact Mater* 2022;**18**:26−41.
305. Tao BL, Yi WW, Qin X, Wu JJ, Li K, Guo A, et al. Improvement of antibacterial, anti-inflammatory, and osteogenic properties of OGP loaded co-MOF coating on titanium implants for advanced osseointegration. *J Mater Sci Technol* 2023;**146**:131−44.
306. Si YH, Liu HY, Yu HY, Jiang XZ, Sun DB. MOF-derived CuO@ZnO modified titanium implant for synergistic antibacterial ability, osteogenesis and angiogenesis. *Colloids Surf B Biointerfaces* 2022; **219**:112840.
307. Ni T, Zhu YM, Hao L, Chen Y, Cheng T. Preparation of photothermal-sensitive PDGF@ZIF-8-PDA@COL/PLGA-TCP composite scaffolds for bone defect repair. *Mater Des* 2022;**217**: 110643.
308. Ma L, Jiang FB, Fan X, Wang LY, He C, Zhou M, et al. Metal-organic-framework-engineered enzyme-mimetic catalysts. *Adv Mater* 2020;**32**:e2003065.
309. Pascanu V, González Miera G, Inge AK, Martín-Matute B. Metal−organic frameworks as catalysts for organic synthesis: a critical perspective. *J Am Chem Soc* 2019;**141**:7223−34.
310. Korzyński MD, Consoli DF, Zhang S, Román-Leshkov Y, Dincă M. Activation of methyltrioxorhenium for olefin metathesis in a zirconium-based metal−organic framework. *J Am Chem Soc* 2018; **140**:6956−60.
311. Deng HX, Doonan CJ, Furukawa H, Ferreira RB, Towne J, Knobler CB, et al. Multiple functional groups of varying ratios in metal-organic frameworks. *Science* 2010;**327**:846−50.
312. Xiao DJ, Oktawiec J, Milner PJ, Long JR. Pore environment effects on catalytic cyclohexane oxidation in expanded Fe_2(dobdc) analogues. *J Am Chem Soc* 2016;**138**:14371−9.
313. Fracaroli AM, Siman P, Nagib DA, Suzuki M, Furukawa H, Toste FD, et al. Seven post-synthetic covalent reactions in tandem leading to enzyme-like complexity within metal−organic framework crystals. *J Am Chem Soc* 2016;**138**:8352−5.
314. Bloch WM, Burgun A, Coghlan CJ, Lee R, Coote ML, Doonan CJ, et al. Capturing snapshots of post-synthetic metallation chemistry in metal−organic frameworks. *Nat Chem* 2014;**6**:906−12.

315. Burgun A, Coghlan CJ, Huang DM, Chen W, Horike S, Kitagawa S, et al. Mapping-out catalytic processes in a metal-organic framework with single-crystal X-ray crystallography. *Angew Chem Int Ed Engl* 2017;**56**:8412−6.
316. Lam WS, Yao YF, Tang CX, Wang Y, Yuan Q, Peng L. Bifunctional mesoporous HMUiO-66-NH2 nanoparticles for bone remodeling and ROS scavenging in periodontitis therapy. *Biomaterials* 2025;**314**: 122872.
317. Xie B, Zeng DL, Yang MJ, Tang ZY, He LZ, Chen TF. Translational selenium nanoparticles to attenuate allergic dermatitis through Nrf2-Keap1-driven activation of selenoproteins. *ACS Nano* 2023;**17**: 14053−68.
318. Surhio MM, Wang Y, Xu P, Shah F, Li J, Ye M. Antihyperlipidemic and hepatoprotective properties of selenium modified polysaccharide from *Lachnum* sp. *Int J Biol Macromol* 2017;**99**:88−95.
319. Ouyang J, Deng B, Zou BH, Li YJ, Bu QY, Tian Y, et al. Oral hydrogel microbeads-mediated *in situ* synthesis of selenoproteins for regulating intestinal immunity and microbiota. *J Am Chem Soc* 2023; **145**:12193−205.
320. Khurana A, Tekula S, Saifi MA, Venkatesh P, Godugu C. Therapeutic applications of selenium nanoparticles. *Biomed Pharmacother* 2019; **111**:802−12.
321. Guo L, Huang K, Liu H. Biocompatibility selenium nanoparticles with an intrinsic oxidase-like activity. *J Nanopart Res* 2016;**18**:74.
322. Huang B, Zhang J, Hou J, Chen C. Free radical scavenging efficiency of nano-Se *in vitro*. *Free Radic Biol Med* 2003;**35**:805−13.
323. Lee SC, Lee NH, Patel KD, Jang TS, Knowles JC, Kim HW, et al. The effect of selenium nanoparticles on the osteogenic differentiation of MC3T3-E1 cells. *Nanomaterials (Basel)* 2021;**11**:557.
324. Zou BH, Xiong ZS, Yu YZ, Shi SJ, Li XL, Chen TF. Rapid selenoprotein activation by selenium nanoparticles to suppresses osteoclastogenesis and pathological bone loss. *Adv Mater* 2024;**36**: 2401620.
325. Gagrani A, Ding B, Wang Y, Tsuzuki T. pH dependent catalytic redox properties of Mn_3O_4 nanoparticles. *Mater Chem Phys* 2019; **231**:41−7.
326. Yang DZ, Li QL, Tammina SK, Gao Z, Yang YL. Cu-CDs/H_2O_2 system with peroxidase-like activities at neutral pH for the co-catalytic oxidation of o-phenylenediamine and inhibition of catalytic activity by Cr(III). *Sens Actuators B Chem* 2020;**319**:128273.
327. Estelrich J, Busquets N. Prussian blue: a nanozyme with versatile catalytic properties. *Int J Mol Sci* 2021;**22**:5993.
328. Feng KZ, Wang GC, Wang S, Jing Y, Wu HA, Ming, et al. Breaking the pH limitation of nanozymes: mechanisms, methods and applications. *Adv Mater* 2024;**36**:2401619.
329. Liu QW, Zhang A, Wang RH, Zhang Q, Cui DX. A review on metal- and metal oxide-based nanozymes: properties, mechanisms, and applications. *Nanomicro Lett* 2021;**13**:154.
330. Ribeiro MEA, Huaman NRC, Folly MM, Gomez JGC, Sánchez Rodríguez RJ. A potential hybrid nanocomposite of poly(3-hydroxybutyrate-*co*-3-hydroxyvalerate) and fullerene for bone tissue regeneration and sustained drug release against bone infections. *Int J Biol Macromol* 2023;**251**:126531.
331. Tanzi L, Terreni M, Zhang Y. Synthesis and biological application of glyco- and peptide derivatives of fullerene C_{60}. *Eur J Med Chem* 2022;**230**:114104.
332. Hou WJ, Shen L, Zhu YM, Wang XJ, Du TY, Yang F, et al. Fullerene derivatives for tumor treatment: mechanisms and application. *Int J Nanomed* 2024;**19**:9771−97.
333. Osuna S, Swart M, Solà M. On the mechanism of action of fullerene derivatives in superoxide dismutation. *Chemistry* 2010;**16**:3207−14.
334. Yin JJ, Lao F, Fu PP, Wamer WG, Zhao Y, Wang PC, et al. The scavenging of reactive oxygen species and the potential for cell protection by functionalized fullerene materials. *Biomaterials* 2009; **30**:611−21.
335. Krusic PJ, Wasserman E, Keizer PN, Morton JR, Preston KF. Radical reactions of C_{60}. *Science* 1991;**254**:1183−5.
336. Yang X, Li CJ, Wan Y, Smith P, Shang G, Cui Q. Antioxidative fullerol promotes osteogenesis of human adipose-derived stem cells. *Int J Nanomed* 2014;**9**:4023−31.
337. Grausova L, Vacik J, Vorlicek V, Svorcik V, Slepicka P, Bilkova P, et al. Fullerene C_{60} films of continuous and micropatterned morphology as substrates for adhesion and growth of bone cells. *Diamond Relat Mater* 2009;**18**:578−86.
338. Geng H, Chang YN, Bai X, Liu S, Yuan Q, Gu W, et al. Fullerenol nanoparticles suppress RANKL-induced osteoclastogenesis by inhibiting differentiation and maturation. *Nanoscale* 2017;**9**: 12516−23.
339. Injac R, Prijatelj M, Strukelj B. Fullerenol nanoparticles: toxicity and antioxidant activity. *Methods Mol Biol* 2013;**1028**:75−100.
340. Yang JL, Zhan ZH, Li XC, Hu M, Zhu Y, Xiao YC, et al. Fullerol-reinforced antioxidantive 3D-printed bredigite scaffold for accelerating bone healing. *Mater Today Bio* 2024;**27**:101120.
341. DeJulius CR, Dollinger BR, Kavanaugh TE, Dailing E, Yu F, Gulati S, et al. Optimizing an antioxidant TEMPO copolymer for reactive oxygen species scavenging and anti-inflammatory effects *in vivo*. *Bioconjug Chem* 2021;**32**:928−41.
342. Soule BP, Hyodo F, Matsumoto K, Simone NL, Cook JA, Krishna MC, et al. The chemistry and biology of nitroxide compounds. *Free Radic Biol Med* 2007;**42**:1632−50.
343. Li JC, Zhang J, Chen Y, Kawazoe N, Chen GP. TEMPO-conjugated gold nanoparticles for reactive oxygen species scavenging and regulation of stem cell differentiation. *ACS Appl Mater Interfaces* 2017;**9**:35683−92.
344. Sadowska-Bartosz I, Bartosz G. The cellular and organismal effects of nitroxides and nitroxide-containing nanoparticles. *Int J Mol Sci* 2024;**25**:1446.
345. Sharma A, Madhunapantula SV, Robertson GP. Toxicological considerations when creating nanoparticle-based drugs and drug delivery systems. *Expert Opin Drug Metab Toxicol* 2012;**8**:47−69.
346. Guo Y, Sun Q, Wu FG, Dai Y, Chen X. Polyphenol-containing nanoparticles: synthesis, properties, and therapeutic delivery. *Adv Mater* 2021;**33**:e2007356.
347. Liu H, Qu X, Tan HQ, Song JL, Lei M, Kim E, et al. Role of polydopamine's redox-activity on its pro-oxidant, radical-scavenging, and antimicrobial activities. *Acta Biomater* 2019;**88**:181−96.
348. Liu Y, Ai K, Lu L. Polydopamine and its derivative materials: synthesis and promising applications in energy, environmental, and biomedical fields. *Chem Rev* 2014;**114**:5057−115.
349. Mostert AB, Rienecker SB, Noble C, Hanson GR, Meredith P. The photoreactive free radical in eumelanin. *Sci Adv* 2018;**4**:eaaq1293.
350. Lee HA, Park E, Lee H. Polydopamine and its derivative surface chemistry in material science: a focused review for studies at KAIST. *Adv Mater* 2020;**32**:1907505.
351. Li ZH, Lu HL, Fan LM, Ma XY, Duan ZW, Zhang YW, et al. Microneedle-delivered PDA@Exo for multifaceted osteoarthritis treatment *via* PI3K−Akt−mTOR pathway. *Adv Sci* 2024;**11**: e2406942.
352. Li B, Liu FL, Ye J, Cai XM, Qian RL, Zhang KW, et al. Regulation of macrophage polarization through periodic photo-thermal treatment to facilitate osteogenesis. *Small* 2022;**18**:e2202691.
353. Li YZ, Liu CD, Cheng XT, Wang JY, Pan Y, Liu C, et al. PDA-BPs integrated mussel-inspired multifunctional hydrogel coating on ppenk implants for anti-tumor therapy, antibacterial infection and bone regeneration. *Bioact Mater* 2023;**27**:546−59.
354. Yu YL, Li XL, Li JR, Li DY, Wang QM, Teng W. Dopamine-assisted co-deposition of hydroxyapatite-functionalised nanoparticles of polydopamine on implant surfaces to promote osteogenesis in environments with high ROS levels. *Mater Sci Eng C* 2021;**131**:112473.
355. Li YZ, Yang L, Hou Y, Zhang ZZ, Chen M, Wang MX, et al. Polydopamine-mediated graphene oxide and nanohydroxyapatite-incorporated conductive scaffold with an immunomodulatory ability accelerates periodontal bone regeneration in diabetes. *Bioact Mater* 2022;**18**:213−27.

356. Yu SF, Du J, Zhang Q, Li Z, Ge SH, Ma BJ. Mitochondria-targeted polyphenol-cysteine nanoparticles regulating AMPK-mediated mitochondrial homeostasis for enhanced bone regeneration. *Adv Funct Mater* 2024;**34**:2402463.
357. Byun HY, Jang GN, Hong MH, Yeo JW, Shin HJ, Kim WJ, et al. Biomimetic anti-inflammatory and osteogenic nanoparticles self-assembled with mineral ions and tannic acid for tissue engineering. *Nano Converg* 2022;**9**:47.
358. Byun HY, Jang GN, Jeong HW, Lee JK, Huh SJ, Lee SM, et al. Development of a composite hydrogel incorporating anti-inflammatory and osteoinductive nanoparticles for effective bone regeneration. *Biomater Res* 2023;**27**:132.
359. Geng H, Zhong QZ, Li J, Lin Z, Cui J, Caruso F, et al. Metal ion-directed functional metal-phenolic materials. *Chem Rev* 2022;**122**: 11432−73.
360. Chen JQ, Pan SJ, Zhou JJ, Lin ZX, Qu YJ, Glab A, et al. Assembly of bioactive nanoparticles *via* metal-phenolic complexation. *Adv Mater* 2022;**34**:e2108624.
361. Guo J, Tardy BL, Christofferson AJ, Dai Y, Richardson JJ, Zhu W, et al. Modular assembly of superstructures from polyphenol-functionalized building blocks. *Nat Nanotechnol* 2016;**11**:1105−11.
362. Lin Z, Richardson JJ, Zhou J, Caruso F. Direct synthesis of amorphous coordination polymers and metal-organic frameworks. *Nat Rev Chem* 2023;**7**:273−86.
363. Ejima H, Richardson JJ, Liang K, Best JP, van Koeverden MP, Such GK, et al. One-step assembly of coordination complexes for versatile film and particle engineering. *Science* 2013;**341**:154−7.
364. Jia X, Wu JZ, Lu K, Li Y, Qiao XS, Kaelin J, et al. Organic−inorganic hybrids of Fe−Co polyphenolic network wrapped Fe_3O_4 nanocatalysts for significantly enhanced oxygen evolution. *J Mater Chem A* 2019;**7**:14302−8.
365. Jeong H, Byun H, Lee J, Han Y, Huh SJ, Shin H. Enhancement of bone tissue regeneration with multi-functional nanoparticles by co-ordination of immune, osteogenic, and angiogenic responses. *Adv Healthc Mater* 2025;**14**:2400232.
366. Xu M, Wu GG, You Q, Chen XY. The landscape of smart biomaterial-based hydrogen therapy. *Adv Sci* 2024;**11**:e2401310.
367. Ohsawa I, Ishikawa M, Takahashi K, Watanabe M, Nishimaki K, Yamagata K, et al. Hydrogen acts as a therapeutic antioxidant by selectively reducing cytotoxic oxygen radicals. *Nat Med* 2007;**13**: 688−94.
368. Zhou G, Goshi E, He Q. Micro/nanomaterials-augmented hydrogen therapy. *Adv Healthc Mater* 2019;**8**:e1900463.
369. Zhou H, He ZY, Cao YD, Chu L, Liang B, Yu KX, et al. An injectable magnesium-loaded hydrogel releases hydrogen to promote osteoporotic bone repair *via* ROS scavenging and immunomodulation. *Theranostics* 2024;**14**:3739−59.
370. Chen SQ, Yu YM, Xie SQ, Liang DN, Shi W, Chen SZ, et al. Local H_2 release remodels senescence microenvironment for improved repair of injured bone. *Nat Commun* 2023;**14**:7783.
371. Ren XX, Liu H, Wu XM, Weng WZ, Wang XH, Su JC. Reactive oxygen species (ROS)-responsive biomaterials for the treatment of bone-related diseases. *Front Bioeng Biotechnol* 2021;**9**:820468.
372. Yao YJ, Zhang HL, Wang ZY, Ding J, Wang SQ, Huang BQ, et al. Reactive oxygen species (ROS)-responsive biomaterials mediate tissue microenvironments and tissue regeneration. *J Mater Chem B* 2019;**7**:5019−37.
373. Gao F, Xiong Z. Reactive oxygen species responsive polymers for drug delivery systems. *Front Chem* 2021;**9**:649048.
374. Martin JR, Gupta MK, Page JM, Yu F, Davidson JM, Guelcher SA, et al. A porous tissue engineering scaffold selectively degraded by cell-generated reactive oxygen species. *Biomaterials* 2014;**35**: 3766−76.
375. Wilson DS, Dalmasso G, Wang L, Sitaraman SV, Merlin D, Murthy N. Orally delivered thioketal nanoparticles loaded with TNF-α-siRNA target inflammation and inhibit gene expression in the intestines. *Nat Mater* 2010;**9**:923−8.
376. McEnery MA, Lu S, Gupta MK, Zienkiewicz KJ, Wenke JC, Kalpakci KN, et al. Oxidatively degradable poly(thioketal urethane)/ceramic composite bone cements with bone-like strength. *RSC Adv* 2016;**6**:109414−24.
377. Zhang Q, Chen WK, Li GF, Ma ZX, Zhu MR, Gao QM, et al. A factor-free hydrogel with ROS scavenging and responsive degradation for enhanced diabetic bone healing. *Small* 2024;**20**: 2306389.
378. Fang X, Hu JF, Hu QY, Li H, Sun ZJ, Xu Z, et al. ROS-responsive resveratrol-loaded cyclodextrin nanomicelles reduce inflammatory osteolysis. *Colloids Surf B Biointerfaces* 2022;**219**:112819.